FOOD AND ECOLOGICAL SYSTEMS MODELLING JOURNAL

Food and Ecological Systems Modelling Journal 7: e169793 (2026)
DOI: https://doi.org/10.3897/fmj.7.169793

Formal Model Article Format

The Formal Model for the hoverfly *Sphaerophoria scripta* (Diptera, Syrphidae) agent-based model in the Animal Landscape and Man Simulation System (ALMaSS)

Elżbieta Ziółkowska[1,2,3], Grzegorz Sowa[2], Xiaodong Duan[1], Christopher John Topping[1]

1 *Social-Ecological Systems Simulation Centre, Department of Agroecology, Aarhus University, Aarhus, Denmark*
2 *Institute of Environmental Sciences, Faculty of Biology, Jagiellonian University, Kraków, Poland*
3 *Institute of Geography and Spatial Management, Faculty of Geography and Geology, Jagiellonian University, Kraków, Poland*

Corresponding author: Elżbieta Ziółkowska (e.ziolkowska@uj.edu.pl)

Abstract

We present a formal model for the aphidophagous hoverfly *Sphaerophoria scripta*, a species widely used for biological control of *Myzus persicae* and other aphids, as well as for pollination services. The model is structured for integration within the Animal Landscape and Man Simulation System (ALMaSS) to investigate population dynamics under variable field conditions, with the overarching aim of improving regulatory risk assessments of pesticide impacts on hoverflies. Our approach is individual-based, spatially explicit, and operates on a daily time step. The principal model drivers include temperature, the spatial and temporal distribution of aphid prey for larvae, and the availability of nectar and pollen resources for adult females. Dispersal functions are designed to interact dynamically with foraging and oviposition behaviours, with daily activity patterns governed by the interplay between reproductive objectives and foraging requirements. Key life-history parameters, including egg incubation duration, larval instar development, pupariation, adult longevity, and fecundity, were derived from available laboratory and field studies. The prototype model defines state transitions, developmental thresholds, mortality functions, and foraging-oviposition behaviours, and is prepared for calibration and scenario-based application.

Key words: Agroecosystem, aphidophagous hoverfly, biological control, Long Hoverfly, pollinator, population dynamics, spatially-explicit model

OPEN ACCESS

Academic editor: Fabio Sgolastra
Received: 26 August 2025
Accepted: 23 January 2026
Published: 27 February 2026

Citation: Ziółkowska E, Sowa G, Duan X, Topping CJ (2026) The Formal Model for the hoverfly *Sphaerophoria scripta* (Diptera, Syrphidae) agent-based model in the Animal Landscape and Man Simulation System (ALMaSS). Food and Ecological Systems Modelling Journal 7: e169793. https://doi.org/10.3897/fmj.7.169793

Copyright: © Elżbieta Ziółkowska et al. This is an open access article distributed under terms of the Creative Commons Attribution License (Attribution 4.0 International – CC BY 4.0).

Introduction

Growing recognition of wild pollinators has highlighted their crucial role in sustainable agriculture and ecosystem functioning. While most research and conservation efforts have historically focused on managed species such as the honey bee, wild pollinators contribute significantly to pollination services and offer additional ecosystem benefits (Garibaldi et al. 2014; Rader et al. 2016; Reilly et al. 2024).

Hoverflies (Diptera, Syrphidae), also known as syrphids or flower flies, are globally distributed and are among the most important insect pollinators

(Wotton et al. 2019; Rader et al. 2020). All adult hoverflies feed primarily on nectar and pollen, although the proportions vary among species (Gilbert 1985b), making them frequent floral visitors and effective pollinators. However, hoverflies also play other essential roles in ecosystems due to the diverse feeding habits of their larvae, which can be phytophagous, mycophagous, zoophagous, or saprophagous, including both aquatic and terrestrial types. Among these, aphidophagous hoverflies are particularly important because their larvae prey on aphids and other major crop pests such as thrips and spider mites, providing a valuable biological control service (Dunn et al. 2020; Pekas et al. 2020).

Given this dual ecological role, pollination by adults and pest control by larvae, we selected *Sphaerophoria scripta* (Linnaeus, 1758) as a focal species for model development. *Sphaerophoria scripta* is one of the most common aphidophagous hoverflies in Central Europe (Reynolds et al. 2024), typically active from May to October with peak abundance in August (Nengel and Drescher 1991). It occurs in diverse habitats, including open grasslands, flower-rich urban wastelands (Stubbs and Falk 2012), and agricultural fields (Madureira et al. 2023, 2024), making it particularly relevant for agroecosystem studies.

This paper follows the formal model structure outlined by Topping et al. (2022a). It presents a prototype spatially-explicit agent-based model for *S. scripta*, prior to its full implementation and calibration. The model is intended for integration into the Animal, Landscape and Man Simulation System (ALMaSS) framework (Topping et al. 2003; Topping 2022b), leveraging its spatially detailed, dynamic landscape features while acknowledging its structural constraints (Topping and Duan 2024).

Several individual-based models have been developed so far to simulate hoverfly population dynamics, particularly focusing on aphidophagous species. RePast hoverfly-aphid model (Parry and Bithell 2011) links a spatially explicit (super) individual-based aphid model (Parry et al. 2006; Parry and Evans 2008) with a simplified hoverfly submodel. Its overall structure is similar to that used by Tenhumberg (2004), with the addition of adult female syrphid movement across the landscape. However, the landscape is represented in a simplified manner, consisting of only two categories: field and field margin. The hoverfly submodel is also highly simplified; development is limited to a single transition from larva to adult, triggered once a larva consumes a minimum number of aphids. Moreover, adult mortality is not included, and larval mortality depends solely on aphid availability (larvae die when no aphids are present).

In contrast, movement and foraging are modelled more realistically, incorporating non-random prey search, oviposition optimisation, and larval predation using an exponential function dependent on hoverfly age and aphid density. Interactions between adult hoverflies and the landscape are not explicitly modelled, aside from oviposition behaviour and larval predation. Notably, pollination by adults and its influence on movement and oviposition are not included.

Two other individual-based models focus specifically on *Episyrphus balteatus* (De Geer, 1776). The 'Hover-Winter' model (Arrignon et al. 2007) simulates winter survival strategies of adult females, examining how landscape structure and climate influence overwintering success. Other life stages are not modelled, and interactions with aphids are absent. Resource acquisition is limited to nectar feeding for energy storage. The landscape is represented as a regular

grid with 25 m resolution, with cells classified into five functional habitat types; forest edges, forest interior, flower-rich semi-natural habitats/field margins, open arable fields, and urban/other non-habitat cells.

The SyrFitSources model (App et al. 2025), implemented in NetLogo, extends the 'Hover-Winter' model by simulating the full life cycle of *E. balteatus*, including interactions with aphids. While development of immature stages is driven solely by temperature, aphid availability influences larval voracity and, consequently, larval mortality. Adult behaviour is governed by resource availability and seasonal dynamics. Adults disperse among habitat patches in search of nectar and pollen, with movement probabilities weighted by patch distance and resource attractiveness. Pollen intake regulates egg maturation, while oviposition rates depend on both nutritional status and local aphid density, reflecting resource-based habitat selection. The landscape is represented as a network of habitat patches derived from raster land-cover data, with each patch characterised by area, habitat type, and dynamic resource availability (nectar, pollen, and aphids), updated daily based on plant phenology and an aphid population model.

Building on concepts from the models described above, our model of *S. scripta* introduces increased realism, particularly in landscape representation. It will be integrated into the highly detailed, dynamic landscape simulation available in ALMaSS, which operates at a spatial resolution of 1 m^2 (Topping et al. 2003; Topping and Duan 2024a, b). This integration enables daily simulation of vegetation dynamics and resource (pollen and nectar) availability across space and time, alongside realistic agricultural management practices. The *S. scripta* model is also designed to run in parallel with the aphid species model (Thomsen et al. 2024), which supports the simulation of multiple aphid species: *Acyrthosiphon pisum* (Harris, 1776), *Aphis fabae* (Scopoli, 1763), *Myzus persicae* (Sulzer, 1776) and *Sitobion avenae* (Fabricius, 1775). Together, these models facilitate the representation of complex trophic interactions between prey and predator species within the same landscape, offering a powerful framework for exploring ecological dynamics and assessing pesticide risks.

To complement the *S. scripta* model and capture the broader functional diversity of hoverflies, a second model is under development for the species *Eristalis tenax* (Linnaeus, 1758), whose larvae are saprophagous (Ziółkowska et al. 2025). Together, these models provide a complementary representation of the ecosystem services delivered by hoverflies and support their integration into ecological based agricultural management.

Aims and purpose

The model provides a spatially explicit, mechanistic representation of *S. scripta* population dynamics in temperate agricultural landscapes, with individual development and survival rates driven by ambient temperature and aphid prey density. Its primary purpose is to evaluate hoverfly efficacy and resilience under alternative climate and crop-management scenarios. A secondary application is to model a representative non-target species within a systems-based environmental risk-assessment framework for agrochemicals, particularly pesticides.

We will implement the model in the ALMaSS framework (Topping et al. 2003; Topping 2022b; Topping and Duan 2024) to exploit its 1 m^2 resolution, dynamic treatment of landscape heterogeneity, and explicit farm-management routines. Simulations will typically span 10 × 10 km^2 landscapes, run at daily time steps, and extend over multi-year to decadal periods. This design captures both seasonal population cycles and longer-term trends in *S. scripta* abundance.

Theoretical framework and modelling approach

The model aims to represent the development, survival, movement, foraging, and reproduction of *S. scripta* using an individual-based approach within the ALMaSS framework. This approach enables a mechanistic simulation of hoverfly population dynamics in response to key ecological drivers, particularly temperature and prey density, with a level of detail suitable for long-term ecological projections and agricultural management scenarios.

As with other published models in ALMaSS (Duan et al. 2022; Ziółkowska et al. 2023; Topping and Duan 2025), we use an agent-based modelling framework (Grimm and Railsback 2005). Each hoverfly is represented as a unique object that exists within a specific behavioural state and possesses properties such as age, developmental stage, location, and aphid intake. These characteristics evolve and influence transitions between behavioural states, such as the shift from feeding to oviposition.

The ALMaSS environment provides a detailed, spatially and temporally dynamic representation of agricultural landscapes. This environment includes a raster-based land-cover map at 1 m^2 resolution, overlaid with polygonal habitat data. Landscapes are composed of individual farm units that are grouped and classified by type (e.g. arable, grassland, non-crop, mixed, or livestock farms), and each farm is governed by tailored crop management regimes. These regimes define the timing and probability of farm activities, including pesticide application and are structured as pluri-annual crop rotations based on real agronomic practices.

Daily updates to landscape conditions include vegetation growth and weather, both of which affect resource availability. The aphid population dynamics could be explicitly simulated (i.e., the model could be linked with the aphid subpopulation model of Thomsen et al. 2024) or externally inputted, allowing the model to respond to spatio-temporal variation in prey availability. Larval development is explicitly linked to aphid prey consumption, as the daily developmental rate depends on the aphid biomass consumed each day. Larval mortality is not directly tied to prey density. In adults, foraging and reproduction are coupled through prey availability, as the daily oviposition rate depends on the number of aphids present. In future extensions, this relationship may also incorporate pollen and nectar intake by adults.

All life stages of *S. scripta*—egg, larva, pupa, and adult—are modelled individually. Parameters are based on the field and laboratory data on *S. scripta* or similar species within the genus if available in the literature. Interactions with the landscape and other individuals are updated daily, enabling realistic simulation of individual and population-level dynamics within complex agricultural mosaics.

Overview of processes

The life cycle of this highly migratory syrphid comprises four principal stages, egg, larva, pupa and adult. It unfolds over multiple generations between April and November (and potentially year-round in southern Europe). Overwintering occurs predominantly at the fully grown larval stage, with individuals remaining inactive in the soil or leaf litter. Following spring warming, larvae resume development, pupate, and subsequently emerge as adults. Newly emerged adults disperse into open habitats and engage in low, erratic flight among grasses while visiting a broad spectrum of flowers (Speight 2024). They feed on nectar and pollen from various wild flowers (e.g. *Achillea*, *Campanula*, *Cirsium*, *Euphorbia* or *Origanum*) (De Buck 1990), thereby contributing to pollination in both natural and agricultural ecosystems.

Gravid females locate aphid-infested host plants, ranging from wild herbaceous species to economically important crops such as *Avena*, *Brassica*, *Cichorium*, *Lactuca*, *Triticum* and *Vicia*, as well as apple orchards, on which they oviposit (Wojciechowicz-Żytko and Wilk 2023; Speight 2024). Upon hatching, larvae immediately search for prey and consume large numbers of aphids. Larval development typically spans three instars over several days up to two weeks, depending on temperature and prey availability.

Fully grown larvae then harden to create a puparium. This pupal phase endures for approximately one week, during which metamorphosis to the adult form occurs (Nengel and Drescher 1991). The overall generation time is quite short, supporting multiple generations per year. That is why emerging adults may join the current season's reproductive cohort, mating and producing subsequent generations. Throughout its range, from subarctic grasslands in Greenland and Fennoscandia to Mediterranean, North African, and high-altitude Asian habitats, this species' flexible phenology and habitat use underscore its ecological resilience and importance as both pollinator and biocontrol agent. More details about each developmental stage are given below.

Growth and development

Egg

Geographical variation in degree-day requirements shows that mean thermal sums for insect egg development increase from tropical to temperate populations, reflecting local adaptation to cooler climates (Honěk 1996). Eggs are laid singly on aphid-infested leaves, ensuring freshly emerged larvae immediate prey access and minimising egg crowding.

During the egg stage, *S. scripta* exhibits a clear inverse relationship between temperature and developmental duration (Table 1). At 10 °C, egg development requires approximately 12 days, whereas at 30 °C, this period is reduced to approximately 2.3 days (Nengel and Drescher 1991). Under moderate temperature conditions (approximately 20 °C), the egg stage typically lasts between 3 and 6 days (Agarwala et al. 1989; Krsteska 2008). When compared to other species (Table 1), *Sphaerophoria rueppellii* (Wiedemann, 1820) shows similar thermal responses, with egg durations ranging from 2.9 to 5.5 days when temperature decreased from 30 °C to 20 °C (Amoros-Jimenez et al. 2012).

Table 1. Summary of thermally induced length of development of subsequent life stages for genus of *Sphaerophoria*.

Life stage	Temperature (°C)	Relative humidity (%)	Type of food	Food availability	Duration (days)	Conditions /Notes	Species	Reference
Egg	≈ 20				3–4	Laboratory temp.	*Sphaerophoria scripta*	Krsteska (2008)
	10	60–70			12		*Sphaerophoria scripta*	Nengel and Drescher (1991)
	15				6			
	20				4			
	25				3			
	30				~2.3			
	20–22				3–4			
	14–17				5–6		*Sphaerophoria scripta*	Agarwala et al. (1989)
	22–32				2–3	Laboratory temp. Very wide temp range and no details on temp regime in the lab.	*Sphaerophoria scripta*	Gafarov (1979)
	20	50			5.50		*Sphaerophoria rueppellii*	Amorós-Jiménez et al. (2012)
	20	90			3.55			
	25	50			4.72			
	25	90			2.93			
	30	50			3.89			
	30	90			2.36			
	20				6–12	Laboratory temp.	*Sphaerophoria cylindrica*	Curran (1920)
	19.33				4.39		*Sphaerophoria sulphuripes*	Hopper et al. (2011)
	27.9 ± 1.1				1.96 ± 0.07		*Allograpta* (*Sphaerophoria*) *javana*	Patro and Behera (2002)
	16–18	80			6–8		*Sphaerophoria scripta*	Kantyerina (1979)
	18–20	70			4–6			
Larva	≈ 20		*Myzus persicae*	Ad libitum	8	50% population Laboratory temp.	*Sphaerophoria scripta*	Krsteska (2008)
	21	80	*Aphis fabae*	Ad libitum	11		*Sphaerophoria scripta*	Wojciechowicz-Żytko (2000)
	27.1	77.3	*Hyalopterus pruni*	Ad libitum	3.19 ± 0.22	First instar	*Sphaerophoria scripta*	Awadallah et al. (1980)
					3.86 ± 0.23	Second instar		
					6.95 ± 0.38	Third instar		
					14.00 ± 0.34	Total		
	20–22		unknown	unknown	4.1 ± 1.0	Third instar	*Sphaerophoria scripta*	Nengel and Drescher (1991)
	≈ 20		*Acyrthosiphon pisum*	unknown	9	Near natural temp.	*Sphaerophoria scripta*	Bańkowska (1978)
	≈ 20		*Acyrthosiphon pisum*	5 larvae/ day	14	Near natural temp.	*Sphaerophoria scripta*	Polak (1980)
				10 larvae/ day	15			
				15 larvae/ day	13			

Life stage	Temperature (°C)	Relative humidity (%)	Type of food	Food availability	Duration (days)	Conditions /Notes	Species	Reference
Larva				20 larvae/ day	13			
				30 larvae/ day	13			
				40 larvae/ day	12			
				60 larvae/ day	10			
	14–17			Ad libitum	13–15		*Sphaerophoria scripta*	Agarwala et al. (1989)
	22–24			Ad libitum	12–15		*Sphaerophoria scripta*	Wnuk and Fuchs (1977)
	22			Ad libitum	9		*Sphaerophoria scripta*	Laska (1959)
	22–32			Ad libitum	9–14	Laboratory temp. Very wide temp range and no details on temp regime in the lab.	*Sphaerophoria scripta*	Gafarov (1979)
	20	90	*Myzus persicae*	Ad libitum	10.95		*Sphaerophoria rueppellii*	Amorós-Jiménez et al. (2012)
	25	90			8.92			
	30	90			8.14			
	20				8.22	High food availability		
					10.42	Low food availability		
	≈ 20				16–27	Laboratory temp.	*Sphaerophoria cylindrica*	Curran (1920)
	19.33				13.50		*Sphaerophoria sulphuripes*	Hopper et al. (2011)
	27.9 ± 1.1				2.07 ± 0.11	First instar	*Allograpta* (*Sphaerophoria*) *javana*	Patro and Behera (2002)
					2.06 ± 0.15	Second instar		
					2.18 ± 0.10	Third instar		
					6.30 ± 0.22	Total		
Pupa	15				16		*Sphaerophoria scripta*	Nengel and Drescher (1991)
	20				10			
	24				7.4 ± 0.5			
	25				7			
	30				6			
	15				15.5		*Sphaerophoria scripta*	Honerk and Kocourek (1988)
	18				11			
	51				8.2			
	24				7.9			
	≈ 20				6–7	Laboratory temp.	*Sphaerophoria scripta*	Bokina (2012)
	≈ 20				6.35 ± 1.5	Laboratory temp.	*Sphaerophoria scripta*	Krsteska (2008)
	21				7.8		*Sphaerophoria scripta*	Laska (1959)
	14–17				14–15		*Sphaerophoria scripta*	Agarwala et al. (1989)

Life stage	Temperature (°C)	Relative humidity (%)	Type of food	Food availability	Duration (days)	Conditions /Notes	Species	Reference
Pupa	22–32				5–7	Laboratory temp. Very wide temp range and no details on temp regime in the lab.	*Sphaerophoria scripta*	Gafarov (1979)
	20	50			8.79		*Sphaerophoria rueppellii*	Amorós-Jiménez et al. (2012)
	20	90			9.14			
	25	50			5.15			
	25	90			5.20			
	30	50			4.90			
	30	90			4.80			
	20				5.66	High food availability at the larval stage		
					5.70	Low food availability at teh larval stage		
	≈ 20				5–10	Laboratory temp.	*Sphaerophoria cylindrica*	Curran (1920)
	19.33				9.77		*Sphaerophoria sulphuripes*	Hopper et al. (2011)
	27.9 ± 1.1				5.38 ± 0.04		*Allograpta* (*Sphaerophoria*) *javana*	Patro and Behera (2002)
Egg–adult total	≈ 20				17 ± 3	Laboratory temp.	*Sphaerophoria scripta*	Krsteska (2008)
	14–17				32–36		*Sphaerophoria scripta*	Agarwala et al. (1989)
	19.33				27.78		*Sphaerophoria sulphuripes*	Hopper et al. (2011)
	27.9 ± 1.1				14.02 ± 0.20		*Allograpta* (*Sphaerophoria*) *javana*	Patro and Behera (2002)

In contrast, *Sphaerophoria cylindrica* (Say, 1824) eggs require 6 to 12 days for development at approximately 20 °C (Curran 1920), and *Allograpta* (*Sphaerophoria*) *javana* (Wiedemann, 1824) demonstrates the shortest egg development time, completing this stage in just 1.96 ± 0.07 days at 27.9 °C (Patro and Behera 2002). Relative humidity appears to play an important role in the development of *Sphaerophoria* eggs as, at 25 °C, *S. rueppellii* eggs incubated at 90% relative humidity hatch in 2.93 days, compared to 4.72 days at 50% humidity (Amorós-Jiménez et al. 2012).

Larva

The larval stage is the longest and most ecologically significant period of syrphid development, as larvae serve as efficient predators of aphids and other soft-bodied insects (Dunn et al. 2020). Developmental duration during this stage is shaped by a complex interplay of temperature, humidity, and prey availability. Total larval development in *Sphaerophoria* ranges from approximately 6 to 27 days, depending on species and environmental conditions (Table 1).

At moderate temperatures (~20 °C), development of *S. scripta* typically spans 8 to 12 days when food is provided ad libitum (Bańkowska 1978; Polak 1980; Krsteska 2008). The larval stage comprises three instars with, at 27 °C, the first instar lasting approximately 3.2 days, the second 3.9 days, and the third 6.9 days, accounting for roughly 23%, 28%, and 50% of the total larval duration,

respectively (Awadallah et al. 1980). Among related species, *S. rueppellii* completes larval development in 8.1 to 10.9 days under similar thermal and humidity conditions (Amoros-Jimenez et al. 2012), while *Sphaerophoria sulphuripes* (Thomson, 1869) requires 13.5 days at 19.3 °C (Hopper et al. 2011). *Allograpta* (*Sphaerophoria*) *javana* again demonstrates the fastest development, completing all three instars in just 6.3 days at 27.9 °C (Patro and Behera 2002).

Prey availability is a critical determinant of aphidophagous hoverfly larval development. At low prey densities, larval development is longer and pupation occurs at lower larval weights (Ruzicka and Cairo 1976; Cornelius and Barlow 1980). Polak (1980) demonstrated a clear inverse linear relationship between both aphid availability (Equation 1; R^2 = 0.87), consumption (Equation 2; R^2 = 0.64), and the developmental time of *S. scripta* larvae reared on *A. pisum* at a temperature of 20 °C (Fig. 1). Developmental time decreased markedly from approximately 15.5 to 9 days as the mean number of aphids per day increased from 5 to 60.

$$D_l = -0.076 \times N_a + 14.817 \quad \text{Equation 1}$$

$$D_l = -0.237 \times N_c + 15.361 \quad \text{Equation 2}$$

where D_l is larva developmental time, N_a is the number of aphids available daily, and N_c is the number of aphids consumed daily.

Similarly, *S. rueppellii* larvae reared on *M. persicae* at 20 °C developed significantly faster under high food availability than under limited prey conditions (8.3 vs. 10.5 days) and pupation occurred at lower larval weights (11 vs. 9.3 mg) (Amorós-Jiménez et al. 2012) (Fig. 2). These findings are consistent with broader patterns observed across aphidophagous hoverflies. For example, Putra and Yasuda (2006) reported that increased aphid density significantly reduced larval development time in both *Episyrphus balteatus* and *Eupeodes* (*Metasyrphus*) *corollae* (Fabricius, 1794). Notably, the effect was prey-specific; *E. balteatus* developed more efficiently on *A. pisum*, whereas *E. corollae* showed faster development on *Aphis craccivora* (Koch, 1854). Collectively, these studies underscore the strong influence of prey availability on hoverfly developmental dynamics, particularly under thermally favourable conditions.

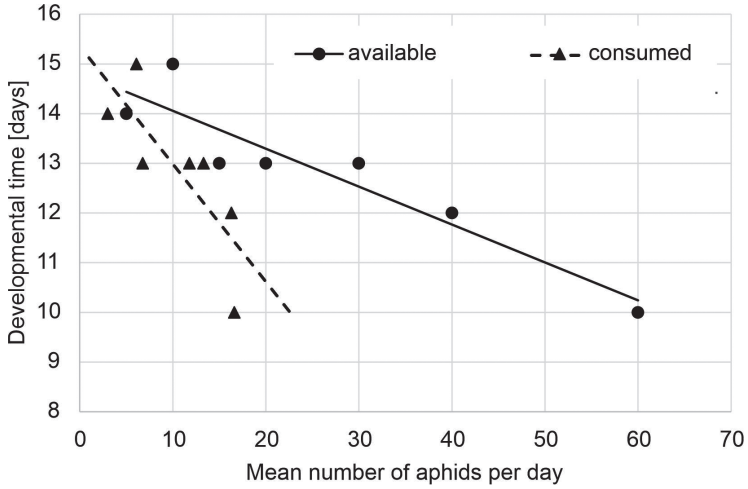

Figure 1. Relationship between number of *Acyrthosiphon pisum* aphids available and consumed daily and developmental time of *Sphaerophoria scripta*. Based on Polak (1980).

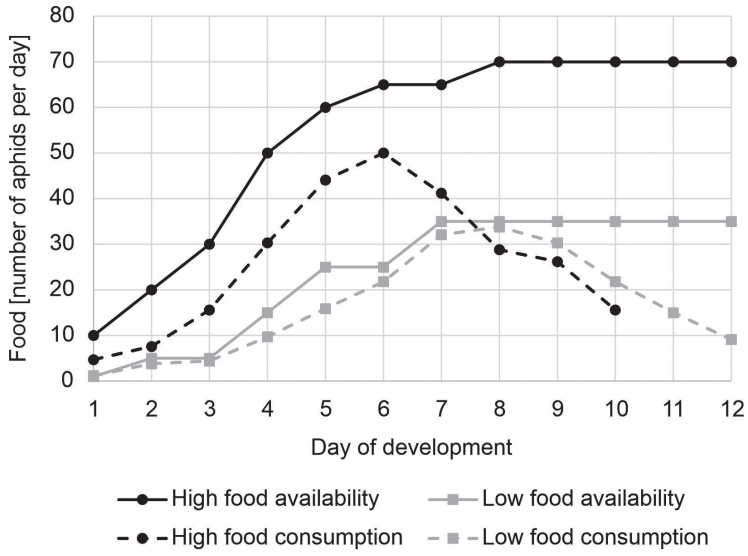

Figure 2. Consumption of *Myzus persicae* aphids by *Sphaerophoria rueppellii* under two feeding regimes: low and high food availability. Based on Amorós-Jiménez et al. (2012).

To date, no published studies have investigated larval longevity under starvation conditions in *S. scripta*. However, Rojo et al. (1996) examined the effects of aphid deprivation on larval survival in *E. corollae* and *E. balteatus* at various ages post-eclosion. In their study, larvae were initially provided with ad libitum access to aphids before being subjected to starvation. The results indicate that younger larvae exhibit greater sensitivity to starvation than older ones. Moreover, *E. balteatus* larvae demonstrated a higher tolerance to starvation compared to *E. corollae*, particularly in later instars (Fig. 3). Based on developmental time estimates, approximately 2 days for the first instar, 2 days for the second, and 3–4 days for the third in *E. corollae* (Li and Wu 2023), and 2–3 days, 3–3.5 days, and 4–6 days respectively for *E. balteatus* (Mushtaq et al. 2014), the mean survival times under starvation could be estimated as 1.0, 1.4, and 2.9 days for the first, second, and third instars of *E. corollae*, and 2.3, 3.5, and 5.8 days for *E. balteatus*. These findings are consistent with those of Ingels et al. (2015), who reported that third instar *E. balteatus* larvae survived an average of 4.6 days under starvation when earlier instars had been fed ad libitum, compared to only 2.9 days when earlier instars had been provided with limited aphid access.

Larvae of *Sphaerophoria* species are generalist predators, primarily consuming a variety of aphid species. Larvae of *S. scripta* have been found feeding on more than 30 genera of aphids. They have also been observed feeding on psyllids (jumping plant lice) and even lepidopteran larvae (e.g., *Pieris brassicae*), although aphids remain their primary prey (Rojo et al. 2003). Cannibalism has also been observed under high-density or food-limited conditions (Bańkowska 1964), suggesting behavioural plasticity in resource-scarce environments.

S. scripta larvae are aphid-feeding on herbaceous plants, including various crop plants, e.g. *Avena*, *Brassica*, *Cichorium*, *Lactuca*, *Triticum*, *Vicia* (Speight 2010). There is no indication of prey preference in *S. scripta*; instead, it tends to exploit local concentrations of aphids, showing opportunistic foraging. However, laboratory tests showed that in *Sphaerophoria* species, fitness-related parameters of adults may depend on the prey species consumed during their larval stage. For example, Amorós-Jiménez and Marcos-García (2020) showed that fecundity

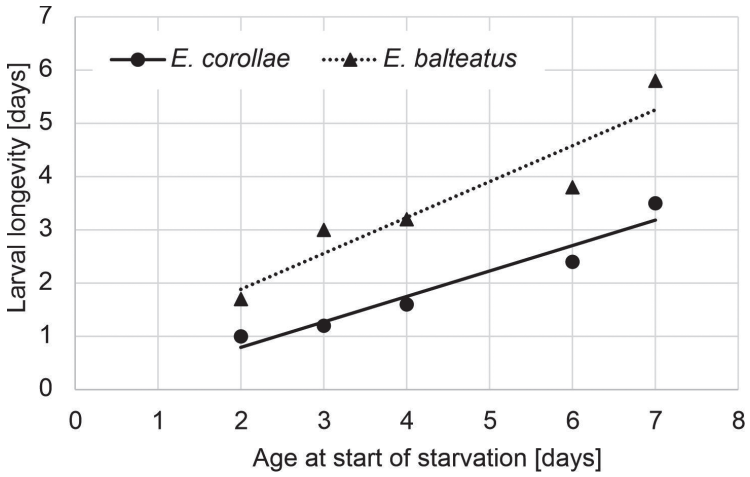

Figure 3. Longevity of *Eupeodes corollae* and *Episyrphus balteatus* larvae exposed to starvation at different developmental days. Before starvation larvae were provided with food ad libitum. Based on Rojo et al. (1996).

(number of eggs produced) and fertility (percentage of eggs hatched) in *S. rueppellii* females were higher when they were fed with *Rhopalosiphum padi* (Linnaeus, 1758) and showed the lowest values with *Aphis nerii* (Fonscolombe, 1841).

Studies indicate that *S. scripta* larvae need a daily minimum of five *A. pisum* aphids for complete development (Polak 1980). Under conditions close to natural and at a temperature of approximately 20 °C, *S. scripta* larvae demonstrated a wide range of aphid consumption, depending on aphid type. According to Krsteska (2008), larvae consumed in total between 300 and 365 individuals of *M. persicae*. In contrast, Bańkowska (1978) reported a mean consumption of 129 aphids of *A. pisum*, while Polak (1980) observed a slightly higher consumption of 167–192 aphids on the same aphid species. In comparison, the total aphid consumption by the smaller larvae of *S. rueppellii* was reported to be approximately 250 individuals of *M. persicae* (Amorós-Jiménez et al. 2012). Under laboratory conditions of 21 °C, *S. scripta* larvae consumed 190–306 *A. fabae* aphids, considerably less than the larger larvae of *E. corollae* and *E. balteatus* (400–500 aphids) (Wojciechowicz-Żytko 2000).

Aphid consumption by *S. scripta* larvae exhibits a pronounced ontogenetic increase, with minimal feeding activity observed during the initial 0–30% of the larval stage. This is followed by a rapid escalation in predation rates between 40 and 70–80% of development, culminating in peak consumption, which then decreases during the final 20–30% prior to pupation (Fig. 4B). These data indicate a strong positive correlation between larval maturity and predatory efficiency, suggesting that feeding behaviour is tightly regulated by developmental stage (Adams et al. 1987; Wojciechowicz-Żytko 2000). Furthermore, interspecific variation in daily consumption rates among *Sphaerophoria* species, as well as differences in aphid prey types, imply that both predator identity and prey characteristics influence feeding dynamics (Fig. 4A).

Adams et al. (1987) suggested that hoverfly larvae kill rates in the field populations are related to two main determinants of their range, i.e., larval size (expressed as body weight) and development rate (expressed as the percentage of development achieved). In controlled laboratory experiments, they examined the growth and predation dynamics of *E. corollae* larvae fed on

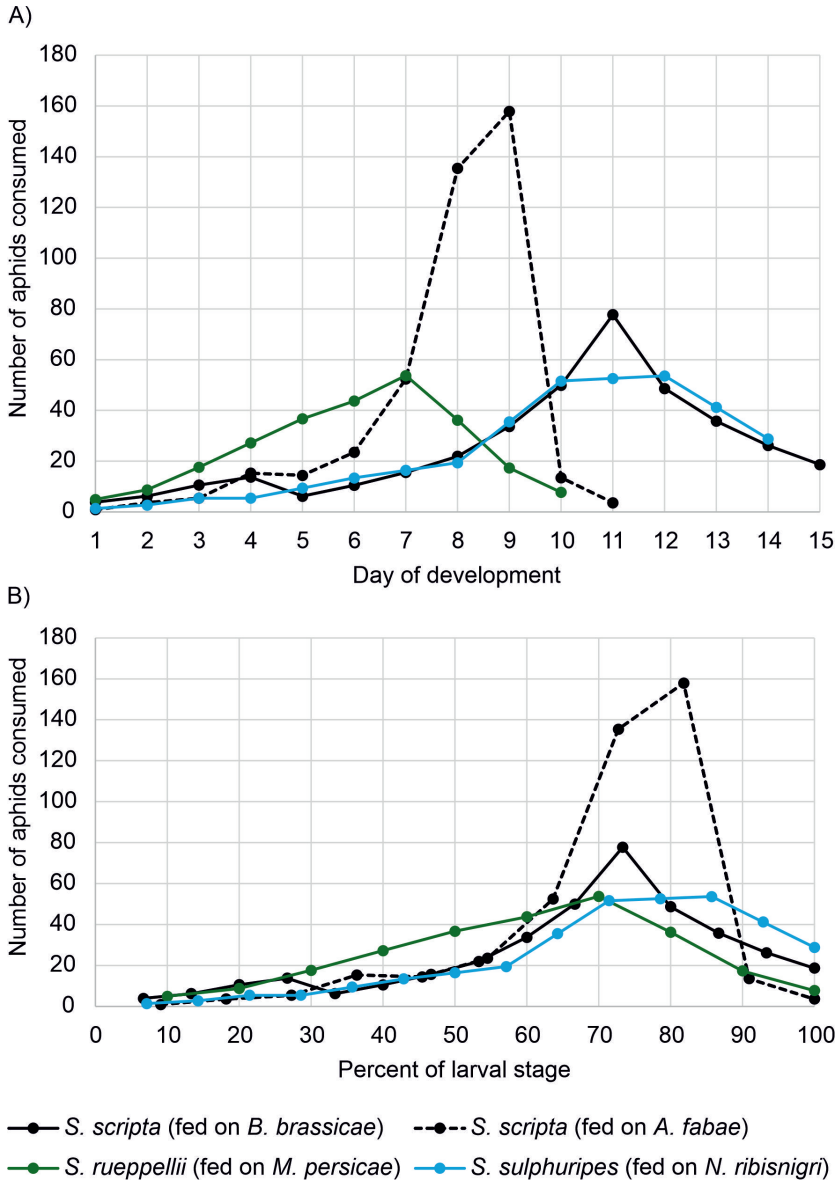

Figure 4. Average number of aphids eaten (**A**) daily and (**B**) in relation to larval developmental time (expressed as % of time taken from egg hatch to pupation) by syrphid larvae from the *Sphaerophoria* genus. Based on studies of Wnuk and Fuchs (1977), Wojciechowicz-Żytko (2000), Amorós-Jiménez R. et al. (2012), and Hopper et al. (2011), in which larvae had ad libitum food access.

S. avenae under two constant temperature regimes (10 °C and 15 °C). Their findings revealed that larval growth (Fig. 5A) and aphid kill (Fig. 5B) followed a similar exponential trajectory during the initial 75% of larval development, underscoring the importance of size as a determinant of predatory capacity. In addition, larval growth and aphid kill rates, expressed as mg per 1% of the larval stage achieved against developmental age, were closely comparable at both temperatures (Fig. 5). This suggests that temperature exerts a proportional influence on development, growth, and predation, allowing for the derivation of a standardised metric, relative kill rate (RKR), defined as the biomass of aphids killed per unit of larval biomass per 1% of the larval period. To further simplify this approach, mean RKR values can be calculated for each instar

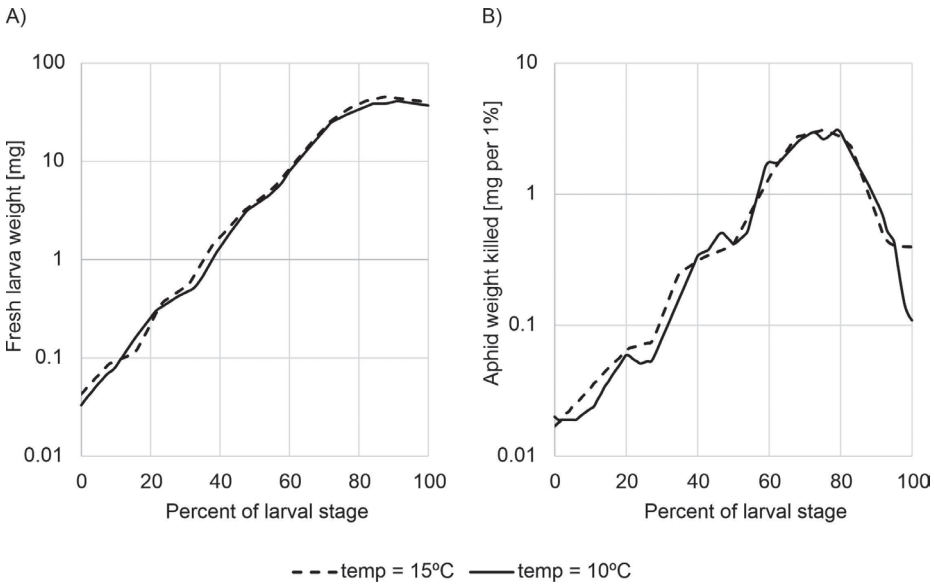

Figure 5. Growth of *Eupeodes* (*Metasyrphus*) *corollae* larvae (**A**) and biomass of *Sitobion avenae* killed by *E. corollae* larvae expressed as mg per 1% of duration of larval stage (**B**) under two constant temperature regimes (10 °C and 15 °C). Based on Adams et al. (1987).

based on daily measurements. Adams et al. (1987) advocated for the application of this model in field settings, enabling the estimation of daily aphid mortality per syrphid larva using field-derived data on predator instar structure, mean weights of each larval instar predator, and ambient temperature, as formalised in their predictive equation (Equation 3):

$$k_d = MRKR \times W_l \times D/W_a \quad \text{Equation 3}$$

where k_d is an estimated number of aphids killed per larva per day, *MRKR* is a mean relative aphid kill rate for the instar, W_l is the weight of the syrphid larva, W_a is a mean aphid weight, and *D* is the percentage of total larval development achieved in one day at the prevailing temperatures. For *E. corollae*, MRKR values were 0.29, 0.16, and 0.09 mg × mg^{-1} × percent^{-1} for first, second, and third instar, respectively.

Although empirical data on the relationship between larval biomass and aphid predation are not available for *S. scripta*, Hopper et al. (2011) investigated this relationship in four hoverfly species, including *S. sulphuripes*, under controlled conditions at 19.33 °C. In their study, larval growth was quantitatively described using a logistic growth model, which relates the day of development to larval fresh weight (Equation 4):

$$M_l = \frac{12.96}{1 + \exp(-0.68 \times (d - 9.22))} \quad \text{Equation 4}$$

where M_l is fresh larva weight and *d* is day of development.

They further investigated daily aphid biomass kill by larvae (B_a) in relation to larva fresh weight (M_l) and described it using the linear relationship (Equation 5):

$$B_a = 0.48 \times M_l + 6.06 \quad \text{Equation 5}$$

Findings for *S. sulphuripes* of Hopper et al. (2011) can be presented in relation to percentage of the larval stage, instead of day of development, making them comparable with results of Adams et al. (1987) for *E. corollae* (Fig. 6).

Food utilisation in *S. scripta* is strongly dependent on aphid density. Experimental data from Khan (2016) reveal a Holling Type II functional response (Equation 6) in both second and third larval instars, characterised by a rapid increase in aphid consumption at low prey densities followed by a decelerating intake rate that asymptotically approaches a plateau as prey availability increases (Fig. 7). This saturation pattern reflects the constraints imposed by handling time. Notably, third instar larvae exhibit higher maximum consumption rates than second instars, indicating a greater predatory capacity at more advanced developmental stages. In contrast, Polak (1980) assessed food utilisation across the entire larval period without distinguishing between instars. Although prey availability was not stratified by developmental stage, the overall consumption pattern similarly conformed to a Holling Type II response (Fig. 7).

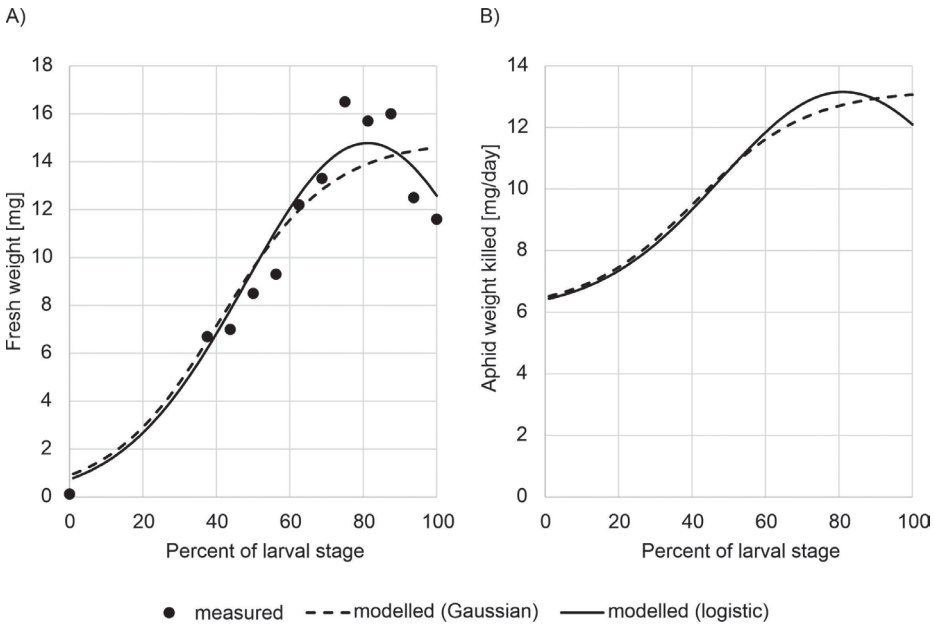

Figure 6. Growth of *Sphaerophoria sulphuripes* larvae (**A**) and biomass of *Nasonovia ribisnigri* (Mosley, 1841) killed by *S. sulphuripes* larvae expressed as mg per 1% of the duration of larval stage (**B**). Functions were fitted based on data from Hopper et al. (2011). Growth of *S. sulphuripes* larvae was modelled using Gaussian and logistic functions (parameters provided in Table 2). Biomass of aphids killed was modelled with Equation 5.

Table 2. Parameters of the logistic and Gaussian functions fitted to the data on growth of *Sphaerophoria sulphuripes* larvae from Hopper et al. (2011) (see Fig. 6).

Parameter	Logistic $M_l = \frac{a}{1+\exp(-b\times(p_l-c))}$	Gaussian $M_l = a\times\exp\left(-\frac{(p_l-b)^2}{2\times c^2}\right)$
a	14.89	14.78
b	0.0665	81.20
c	41.22	33.13
R^2	0.92	0.96

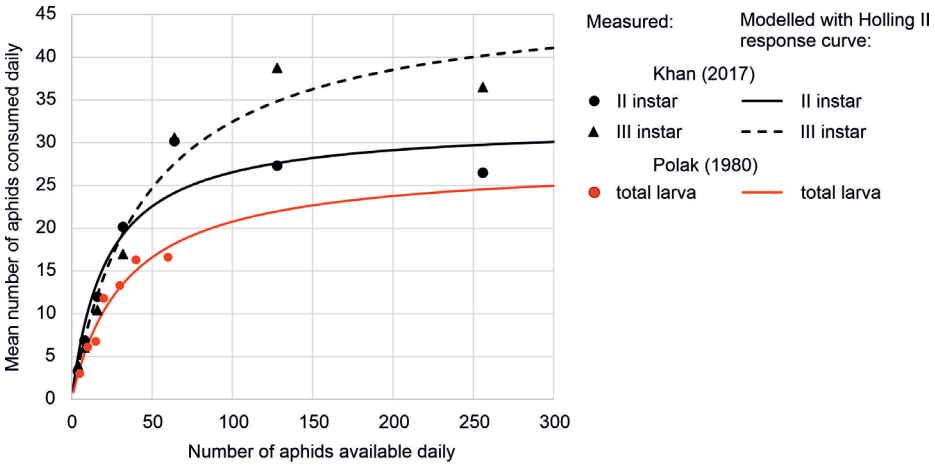

Figure 7. Functional response *Sphaerophoria scripta* larvae modelled with Holling II response curve based on data for II and III instars from Khan (2016) and for larvae in general from Polak (1980).

These findings collectively support the conclusion that *S. scripta* larvae exhibit a saturating functional response to increasing aphid density, with developmental stage influencing the magnitude of consumption. The parameters of the fitted models are presented in Table 3.

$$f(R) = \frac{a \times R}{1 + a \times h \times R} \qquad \text{Equation 6}$$

where *f* denotes the intake rate and *R* denotes food (or resource) density; *a* is the attack rate (i.e., the rate at which the hoverfly larva encounters food items per unit of food density), and *h* is handling time (i.e., the average time spent on processing a food item).

Table 3. Parameters of the Holling Type II response functions fitted to the data on food utilisation from Khan (2016) for second and third instars of *Sphaerophoria scripta* larvae reared in 25 °C and fed on *Brevicoryne brassicae*, and from Polak (1980) for *S. scripta* larvae reared in 20 °C and fed on *Acyrthosiphon pisum* aphids (see Fig. 7).

Parameter	II instar	III instar	Total larva
a	1.495	1.028	0.820
h	0.031	0.021	0.036
R^2	0.92	0.96	0.95

Pupa

During the pupal stage, syrphid larvae undergo metamorphosis into adults. This transformation is also temperature-dependent. At 15 °C, pupation requires up to 16 days (Nengel and Drescher 1991), whereas at 30 °C, this stage is completed in approximately 6 days. According to Nengel and Drescher (1991) emergence does not occur at or below 10 °C. Under standard laboratory conditions (~20 °C), the pupal stage typically lasts between 6 and 10 days (Krsteska 2008; Bokina 2012), providing a relatively short final step before adult emergence. In comparison, *S. rueppellii* pupates in 4.80 to 9.14 days depending on temperature and humidity (Amoros-Jimenez et al. 2012), *S. sulphuripes* requires 9.77

days at 19.33 °C (Hopper et al. 2011), and *A. javana* completes pupation in 5.38 ± 0.04 days at 27.9 °C (Patro and Behera 2002). Humidity exerts a minor influence, with slightly longer durations observed at higher relative humidity levels. Food availability during the larval stage seems to have minimal impact on pupal duration in *Sphaerophoria* species, with only marginal differences observed (less than 0.1 day) in *S. rueppellii* (Amoros-Jimenez et al. 2012).

Planned implementation in the model

The model will consider *S. scripta* behaviour of all four life stages (i.e., egg, larva with three instars, pupa, and adult) daily. We assume a ratio of 1:1 of females to males at the population level and thus, males will not be included in the model. It is further assumed that all adult females are fertilised; therefore, mating behaviour is not explicitly modelled, although it is implicitly incorporated into the timing of the reproductive process.

The development will be modelled according to the life-stage state machine and transition path (Fig. 8). Although some literature references the pupal stage as a potential overwintering form for *S. scripta*, the majority of sources identify the fully grown larva as the primary overwintering stage. This assumption is adopted in the present model. Following emergence from overwintering in early spring, larvae resume development and transition into the pupal stage. Upon adult emergence, females begin interacting with their environment, engaging in dispersal, foraging for nectar and pollen, and reproduction (see section 'Adults' for further details). Oviposition occurs with eggs laid singly, directly on or in close proximity to aphid colonies, ensuring immediate prey access for the hatching larvae. Egg development is governed by temperature and humidity. Upon hatching, a 1:1 sex ratio is assumed, and male larvae are excluded from the model.

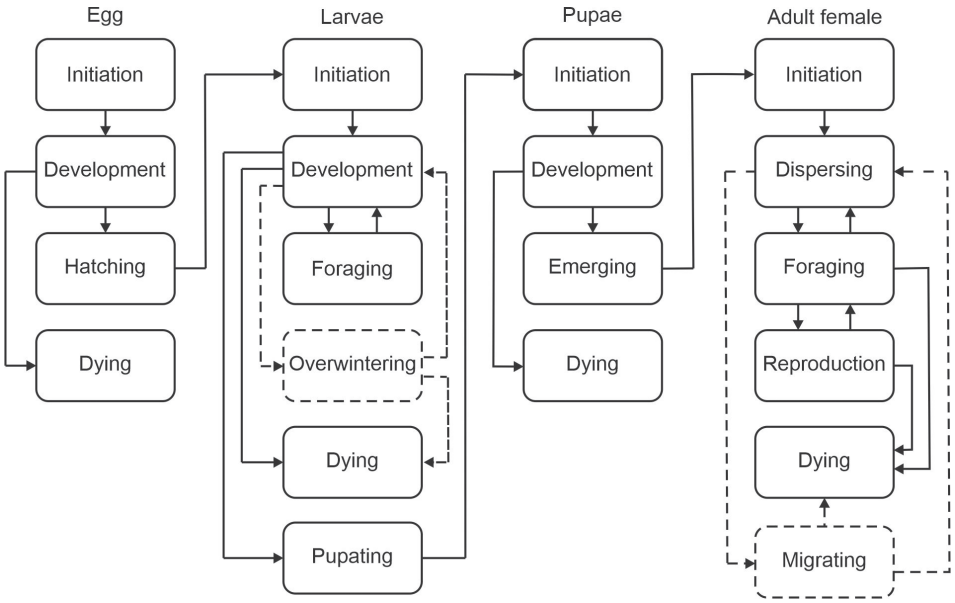

Figure 8. *Sphaerophoria scripta* state diagram showing development from egg to adult female. All stages could transition to state Dying from any other behavioural state due to external messaging. The Overwintering and Migration states (dashed lines) only occurs for the last, autumn generation. It is assumed that a proportion of the population migrates, whereas the remainder reproduces, producing larvae that subsequently enter overwintering. Additionally, a subset of individuals may migrate into the landscape during the subsequent spring.

Larval development occurs on herbaceous vegetation and aphid-infested crops, and is driven by ambient temperature and aphid biomass consumption, which is a function of aphid density. Larvae are capable of moving across plant surfaces in search of prey. This movement is assumed to be density-dependent; in high-density aphid colonies, larvae are likely to remain localised, whereas in low-density conditions, they may actively search for prey. Although precise data on larval mobility are lacking, movement is generally slow and localised, likely limited to several centimetres to tens of centimetres per day, depending on prey availability and plant architecture. First instar larvae are less mobile than later instars and typically remain near the hatching site. Nengel and Drescher (1991) reported that larval voracity and survival increase significantly in later instars, correlating with enhanced mobility and prey-handling capacity.

The model assumes that aphid density is provided daily at a spatial resolution of 10 × 10 metres, consistent with the resolution of the ALMaSS aphid subpopulation model (Thomsen et al. 2024; Duan and Topping 2024), facilitating integration between models. Thus, *S. scripta* larvae and adult females are able to sense aphids at this resolution. First instar larvae are assumed to move only within the 10 × 10 m grid cell in which they hatched. In addition, we assume that their sensing of aphids may be restricted to a smaller surrounding than the 10 × 10 m grid cell in which they hatched; thus a scaling (fitting) parameter will be applied for the calculation of available aphid density and biomass. For second and third instars, if aphid density in their current 10 × 10 m grid cell exceeds a defined threshold D_a, larvae will remain within it. If aphid density falls below D_a, larvae will initiate active search behaviour, prioritising adjacent cells with higher aphid densities. The threshold D_a, below which intercellular movement is triggered, is treated as a model calibration parameter.

Larvae eventually pupate, entering a non-mobile stage with temperature-dependent development. Pupae develop into adult females, initiating the next generation. Under favourable conditions, one generation follows another without interruption until autumn. The final generation of the season either migrates or produces larvae that overwinter in a fully developed state. Each ontogenetic stage is associated with a distinct, stage-specific probability of mortality (refer to section 'Mortality').

Temperature-dependent development of pre-imaginal stages of *S. scripta* was modelled using development rates (inverse of development time, day^{-1}). Exploratory analyses indicated that the relationship between temperature and development rate differed among life stages. For egg and pupal stages, the development rate increases monotonically across the observed temperature range, with no evidence of a decline at high temperatures. Consequently, these stages will be modelled using linear degree-day models (Equation 7), expressed as:

$$r(T) = a \times (T - T_0) \quad \text{Equation 7}$$

where $r(T)$ is the development rate, T is temperature, a is the thermal sensitivity (slope), and T_0 is the lower developmental threshold. Linear degree-day models are appropriate when the development rate responds linearly to temperatures above a threshold and when experimental data do not include temperatures near the upper thermal limit. For these stages, the thermal constant (degree-days required to complete development) was calculated as the inverse of the slope

parameter (Table 4). Note that a linear degree-day model for pupae suggests a lower developmental threshold of 3.6 °C; however, confidence intervals are wide (-7.5 to 8.0 °C), indicating limited information on low-temperature constraints.

In contrast, larval development exhibited a unimodal response to temperature, with a clear maximum at intermediate temperatures and reduced development rates at higher temperatures. Because larval development is strongly influenced by aphid prey availability, model fitting for this stage was restricted to experiments conducted under ad libitum food conditions to minimise confounding effects of resource limitation. For larvae, a Gaussian thermal performance curve (Equation 8) was used to estimate the thermal optimum, as this model provides a stable description of unimodal thermal responses when data near upper thermal failure are limited.

$$r(T) = r_{max} \times \exp\left(-0.5 \times \left(\frac{(T - T_{opt})}{a}\right)^2\right) \quad \text{Equation 8}$$

where $r(T)$ is the development rate, T is temperature, r_{max} is maximum rate at optimum temperature, T_{opt} is the optimum temperature, and a scales the full curve width. The model parameters r_{max}, T_{opt}, and a were estimated by fitting the model to the empirical data, resulting in values of 0.102, 20.583, and 6.705, respectively.

Several alternative non-linear thermal performance models (including Logan, Lactin, Brière, and Sharpe–Schoolfield formulations) were evaluated for all stages. However, these models explicitly estimate upper critical thermal limits and require empirical observations of declining development rates at high temperatures to produce identifiable and biologically meaningful parameter estimates. Because such declines were not observed for egg and pupal stages, and were only weakly represented for larvae, parameters related to upper thermal limits were not statistically identifiable and resulted in unstable estimates. Consequently, these non-linear models were not retained for inference.

Upper critical thermal limits (CT_{max}) could therefore not be empirically estimated from the available data and were treated as calibration parameters in subsequent simulations. This modelling strategy ensures that parameter estimates are supported by the experimental data and avoids extrapolation beyond the observed temperature range (Fig. 9).

In addition to temperature, the growth of eggs will be influenced by the relative humidity. The linear degree-day relationship estimated for eggs is assumed to be valid for a relative humidity of approximately 65% (as eggs in the study of Nengel and Dreschel (1991) were kept in 60–70% relative humidity conditions).

Table 4. Stage-specific parameter for relationship describing temperature-related development in pre-imaginal stages of *Sphaerophoria scripta*. Functions fitted based on data in Table 1. * For the larval stage, a mean from values reported for 20 °C in the study of Polak (1980) was taken for model fitting. a – thermal sensitivity (slope), T_0 – lower developmental threshold, T_{opt} – thermal optimum, K – the thermal constant (degree-days). Confidence intervals (CI) were obtained by bootstrap resampling.

Developmental stage	Model type	a [day^{-1}×°C]	T_0 [°C)]	*95% CI* [°C]	K [degree-days]	*95% CI* [DD]	T_{opt} [°C]	R^2
Egg	Degree-day (linear)	0.0180	6.1	4.6–8.9	55.6	~50–65	–	0.93
Larva*	Gaussian	–	–	–	–	–	20.6	0.56
Pupa	Degree-day (linear)	0.0068	3.6	-7.5–8.0	146.2	~100–250	–	0.88

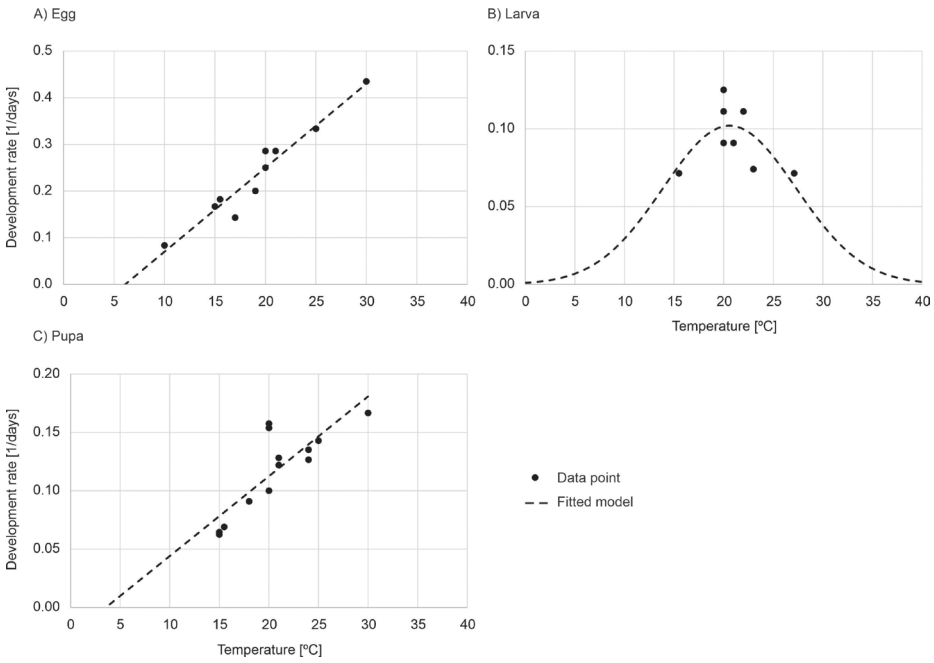

Figure 9. Temperature-related development rate for (**A**) egg, (**B**) larva and (**C**) pupa of *Sphaerophoria scripta*. Stage-specific parameters of fitted models are provided in Table 4. Input data are provided in Table 1.

This temperature–humidity combination was therefore used as a reference state. Under this assumption, egg development rate can be expressed as a temperature-driven baseline rate modified by a humidity-dependent correction term (Equation 9):

$$r(T, RH) = r(T) + \Delta_{RH}(RH, T) \quad \text{Equation 9}$$

where $r(T)$ is provided by Equation 7 with parameters from Table 4, and $\Delta_{RH}(RH,T)$ is the correction due to humidity, which is derived from the data on *S. rueppellii* from Amorós-Jiménez et al. (2012) study. The rate of change β_T in developmental time per 1% relative humidity increase changes with temperature (Equation 10):

$$\beta_T = 0.00105 \times T - 0.0708 \quad \text{Equation 10}$$

Centering the effect at 65% RH, the change in development rate due to relative humidity can be approximated as:

$$\Delta_H(RH, T) = -r \times (T)^2 \times \beta_T \times (RH - 65) \quad \text{Equation 11}$$

where $r(T)=a\times(T-T_0)$ is the temperature-driven linear degree-day rate. This formulation allows the combined effect of temperature and humidity on egg development to be consistently incorporated into the degree-day framework.

In addition to temperature, the growth of larvae will be influenced by the aphid biomass consumed/prey density. In extreme situations, first instar larvae will die after one consecutive day of starvation, while the longevity of second and third instar larvae under starvation conditions will be set to two and three

days, respectively. These assumptions are based on the starvation experiment conducted by Rojo et al. (1996) on *E. corollae*, as this species is comparable to *S. scripta* in terms of weight and larval developmental time.

We assume that the dependence on the number of aphids consumed (Fig. 1, Equation 2), which shows that larvae require more time to develop at low aphid densities, is valid for a temperature of 20 °C (as this was the mean temperature in the laboratory during Polak's experiment; Polak 1980). We therefore assume that the measured relationship between larval development and consumed aphid biomass is valid at 20 °C and extrapolate the proportional effect of prey limitation to other temperatures. If we then assume that in the experiment of Polak (1980), larvae were provided with late third instar or adult aphids, which weighed ~1.3 mg per individual (Putra and Yasuda 2006), then we can relate the development of larvae to aphid biomass consumed (B_c) instead of the number of aphids consumed (N_c).

To combine the prey limitation with the Gaussian temperature response, we define a multiplicative scaling factor $f(B_c)$ (Equation 12) relative to the ad libitum biomass B_c^{max}. We will define B_c^{max} based on the maximum number of aphids consumed in the experiment of Polak (1980) being N_c^{max} = 16.61 aphids/day (thus B_c^{max} = 21.59 mg/day).

$$f(B_c) = \frac{-0.237 \times \left(\frac{N_c^{max}}{1.3}\right)}{-0.237 \times \left(\frac{N_c}{1.3}\right)} = \frac{-0.1823 \times B_c^{max} + 15.361}{-0.1823 \times B_c + 15.361} \approx \frac{11.416}{-0.1823 \times B_c + 15.361} \quad \text{Equation 12}$$

The combined larval development rate as a function of temperature and consumed aphid biomass is then (Equation 13, Equation 14):

$$r(T, B_c) = r(T) \times f(B_c) \quad \text{Equation 13}$$

$$r(T, B_c) = 0.102 \times \exp\left(-0.5 \times \left(\frac{(T - 20.583)}{6.705}\right)^2\right) \times \frac{11.416}{15.361 - 0.1823 \times B_c} \quad \text{Equation 14}$$

At $B_c = B_c^{max}$, the factor $f(B_c)$ = 1 and $r(T, B_c) = r(T)$, recovering the Gaussian thermal performance curve fitted under ad libitum conditions. At lower aphid biomass, the development rate will decrease proportionally, reflecting prey limitations. This formulation allows larval development to be simulated as a function of both temperature and prey biomass, while explicitly acknowledging that the prey limitation effect was measured at 20 °C and extrapolated to other temperatures (Fig. 10).

To account for individual variability, a stochastic component will be incorporated, allowing developmental duration to fluctuate within ± 10% of the maximum developmental rate. The total larval developmental period will be partitioned into three instars, allocated as 25%, 25%, and 50% of the total duration, respectively, in accordance with Awadallah et al. (1980).

Given that *S. scripta* larvae are generalist predators, no preference for specific aphid species is assumed. Larvae are assumed to attack aphids opportunistically, while differences in realised biomass consumption among aphid species arise from nutritional quality rather than prey choice. Consequently, the number of aphids of various species present within each 10 × 10 m^2 landscape grid cell will

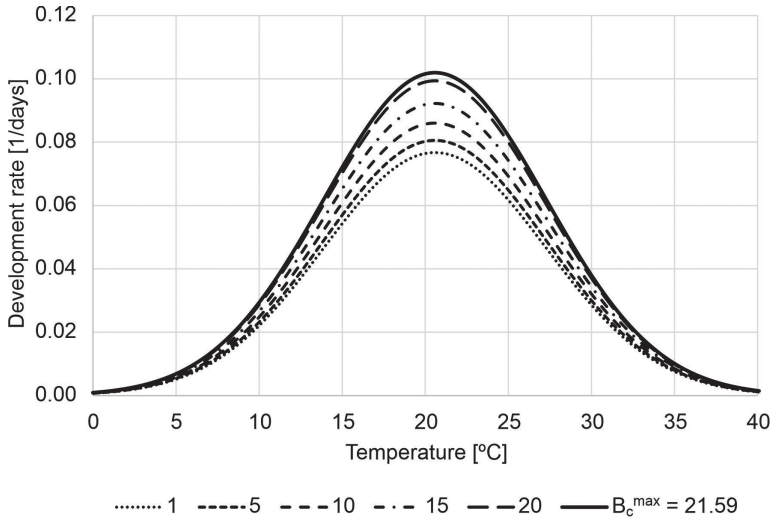

Figure 10. Dependence of *Sphaerophoria scripta* larval development rate on temperature and aphid biomass consumed daily. A family of Gaussian curves describing temperature-dependent development rate is shown for daily aphid biomass consumption [mg] ranging from 1 to B_c^{max} = 21.59 mg, corresponding to mean larval food intake under constant, non-limiting food conditions in the experiment of Polak (1980), after conversion from aphid counts to biomass.

be converted into total available aphid biomass, using species-specific biomass values provided in Table 5. Food utilisation by larvae will be modelled separately for each instar using a Holling Type II functional response (Equation 6), with parameter values for the second and third instars derived from Table 3. Based on the observed trend in Table 3, where both attack rate and handling time decrease by a factor of 1.5 between the second and third instars, we will assume a similar reduction factor between the first and second instars. Furthermore, since experimental data on aphid consumption by *S. scripta* larvae were obtained from individuals reared in isolation within Petri dishes, we introduce an instar-specific perception factor. This factor represents the proportion of aphids perceived by larvae at the 10 × 10 m^2 grid cell scale and will be treated as a calibrated parameter.

Using species-specific biomass values from Table 5, aphid counts consumed during larval development of various *Sphaerophoria* species (Fig. 4) can be converted into total aphid biomass consumed. Assuming a linear relationship between larval body mass and aphid biomass consumption, i.e., that consumption scales proportionally with larval weight, we can infer biomass consumption patterns across larval development for *S. scripta* based on data from other *Sphaerophoria* species, provided that larval weights are available. These patterns were informed by published studies on *S. scripta* (Wnuk and Fuchs 1977; Wojciechowicz-Żytko 2000), *S. rueppellii* (Amorós-Jiménez et al. 2012), and *S. sulphuripes* (Hopper et al. 2011). To enable cross-species comparison, aphid biomass consumption data for *S. rueppellii* and *S. sulphuripes* were rescaled to *S. scripta* equivalents using scaling factors of 1.6 and 1.3, respectively (Fig. 11). These factors were derived from the relative weights of third instar larvae; 17.7 mg for *S. scripta*, 11.0 mg for *S. rueppellii*, and 14.0 mg for *S. sulphuripes*. Patterns presented in Fig. 11 are comparable for all aphid species except *A. fabae*, showing total aphid biomass consumption at a level of 220–240 mg, when aphids are available ad libitum.

Table 5. Re-calculation of different aphid species to biomass (in mg). Scaling factors were calculated comparing the total number of aphids of different types consumed during *Sphaerophoria scripta* larval development when food was provided ad libitum (see Table 6), assuming (after Adams 1987) that under ad libitum food availability, larvae tend to consume a certain aphid biomass during their development regardless of the temperature experienced.

Aphid species	Aphid instar				Reference
	I	II	III early	III late	
Acyrthosiphon pisum	0.07	0.18	0.51	1.27	Putra and Yasuda (2006)
Aphis craccivora	0.03	0.07	0.19	0.48	
Aphis fabae	0.04	0.12	0.33	0.82	Recalculated from *A. pisum* using scaling factor from Table 6.
Myzus persicae	0.03	0.08	0.24	0.59	
Brevicoryne brassicae	0.03	0.09	0.24	0.60	
Hyalopterus. pruni	0.07	0.17	0.48	1.21	
Nasonovia ribisnigri	0.03	0.07	0.20	0.51	

Table 6. Summary of studies providing data on the total number of aphids consumed by *Sphaerophoria scripta* larvae during development. * To calculate the scaling factor, a base for *Acyrthosiphon pisum* was set to 154 aphids (mean value from those reported by Bańkowska 1978 and Polak 1980). ** Recalculated from *Sphaerophoria sulphuripes* based on comparison of larvae weights.

Aphid species	Total number of aphids consumed		Reference	Scaling factor (compared to *A. pisum*)*
	Range	Mean		
Acyrthosiphon pisum	129	129	Bańkowska (1978)	1.0 (base)
Acyrthosiphon pisum	167–192	179	Polak (1980)	
Aphis fabae	190–306	234	Wojciechowicz-Życzko (2000)	1.5
Myzus persicae	300–365	333	Krsteska (2008)	2.2
Brevicoryne brassicae		326	Wnuk and Fuchs (1977)	2.1
Hyalopterus pruni	96–226	162	Awadallah et al. (1980)	1.1
Nasonovia ribisnigri		385**	Hopper et al. (2011)	2.5

The empirical pattern of aphid biomass consumption across larval development, derived from Wnuk and Fuchs (1997) for *S. scripta*, was further used to fit a Gaussian model describing the relationship between consumption rate and the percentage of larval development (Fig. 12, Equation 15). In accordance with findings from Adams et al. (1987), this consumption pattern is assumed to be independent of the temperature experienced during development. We can further use Equation 5 to derive the pattern of larval fresh weight at pupation across percent of larval development if food is available at libitum. When aphid availability is restricted then larval weight will be scaled accordingly, resulting in population-level variability of larval weight at pupation depending on patterns of aphid density across the landscape.

$$B_{cr} = 36.38 \times \exp\left(\frac{-(D_{per} - 73.64)^2}{2 \times 15.08^2}\right) + 2.30 \qquad \text{Equation 15}$$

where B_{cr} is aphid biomass [mg] required daily based on the development percentage, and D_{per} is percentage of larval development. An offset of 2.30 is applied to account for non-zero aphid consumption of one day larvae. In the model, the developed percentage from the preceding day will be utilised to calculate the requisite aphid biomass for the current day.

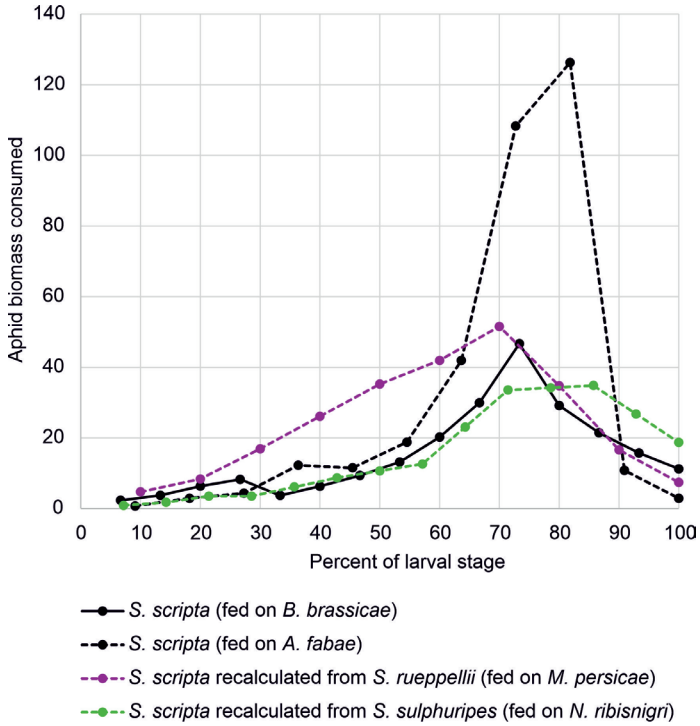

Figure 11. Aphid biomass consumption patterns for *Sphaerophoria scripta* generated based on published studies on *S. scripta* (Wnuk and Fuchs 1977; Wojciechowicz-Żytko 2000), *Sphaerophoria rueppellii* (Amorós-Jiménez et al. 2012), and *Sphaerophoria sulphuripes* (Hopper et al. 2011). Details of the re-calculation are provided in the text.

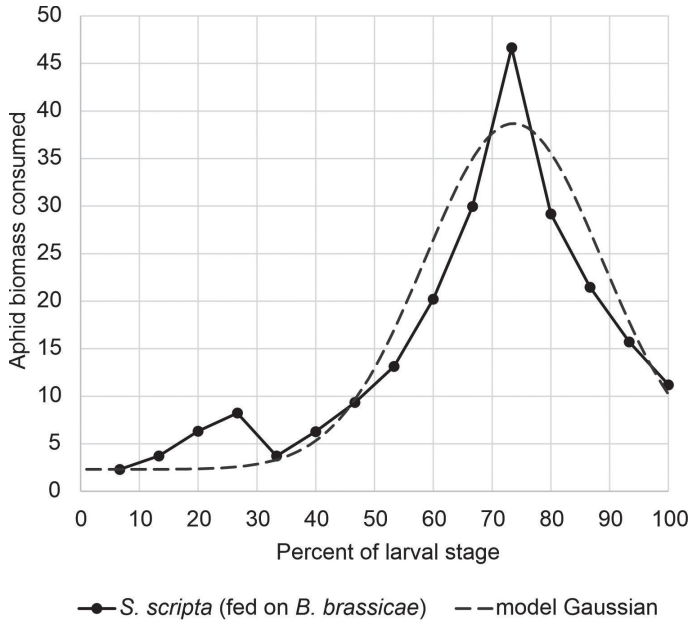

Figure 12. Gaussian model fitted to the aphid biomass consumption pattern for *Sphaerophoria scripta* generated based on Wnuk and Fuchs (1977).

Adults

Diurnal activity

S. scripta is strictly diurnal, with adults active only in daylight hours (Gilbert 1985a; D'Amen et al. 2013). Like most syrphid pollinators, it visits flowers during sunny periods and different hoverfly species tend to forage in sequence over the course of a day (D'Amen et al. 2013). According to Gilbert (1985a), *S. scripta* spends 67.4% of the time feeding, 21.7% resting, and 8.7% flying, with female hoverflies spending more time feeding than males. Diurnal activity can be explained in terms of the temporal variation in floral resources and physiological limits of the species, which determine when during the day the flower-pollinator interactions occur. During the morning, more flowers open and pollen and nectar are more abundant, while the amount of nectar secreted per flower tends to decrease towards evening (Pleasants and Chaplin 1983). Nocturnal activity is absent except during long-distance migration (see Dispersal section). In practice, *S. scripta* is most often observed flying and feeding in mid-morning to afternoon, when temperature and light levels favour flight. Its daytime activity leads to a succession of pollinator visits throughout the day (D'Amen et al. 2013), partitioning floral resources temporally.

There are no published studies measuring an intrinsic circadian clock in *Sphaerophoria* itself, but data from related hoverflies imply a robust endogenous rhythm. For example, *Eristalis* hoverflies remained continuously active throughout the 12-hour light phase of a 12L:12D cycle, and showed only minimal increases in night time activity when lights were briefly turned on; importantly, this did not shift their next-day activity peak (Thyselius and Nordström 2016). In that experiment, locomotor activity stayed consistent across the lifespan and was not altered by age or diet. These results indicate that hoverflies possess a self-sustained ~24-h rhythm largely driven by an internal clock. By analogy, *Sphaerophoria* species are presumed to have similar circadian control over their daytime activity, with very little spontaneous nocturnal activity in constant conditions. *Sphaerophoria* do respond to photoperiodic changes over longer timescales. For example, in the hoverfly *S. rueppellii*, switching from a short day (12L:12D) to a long day (14L:10D) significantly altered development and reproductive output (Orengo-Green et al. 2022). These experiments showed that longer light periods (and higher temperatures) accelerated gonad maturation and oviposition in *S. rueppellii*. Although this study focused on reproduction rather than direct activity, it demonstrates that seasonal daylength cues affect *Sphaerophoria* biology (Orengo-Green et al. 2022).

Ambient temperature plays a critical role in modulating the diurnal activity patterns of hoverflies. Field observations of syrphid species indicate that activity is predominantly concentrated within a moderate thermal range of approximately 15–25 °C, with minimal activity recorded below 8–10 °C, suggesting a lower thermal threshold near 10 °C (Gilbert 1985). Conversely, peak activity levels are typically observed at higher temperatures of 20 °C and higher. In a field study conducted by Bańkowska (1961), diurnal activity patterns of *Melanostoma mellinum* (Linnaeus, 1758), *S. scripta*, and *Chrysogaster viduata* (Walker, 1852) were examined under sunny, windless conditions with maximum daily temperatures reaching 28 °C. All three species exhibited a bimodal

activity pattern, characterised by an initial peak occurring prior to the daily thermal maximum and a secondary peak following the hottest part of the day (Fig. 13). Hoverflies remained inactive during early morning hours until ambient temperatures rose to approximately 16–17 °C, at which point activity gradually increased. However, when temperatures approached 27–28 °C, flight activity declined markedly, with individuals seeking shaded microhabitats to mitigate desiccation risk. For *S. scripta*, Bańkowska (1961) identified a thermal optimum in the range of 22–24 °C. These findings align with earlier studies on *Eristalis tenax* (Campan 1968, 1973), which also reported temperature-dependent shifts in diurnal activity rhythms. Specifically, *S. scripta* appears to transition from a unimodal to a bimodal activity pattern as ambient temperatures exceed approximately 25 °C, indicating a behavioural adaptation to thermal stress.

Flight activity in hoverflies is further influenced by weather conditions (Bańkowska 1964); rain and strong wind halt movement entirely, forcing flies to shelter under vegetation, and prolonged rain can result in significant mortality (Bańkowska 1961).

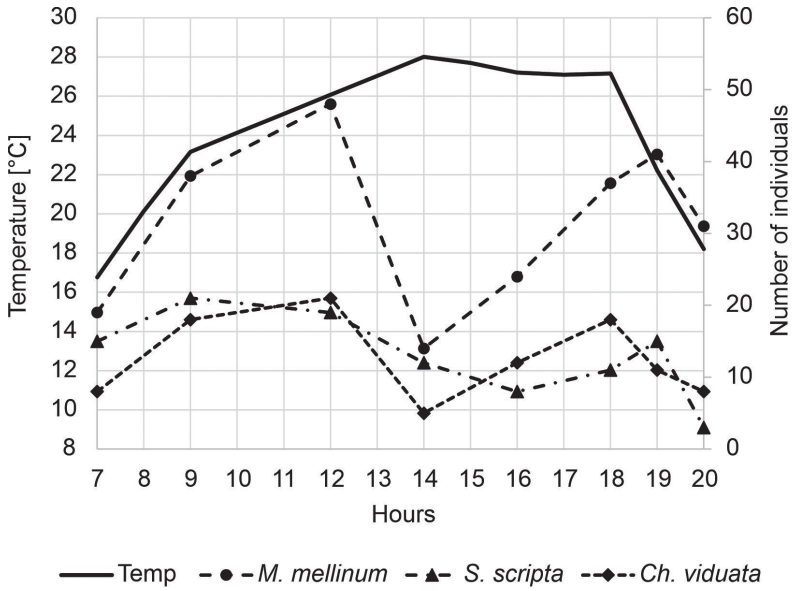

Figure 13. Diurnal activity of selected hoverflies, including *Sphaerophoria scripta*, observed in a meadow on a sunny, windless day in mid-May 1958 by Bańkowska (1961).

Planned implementation in the model

We will incorporate weather effects on hoverfly activity through an hourly weather assessment. Gilbert (1985a) provides the lowest temperatures at which different hoverfly species were seen, and temperatures at which more than 50% of flies seen were active. *Sphaerophoria scripta* was omitted, but data for a similar species, *E. balteatus*, indicates that 50% of the population becomes active when the hourly daytime temperature reaches 12 °C. Furthermore, if we assume that the minimum temperature at which *E. balteatus* was seen active, being 10 °C (Gilbert 1985a), is the minimum temperature for activity for *S. scripta*, and the temperature optimum is around 22–24 °C (after Bańkowska 1961), we can model the fraction of the

S. scripta population being active (F_{activ}) at specific hourly temperatures (T_h) during the day with linear functions (Equation 16).

$$F_{activ}(T_h) = \begin{cases} 10 \times T_h - 100, \text{if} \quad T_h \in [10, 20) \\ -10 \times T_h + 350, \text{if} \quad T_h \in (25, 35] \\ 100, \text{if} \quad T_h \in [20, 25] \\ 0, \text{if} \quad T_h < 10 \quad \text{or} \quad T_h > 35 \end{cases} \qquad \text{Equation 16}$$

With Equation 16, the temperature at which 50% of *S. scripta* population becomes active is 15 °C, thus higher than the one provided by *E. balteatus* by Gilbert (1985a). However, it corresponds well with observations of Bańkowska (1961), in which S. scripta started to be active in the morning when temperatures exceeded 16 °C.

This activity is further restricted to daylight hours only (Fig. 14), and to specific rainfall and wind conditions (maximum acceptable rainfall R_{max} and wind speed $W_{max,}$ which will be calibrated). Individuals that become active at a given temperature are selected randomly from the population, reflecting the influence of varying local microclimatic conditions. In addition, after Nangel and Drescher (1991), we will assume that the maximum temperature for activity is 35 °C (as the temperature in their greenhouse experiment varied between 15 and 35 °C).

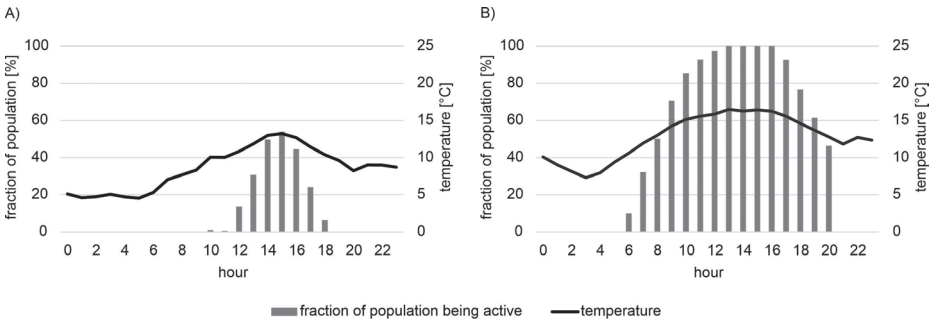

Figure 14. Fraction of hoverfly population being active on two selected days near Warsaw (Poland) in 2009, calculated based on Equation 16: (**A**) on March 28th, and (**B**) on June 1st. The activity is restricted by the temperature and photoperiod.

Knowing when a given hoverfly starts and ceases to be active during the day (based on temperature, rainfall and wind profiles during the day), we can calculate the total number of activity hours per day (h_{tot}). The total activity hours per day will then be divided into time spent on feeding (h_f), resting (h_r), and flying (h_m) based on proportions provided by Gilbert (1985a). These proportions were derived from instantaneous behavioural observations recorded at the moment of first sighting, with the aggregated data interpreted as representative of the species' energy budget. For the purposes of this study, we assume that 'feeding' time includes all local movements within the flower patch, whereas 'flying' time covers movements between flower patches. This would imply that there is a local movement distance threshold d_l (to be calibrated) above which a movement bout is considered to be long enough to allow a hoverfly reaching flight speed to find a new flower patch (see 'Dispersal' for details). We further assume, following Thyselius's (2022) study on *E. tenax*, that activity pattern of *S. scripta* does not change with hoverfly age.

Foraging

Gilbert (1985b) analysed dietary preferences (estimated feeding-time-budgets) of hoverflies based on field observations and categorised hoverflies according to the proportion of time spent feeding on nectar versus pollen. In this study, *S. scripta* was categorised as a mixed-feeder, feeding similarly frequently on pollen and nectar. Nectar serves as a main energy source, needed for flying, mate searching, and thermoregulation. Pollen, on the other hand, is required for oogenesis in females.

To date, detailed information on the energetics of *S. scripta* and other hoverfly species remains scarce. The most comprehensive analyses of foraging energetics are available for *E. tenax* (Sotavalta and Laulajainen 1961; Gilbert 1983). Gilbert (1983) quantified the net energy gain of *E. tenax* during continuous foraging on *Aster* flowers as rather low (0.01 W), while Sotavalta and Laulajainen (1961) reported an average flight energy consumption rate (C_f) of approximately 8.6×10^{-4} mg of sugar per second (after App et al. 2025). When converted using an energy density of 17 J/mg for sugar, this corresponds to an energy consumption rate of approximately 0.015 W during flight. Sotavalta and Laulajainen (1961) (after App et al. 2025) also described *E. tenax* energy consumption rate while resting (C_r) with the following equation (Equation 17):

$$C_r = k_r \times M^{0.73} \quad \text{Equation 17}$$

where k_r is the scaling parameter [J/(s × mg)] and M is the hoverfly mass [mg].

App et al. (2025) proposed to estimate C_r [W] based on the maximum possible daily energy gain E_{max} [J] (which provides an estimate of the upper energetic ceiling available to an organism for allocation to flight, maintenance, and reproduction within a 24-hour period) and the maximum starvation time $t_{starvationmax}$ [s] (the time an individual is able to survive without feeding) using the following equation (Equation 18):

$$C_r = E_{max} \times \frac{1}{t_{starvationmax}} \quad \text{Equation 18}$$

where

$$E_{max} = C_f \times t_{flightmax} + Fat\% \times M \times E_{fatdensity} \quad \text{Equation 19}$$

where $t_{flightmax}$ is maximum possible time of flight without feeding, *Fat%* is percentage of fat deposit related to mass, and $E_{fatdensity}$ is the energy density of fat (assumed to be 37 J/mg).

Given the lack of direct measurements for *S. scripta*, we can estimate its flight and resting energy consumption using an allometric scaling approach. This method applies a mass-dependent scaling law with an exponent $b < 1$, consistent with empirical findings in insect flight energetics. The scaling relationship is expressed as (Equation 20):

$$MR_{S.scripta} = MR_{E.tenax} \times \left(\frac{M_{S.scripta}}{M_{E.tenax}} \right)^b \quad \text{Equation 20}$$

where *MR* is metabolic rate, and *M* is body mass.

As data on the body mass of adult *S. scripta* are scarce (with only one study of Belyaev and Farisenkov (2019) mentioning the body mass of males to be 15.4 mg), we decided to estimate the body mass employing a general allometric scaling approach (Equation 21):

$$M = a \times L^b \quad \text{Equation 21}$$

where *L* is body length (mm), and *a* and *b* are scaling constants. Using *E. balteatus* as a reference species, with a reported mean body mass of 22.3 mg (App et al. 2025) and *S. scripta* body length range of 9–12 mm, we assumed an allometric exponent *b* = 3, a commonly accepted value for insects. The scaling constant *a* was derived from the average length and mass of *E. balteatus*, and subsequently applied to the length range of *S. scripta* (7–12 mm) to estimate its body mass. This yielded an estimated weight range of approximately 6.6 mg to 33.3 mg for *S. scripta*, with an average of 16.5 mg. This estimate aligns well with the body mass of *S. scripta* males reported by Belyaev and Farisenkov (2019).

Assuming an allometric scaling exponent of approximately 0.85 (which is typical for flying insects) in Equation 19, and using a mean body mass of 149 mg for *E. tenax* females (based on field-collected specimens, Nicholas et al. 2018), the predicted flight energy consumption rate C_f for *S. scripta*, with an estimated body mass range of 6.6–33.3 mg (with mean of 16.5 mg), falls between approximately 0.00106 W and 0.00419 W (with a mean of 0.00231 W).

To estimate the maximum possible daily energy gain (*Emax*) and, consequently, the resting energy consumption rate (C_r), the maximum starvation time ($t_{starvationmax}$) and the maximum possible time of flight without feeding ($t_{flightmax}$) need to be assessed for *S. scripta*. Arrington et al. (2007) reported $t_{starvationmax}$ of 7 days for *E. balteatus*, while Sotavalta and Laulajainen (1961) reported $t_{flightmax}$ of 7 hours for *E. tenax*. Energy reserves generally scale roughly linearly with body mass, assuming similar relative lipid and glycogen storage. Thus, to calculate the total time until reserves are depleted, we can apply a metabolic scaling relationship with an exponent of *b* = 0.75 (Equation 22):

$$t_{scaled} = t_{reference} \times \left(\frac{M_{scripta}}{M_{reference}} \right)^{0.75} \quad \text{Equation 22}$$

If we further assume that $t_{starvationmax}$ for *E. balteatus* is valid for a hoverfly of mean body mass of 22.3 mg (App et al. 2025), and $t_{flightmax}$ for *E. tenax* is valid for a hoverfly of mean body mass of 148 mg (Nicholas et al. 2018), then maximum starvation and flight times rescaled for *S. scripta* can be calculated as (assuming mean body mass for *S. scripta* of 16.5 mg):

- $t_{starvationmax}$ = 7 days × $(16.5/22.3)^{0.75}$ ≈ 5.6 days
- $t_{flightmax}$ = 7 h × $(16.5/148)^{0.75}$ ≈ 80 min

If we assume that body mass of *S. scripta* can vary between 6.6 and 33.3 mg (see above), we can estimate the maximum possible daily energy gain E_{max} of *S. scripta* as varying from 14.8 J to 96.1 J depending on body mass (with a mean of 43.3 J for a mean body mass of 16.5 mg), assuming fat deposit of 5% (the same as in *E. balteatus*, Hondelmann and Poehling 2007). Thus, the energy

consumption rate of *S. scripta* during resting C_r can be estimated to vary between 6.1 × 10^{-5} and 11.8 × 10^{-5} W (with a mean of 8.6 × 10^{-5} W for a mean body mass of 16.5 mg).

On the other hand, maximum nectar intake per foraging bout is constrained by the crop capacity. Gilbert (1983) provides average and maximum gut volumes for *E. tenax* of 5.8 and 17.2 µl, respectively. We can predict gut volume for *S. scripta* using an allometric re-scaling approach, applying a metabolic scaling relationship with an exponent *of b* = 0.75, based on the average gut volume (11.08 µl) and body mass (148 mg) reported for *E. tenax*. To simplify practical application, we then fitted a linear regression to the scaled values (Equation 23):

$$G_v(M) = 0.094 \times M + 0.537 \quad \text{Equation 23}$$

This equation gives us gut volumes for *S. scripta* between 1.08 and 3.62 µl across a body mass range of 6.6–33.3 mg (with a mean value of 2.14 µl for a hoverfly with a body mass of 16.5 mg).

The maximum gut fill can be translated into the maximum energy per gut fill $E_{max(Gv)}$ (reflecting the instantaneous energy intake capacity per feeding event), based on nectar sugar concentration (Equation 24):

$$E_{max(G_v)} = G_v \times \rho_{solution} \times C_{sugar} \times e_{sugar} \times \eta_{assim} \quad \text{Equation 24}$$

where $\rho_{solution}$ is the density of the sugar solution (depends on concentration, ~1.0–1.4 mg/ µl), C_{sugar} is the sugar mass fraction (e.g., sugar concentration of 30% = 0.30 g sugar per g solution), e_{sugar} is energy content of sugar (assumed to be 17 J/mg), and η_{assim} is the assimilation efficiency (if all of the energy ingested is absorbed, then η_{assim} = 1).

Assuming a mean gut volume of 2.14 µl (for *S. scripta* with a mean body mass of 16.5 mg), the maximum energy per gut fill $E_{max(Gv)}$, calculated for a 50% sugar concentration ($\rho_{solution}$ = ~ 1.23 mg/µl) and an assimilation efficiency of 1, is estimated at 22.4 J.

The observed difference between the maximum possible daily energy gain E_{max} and the maximum energy per gut fill $E_{max(Gv)}$ is expected because E_{max} integrates longer-term energy reserves (fat), whereas $E_{max(Gv)}$ reflects only short-term carbohydrate intake. For energy-budget modelling, this distinction is crucial: $E_{max(Gv)}$ constrains the instantaneous rate of energy acquisition and thus short-term activity patterns, while E_{max} defines the maximum daily energy allocation potential, including contributions from stored reserves. Comparing these two metrics allows estimation of gut-filling frequency necessary to sustain activity (E_{max} / $E_{max(Gv)}$ ≈ 2 gut fills/day in case of *S. scripta* of 16.5 mg body mass feeding on nectar with 50% sugar concentration) and provides a framework for modelling trade-offs between feeding, flight, and reproductive investment under varying ecological conditions.

Food requirements

Female *Sphaerophoria* require pollen to mature their ovaries. As in other syrphids, newly emerged females are not sexually mature until they have fed on pollen (Amorós-Jiménez et al. 2014; Orengo-Green et al. 2022). In *S. scripta*, for

example, laboratory studies found that females given sugar plus pollen mated and laid hundreds of eggs, whereas females on sugar alone laid no eggs (Nengel and Drescher 1991). Pollen nutrition also greatly extended adult longevity (e.g. mean female lifespan ~31 days with pollen vs ~9.5 days without, Nengel and Drescher 1991). Male *Sphaerophoria* mature their reproductive organs more rapidly. In *S. rueppellii*, one-day-old males at 25 °C were able to mate (though initial matings were infertile) by day 2, and produced fertile matings by day 3, while at 20 °C, full maturation took ~5–6 days (Orengo-Green et al. 2022). These results imply that males rely mainly on carbohydrate (nectar) reserves to fuel rapid maturation and mating activity.

To our knowledge, detailed information on the nectar preferences of *S. scripta*, particularly regarding sugar concentration preferences, is lacking. Gilbert (1981) investigated the sucking and ingestion rates of sugar solutions ranging from 10% to 67% in various hoverfly species, including two aphidophagous ones, *Syrphus ribesii* (Linnaeus, 1758) and *Scaeva pyrastri* (Linnaeus, 1758). For both species, sucking rates are at the level of around 0.3–0.4 µl per second for sucrose concentrations between 10 and 50%, and then drops with further increase of sucrose concentration (Fig. 15). Sugar ingestion in *S. ribesii*, on the other hand, indicate an optimal energy intake rate at approximately 50% sugar concentration (Fig. 15).

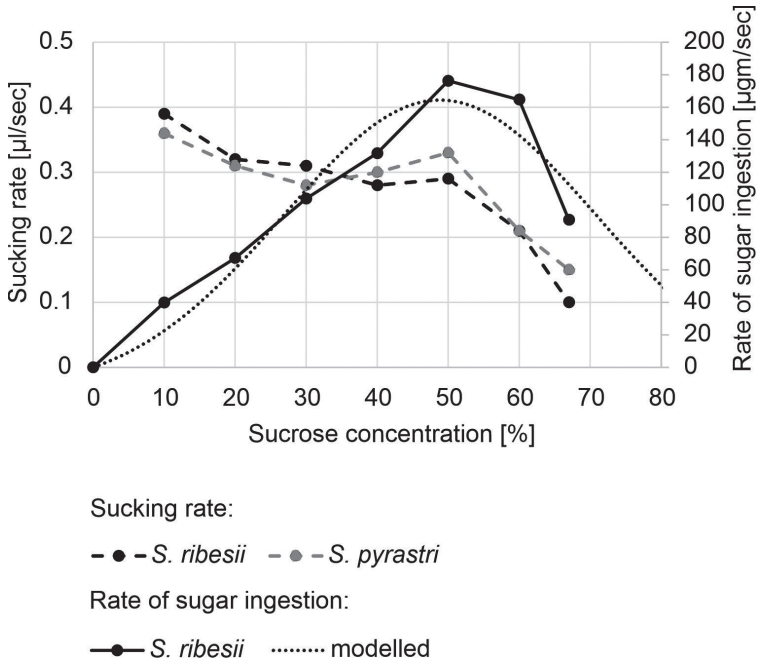

Figure 15. The rate of sucking and sugar ingestion in aphidophagous hoverflies. The rate of sugar ingestion for *Syrphus ribesii* was modelled with the constrained Gaussian model (Equation 27). Based on Gilbert (1981).

Food preferences

Adults are flower-visiting generalists (Madureira et al. 2024). They forage on a wide variety of blossoms (especially open, bowl-shaped flowers), feeding on both nectar and pollen (Klecka et al. 2018; Villa et al. 2021) (Table 7). In agricultural and urban habitats they are attracted to flowering plants (e.g. Asteraceae, Apiaceae) and

even ornamental gardens (Wojciechowicz-Żytko and Dobińska-Graczyk 2025). For example, surveys in olive groves found *S. scripta* present wherever groundcover plants like daisies and plantains were in bloom (Madureira et al. 2024). In green spaces and orchards, adults locate flowering shrubs and herb layers and use these as sources of carbohydrates and protein. This floral visitation also makes *S. scripta* an important pollinator of various plants (Klecka et al. 2018).

Experiments with floral resources have shown that hoverfly flower choice is influenced by flower colour, shape, and abundance. A study on *S. rueppellii* by Gasol et al. (2019) demonstrated that while mating status affected overall foraging activity, with mated females moving less than virgins, it did not alter floral preferences. Both virgin and mated adults consistently favoured flat, circular, white or yellow flowers, indicating that visual floral traits are key determinants of foraging behaviour regardless of reproductive condition. In addition, adults of *Sphaerophoria* and other aphidophagous hoverflies possess a relatively short, sponging proboscis that is structurally adapted for nectar and pollen uptake from open flowers with accessible rewards, rather than from flowers with long corolla tubes (Gilbert 1981). This morphological trait underlies their preference for shallow-flowered taxa such as Asteraceae and Apiaceae, further constraining the set of floral resources effectively used by these species.

Planned implementation in the model

Since foraging movements are intertwined with reproduction and dispersal, we treat them under the heading 'Dispersal' below.

The amount of pollen, nectar, and sucrose concentration available to *S. scripta* from each habitat patch in the landscape per day will be modelled in ALMaSS using the floral resource models. The floral resource models have been developed within the B-GOOD Horizon 2020 project (Ziółkowska et al., unpublished). The framework integrates data on the amount of pollen, nectar, and sugars produced by a single flower/inflorescence of a given plant species with information on flower/inflorescence abundance (i.e. density of flowers/inflorescences per unit area), flowering phenology, plant composition of the habitat, and habitat composition and configuration within the landscape. This approach enables prediction of the spatio-temporal availability of floral resources across different habitat types and landscapes.

The amount of pollen and nectar available to *S. scripta* in the landscape will be limited to those plants visited only by *S. scripta*. Such a list of plants will be available based on analysis of plant-pollinator interactions. Table 7 presents a preliminary list of plants visited by *S. scripta*, which could be further revised by additional literature searches and expert knowledge.

When foraging, a hoverfly will perceive the landscape as consisting of patches of different landscape elements. All vegetated patches are attributed daily with the amount of floral resources provided by different plants composing those patches. The local perception range for resources is assumed as 150–200 m, similar to the perception range for *E. balteatus* provided by Arrignon et al. (2007) based on field observations. Thus, a hoverfly in a given location will only sense resources within this perception range. As individual flower positions are not modelled, floral resource availability in a given location will be assessed at the patch level, scaled by the area within the perceptual range.

Table 7. Example of some plant species visited by *Sphaerophoria scripta* (Klecka et al. 2018; Villa et al. 2021; Capela et al. 2025).

Species	Genus	Family
Achillea millefolium	*Achillea*	Asteraceae
Aegopodium podagraria	*Aegopodium*	Apiaceae
Agrimonia eupatoria	*Agrimonia*	Rosaceae
Allium scorodoprasum	*Allium*	Amaryllidaceae
Anethum graveolens	*Anethum*	Apiaceae
Anthemis arvensis	*Anthemis*	Asteraceae
Anthericum ramosum	*Anthericum*	Asparagaceae
Anthriscus sylvestris	*Anthriscus*	Apiaceae
Aphanes spp.	*Aphanes*	Rosaceae
Aristolochia spp.	*Aristolochia*	Aristolochiaceae
Asphodelus spp.	*Asphodelus*	Xanthorrhoeaceae
Aster spp.	*Aster*	Asteraceae
Borago officinalis	*Borago*	Boraginaceae
Brassicaceae spp.		Brassicaceae
Calendula officinalis	*Calendula*	Asteraceae
Calluna vulgaris	*Calluna*	Ericaceae
Calystegia spp.	*Calystegia*	Convolvulaceae
Campanula patula	*Campanula*	Campanulaceae
Campanula spp.	*Campanula*	Campanulaceae
Cardueae spp.	Cardueae	Asteraceae
Carum carvi	*Carum*	Apiaceae
Centaurea cyanus	*Centaurea*	Asteraceae
Centaurea jacea	*Centaurea*	Asteraceae
Centaurea nigra	*Centaurea*	Asteraceae
Centaurea scabiosa	*Centaurea*	Asteraceae
Centaurium spp.	*Centaurium*	Gentianaceae
Centranthus spp.	*Centranthus*	Valerianaceae
Cichorioideae spp.	Cichorioideae	Asteraceae
Cirsium arvense	*Cirsium*	Asteraceae
Cistus monspeliensis	*Cistus*	Cistaceae
Clinopodium vulgare	*Clinopodium*	Lamiaceae
Convolvulus arvensis	*Convolvulus*	Convolvulaceae
Coronilla varia	*Coronilla*	Fabaceae
Corrigiola telephiifolia	*Corrigiola*	Caryophyllaceae
Crassula	*Crassula*	Crassulaceae
Crepis capillaris	*Crepis*	Asteraceae
Daphne gnidium	*Daphne*	Thymelaeaceae
Daucus carota	*Daucus*	Apiaceae
Dracocephalum moldavica	*Dracocephalum*	Lamiaceae
Echium spp.	*Echium*	Boraginaceae
Echium vulgare	*Echium*	Boraginaceae
Epilobium hirsutum	*Epilobium*	Onagraceae
Erica cinerea	*Erica*	Ericaceae
Erica tetralix	*Erica*	Ericaceae
Erigeron annus	*Erigeron*	Asteraceae

Species	Genus	Family
Eucalyptus spp.	*Eucalyptus*	Myrtaceae
Euphorbia spp.	*Euphorbia*	Euphorbiaceae
Foeniculum vulgare	*Foeniculum*	Apiaceae
Fumaria spp.	*Fumaria*	Papaveraceae
Galium mollugo	*Galium*	Rubiaceae
Galium verum	*Galium*	Rubiaceae
Gentiana cruciata	*Gentiana*	Gentianaceae
Geranium spp.	*Geranium*	Geraniaceae
Hedera helix	*Helix*	Araliaceae
Helianthemum grandiflorum	*Helianthemum*	Cistaceae
Helianthemum nummularium	*Helianthemum*	Cistaceae
Heracleum sphondylium	*Heracleum*	Apiaceae
Hypericum perforatum	*Hypericum*	Hypericaceae
Hypericum spp.	*Hypericum*	Hypericaceae
Hypochaeris radicata	*Hypochaeris*	Asteraceae
Inula salicina	*Inula*	Asteraceae
Jasione	*Jasione*	Campanulaceae
Juniperus	*Juniperus*	Cupressaceae
Knautia arvensis	*Knautia*	Dipsacaceae
Lactuca serriola	*Lactuca*	Asteraceae
Lamium album	*Lamium*	Lamiaceae
Lavandula angustifolia	*Lavandula*	Lamiaceae
Leontodon autumnalis	*Leontodon*	Asteraceae
Leontodon hispidus	*Leontodon*	Asteraceae
Leontodon saxatilis	*Leontodon*	Asteraceae
Leucanthemum vulgare	*Leucanthemum*	Asteraceae
Linum catharticum	*Linum*	Linaceae
Lonicera periclymenum	*Lonicera*	Caprifoliaceae
Lotus corniculatus	*Lotus*	Fabaceae
Lycopus europaeus	*Lycopus*	Lamiaceae
Malva moschata	*Malva*	Malvaceae
Malva sylvestris	*Malva*	Malvaceae
Medicago lupulina	*Medicago*	Fabaceae
Melampyrum nemorosum	*Melampyrum*	Orobanchaceae
Mentha spp.	*Mentha*	Lamiaceae
Myosotis arvensis	*Myosotis*	Boraginaceae
Olea europaea	*Olea*	Oleaceae
Origanum vulgare	*Origanum*	Lamiaceae
Papaver rhoeas	*Papaver*	Papaveraceae
Pastinaca sativa	*Pastinaca*	Apiaceae
Pilosella officinarum	*Pilosella*	Asteraceae
Pimpinella saxifraga	*Pimpinella*	Apiaceae
Pinus pinaster	*Pinus*	Pinaceae
Plantago lanceolata	*Plantago*	Plantaginaceae
Plantago suma	*Plantago*	Plantaginaceae
Poaceae spp.	Poaceae	Poaceae
Polygonum aviculare	*Polygonum*	Polygonaceae
Potentilla argentea	*Potentilla*	Rosaceae

Species	Genus	Family
Potentilla erecta	*Potentilla*	Rosaceae
Potentilla reptans	*Potentilla*	Rosaceae
Quercus spp.	*Quercus*	Fagaceae
Ranunculus acris	*Ranunculus*	Ranunculaceae
Ranunculus bulbosus	*Ranunculus*	Ranunculaceae
Ranunculus repens	*Ranunculus*	Ranunculaceae
Raphanus raphanistrum	*Raphanus*	Brassicaceae
Rhinanthus	*Rhinanthus*	Orobanchaceae
Rhinanthus major	*Rhinanthus*	Orobanchaceae
Rubus spp.	*Rubus*	Rosaceae
Rubus spp.	*Rubus*	Rosaceae
Rumex spp.	*Rumex*	Polygonaceae
Salvia verticillata	*Salvia*	Lamiaceae
Sanguisorba spp.	*Sanguisorba*	Rosaceae
Saxifraga aizoides	*Saxifraga*	Saxifragaceae
Senecio jacobaea	*Senecio*	Asteraceae
Sinapis arvensis	*Sinapis*	Brassicaceae
Sonchus arvensis	*Sonchus*	Asteraceae
Stellaria graminea	*Stellaria*	Caryophyllaceae
Succisa pratensis	*Succisa*	Caprifoliaceae
Teucrium chamaedrys	*Teucrium*	Lamiaceae
Thymus pulegioides	*Thymus*	Lamiaceae
Thymus vulgaris	*Thymus*	Lamiaceae
Tribulus spp.	*Tribulus*	Zygophyllaceae
Trifolium campestre	*Trifolium*	Fabaceae
Trifolium medium	*Trifolium*	Fabaceae
Trifolium pratense	*Trifolium*	Fabaceae
Ulex gallii	*Ulex*	Fabaceae
Ulex minor	*Ulex*	Fabaceae
Verbascum chaixii	*Verbascum*	Scrophulariaceae
Veronica teucrium	*Veronica*	Plantaginaceae
Vicia sativa	*Vicia*	Fabaceae
Viola arvensis	*Viola*	Violaceae

In addition, the daily pollen attractiveness P_h of a given habitat patch *h* will be calculated by multiplying the amount of pollen resources *P* available to *S. scripta* from each plant *p* in the patch on day *d* by the plant's pollen preference score p_s (Equation 25). The amount of pollen resources produced by plant *p* on day *d* in habitat patch *h* results from the daily pollen production of the plant, the proportion of the plant in the habitat patch and the area of the habitat patch. The pollen preference score p_s of a plant is a pollinator-specific measure defined on a semi-quantitative scale from 0 to 3. It is being developed within the Better-B Horizon Europe project and is intended to be linked to the floral resource models of the ALMaSS modelling framework. The pollen preference score was originally developed for bees and is based on documented plant-pollinator interactions, along with the nutritional and chemical properties of pollen, including the protein-to-lipid (P:L) and potassium-to-sodium (K:Na) ratios. While pollen nutritional traits are known to influence pollen selection in bees, no empirical

studies are currently available that directly link pollen nutritional composition to pollen preference in hoverflies. Consequently, for *S. scripta*, the pollen preference score is presently derived solely from documented plant-hoverfly interaction data, reflecting whether a given plant species is known to be used as a pollen source. The integration of additional modifiers relevant to hoverflies (e.g. flower colour, floral morphology, or pollen accessibility) is under development and will be incorporated into future model versions once sufficient empirical evidence becomes available.

$$P_h = \sum_p P_{p,d} \times p_s \quad \text{Equation 25}$$

The daily pollen attractiveness P_h of a given habitat patch *h* in a landscape will be further scaled by the nectar attractiveness N_h to obtain the daily food attractiveness F_h of the patch (Equation 26). Scalars c_p and c_n, for the pollen and nectar attractiveness components, will be calibrated parameters.

$$F_h = \left(c_p \times P_{h)} \times (c_n \times N_h\right) \quad \text{Equation 26}$$

The daily nectar attractiveness of a given habitat patch N_h will combine the total amount of nectar produced by each plant species with the relative preference for sucrose concentration, modelled with constrained Gaussian model on observed ingestion rates of *S. ribesii*, a closely related aphidophagous species in terms of preferred habitats (meadows, grasslands, crop fields) and egg-laying preferences (herbaceous plants, crops), across a gradient of sucrose concentrations (Equation 27):

$$N_h = \sum_{i=1}^{n} N_i \times w\left(S_i\right) \quad \text{Equation 27}$$

where N_i is the total nectar amount (mg/day) produced by plant species *i* in a patch, S_i is sucrose concentration (%) of nectar from species *i*, and $w(S_i)$ is weight assigned to sucrose concentration, modelled by the constrained Gaussian ingestion function $I(S_i)$ (Equation 28):

$$w\left(S_i\right) = \frac{I\left(S_i\right) - I(S_i)_{min}}{I(S_i)_{max} - I(S_i)_{min}} \quad \text{Equation 28}$$

$$I\left(S_i\right) = a \times \left[exp\left(-\frac{\left(S_i - b\right)^2}{2 \times c^2}\right) - exp\left(-\frac{(0-b)^2}{2 \times c^2}\right)\right] \quad \text{Equation 29}$$

Parameters *a* = 179.73, *b* = 48.84 and *c* = 21.98 for Equation 29 were derived from the best-fit ingestion model (R^2 = 0.93) to data on *S. ribesii* from Gilbert (1981) (Fig. 15).

The daily food attractiveness F_h of a patch will be used to drive the long-distance movement between floral patches (see section 'Dispersal' for details).

Furthermore, multiple feeding bouts (i.e., discrete foraging events during which the hoverfly fills its gut to its maximum capacity G_v, after which it leaves the flower patch or reduces intake until the gut is sufficiently emptied to resume feeding) need to be considered during the day. In reality, hoverflies will combine foraging and reproduction and integrate these activities together.

From the modelling perspective, this integration is not easy, so we suggest viewing this as maximum of N_f feeding bouts where the maximum intake of nectar is limited by the gut volume (Equation 23). During a foraging bout, the hoverfly will attempt to fill its gut to maximum capacity. Each feeding bout can be then translated to the maximum energy per gut fill $E_{max(Gv)}$, depending on sugar concentration in nectar (Equation 24). The actual energy gain during a feeding bout will be, however, a difference between potential energy gain per bout and the energy loss per bout associated with local foraging movements and flower handling (see 'Dispersal' section for energy budget details).

Number of feeding bouts actually performed during a day (N_{real}) will be restricted by a time spent on each foraging bout t_s^{bout} (which includes time spent in local foraging flights within the patch and total flower handling time in the bout) and time available for foraging per day (being a fraction of time available for all activities daily; see 'Diurnal activity' section for details). The time spent within a patch will be estimated based on the mean foraging speed (see 'Dispersal' section), the mean distance between floral units of plant species accepted by *S. scripta* within the patch, and the number of floral units required to obtain the assumed nectar intake (i.e., to fill the gut). The nectar reward per floral unit will be represented by the mean nectar amount per flower unit across all plant species accepted by *S. scripta* in the patch. This generalisation is necessary because the model does not operate at the level of individual plants; thus, the specific sequence of floral units visited by an individual cannot be determined.

The daily activity of *S. scripta* will be simulated as a state-dependent sequence of foraging, dispersal, reproduction, and resting, constrained by both time budgets and energetic state (see 'Dispersal' section for details. Foraging will be initiated whenever the current short-term energy level $E_{current}$ falls below a predefined threshold $E_{forage_threshold}$, which will be calibrated as a model parameter.

Reproduction and oviposition

S. scripta is a highly multivoltine species (Bańkowska 1961). Laboratory and field studies have demonstrated that *S. scripta* can complete a generation in approximately 16 days under optimum conditions (Krsteska 2008; Rader et al. 2020), enabling several generations to be produced in a single year. Males reach sexual maturity a few days after adult emergence. For example, males of *S. rueppellii* kept at 25 °C were capable of copulating by day 2 and could fertilise eggs by day 3. In contrast, those kept at 20 °C required around 6 days to achieve successful fertilisation (Orengo-Green et al. 2022). Information on the exact number of mating events is lacking for *Sphaerophoria* species. Nengel and Drescher (1991) reported oviposition under greenhouse conditions, but did not systematically record the number of matings per female. They only mentioned that multiple mating is possible and that the first mating occurs two to three days after the female emerges. Multiple mating is common in Syrphinae (Rojo et al. 2003). For example, Hondelmann and Poehling (2007) reported two to five mating events for *E. balteatus* under laboratory conditions. Polyandry appears to be possible but not necessary, as females can store sperm and lay fertile eggs from a single mating for most of their reproductive lifespan (Rojo et al. 2003). Nengel and Drescher (1991) reported that *S. scripta* mating occurs on

plants or near prey sources. While there are no direct measurements of mating duration for *S. scripta*, general observations of Syrphinae suggest that copulation times are short (~1–5 minutes), similar to those of *E. balteatus* (Branquart and Hemptinne 2000; Hondelmann and Poehling 2007).

The selection of oviposition sites by aphidophagous hoverflies involves the complex integration of visual, auditory, olfactory, and gustatory stimuli (Almohamad et al. 2009; Amorós-Jiménez et al. 2015). However, volatile compounds released by aphids and their host plants can elicit oviposition behaviour in females independently, even in the absence of other sensory inputs (Amorós-Jiménez et al. 2015). Almohamad et al. (2009) described the oviposition site selection process in aphidophagous hoverflies as comprising four stages involving long-range visual cues (e.g. plant patch size and colour), short-range cues for aphid detection, olfactory processing of aphid and plant volatiles, and gustatory cues such as honeydew to confirm the presence of prey.

S. scripta females lay their eggs individually on leaves or stems close to aphid colonies. This trait minimises larval competition and facilitates access to prey (Chandler 1968; Rojo et al. 2003). Chandler's (1968) observations demonstrated that *S. scripta* females can distinguish between infested and uninfested plants and prefer sites with dense aphid populations. Greenhouse trials by Nengel and Drechsler (1991) confirmed that oviposition is concentrated in canopy regions where aphids are abundant. As related species, such as *S. rueppellii*, exhibit similar prey-dependent oviposition patterns (Amorós-Jiménez et al. 2015; Orengo-Green et al. 2022), this behaviour appears to be conserved within the genus, emphasising the significance of prey availability in oviposition site selection. However, the exact relationship between aphid colony size and the number of eggs laid is unknown for this species. In his field observations of hoverflies ovipositing eggs on Brussels sprouts infested with *B. brassicae*, Chandler (1968) found that *Platycheirus peltatus* (Meigen, 1822) preferred smaller aggregates, *Platycheirus scutatus* (Meigen, 1822) preferred aggregates containing twenty-one to fifty aphids, and *S. balteatus* and *Eupeodes* (*Syrphus*) *luniger* (Meigen, 1822) preferred larger aphid aggregates. *Sphaerophoria scripta* showed no evident preference. Wnuk and Starmach's (1977) observations showed that the colony size of *A. fabae* determined oviposition site selection in *E. balteatus*, *E. corollae*, and *Syrphus vitripennis* (Meigen, 1822). In general, these species selected plants that were more heavily infested with aphids (Fig. 16), mainly favouring small and large colonies. No variation in the number of eggs laid was observed with medium-sized colonies.

According to Nengel and Drescher (1991), under optimal environmental conditions (i.e. no shortage of pollen or aphid-infested plants for oviposition and temperatures ranging from 15 to 35 °C in climatically controlled greenhouse cabins), the female *S. scripta* begins oviposition 5–6 days after adult emergence and lays from 228 to 551 (with an average of 365) eggs during its lifetime. Conversely, when pollen was not provided, no eggs were laid, confirming that pollen is essential for egg maturation in hoverflies (Gilbert 2015). Pollen availability also impacted female longevity. Females with ad libitum access to pollen lived for an average of 31.3 days, while those with no access to pollen lived for an average of only 9.5 days. However, Stürken (1964) reported that a lack of pollen had no impact on the lifespan of *E. corollae*, suggesting that lifespan depends mostly on carbohydrate supply.

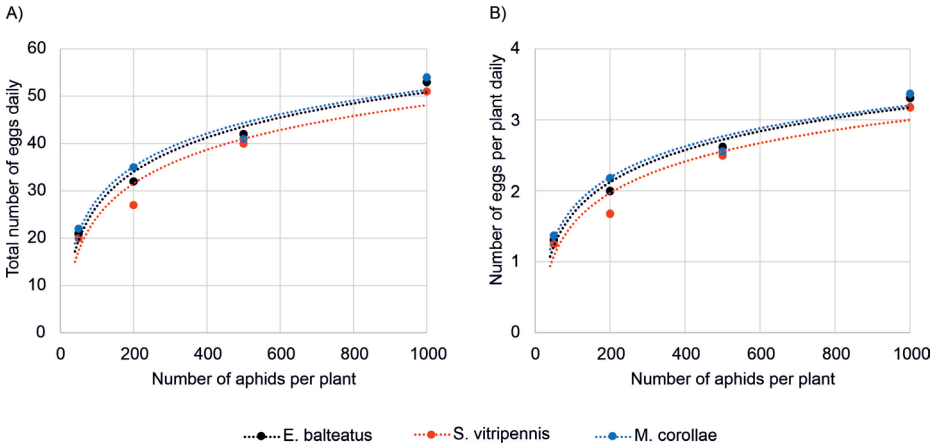

Figure 16. The effect of prey density (number per plant) on eggs oviposited per *Episyrphus balteatus*, *Syrphus vitripennis* and *Eupeodes* (*Metasyrphus*) *corollae* females per day (**A**) or daily per plant (**B**). Based on Wnuk and Starmach (1977) controlled field experiment. The relationships between prey density and number of eggs laid daily or daily per plant follow a similar logarithmic function y = a × lnx +b with parameters provided in Table 8.

Table 8. Parameters for logarithmic functions describing the relationship between aphid colony size (number of aphids per plant) and total number of eggs laid or number of eggs laid per plant per day. Based on Wnuk and Starmach (1977), see Fig. 16.

Species	Total number of eggs daily		Number of eggs per plant per day		R^2
	a	b	a	b	
E. corollae	10.081	-18.287	0.630	-1.150	0.97
S. vitripennis	10.284	-22.915	0.641	-1.427	0.93
E. balteatus	10.446	-21.322	0.652	-1.333	0.98

As females can lay eggs right up until the day they die (Nengel and Drescher 1991), the oviposition period for *S. scripta* females lasts around 25–26 days under favourable environmental conditions. Therefore, we can conclude that *S. scripta* can lay 9–22 eggs daily (with a mean of around 14 eggs). This is a slightly higher daily egg-laying rate than that of *S. rueppellii*, which can lay from two to 15 eggs per day depending on environmental conditions, with a higher rate under warmer conditions and a longer photoperiod (Orengo-Green et al. 2022). According to Almohamad et al. (2009), some hoverfly species can retain mature eggs when aphids are absent; this behaviour is influenced by egg load and age. For instance, *E. balteatus* and *S. ribesii* females do not waste eggs in the absence of hosts and can retain them for weeks. Although there is little specific data on egg retention in *S. scripta*, its ability to lay eggs on aphid-infested plants and its multivoltine life cycle suggest that it may possess similar physiological adaptations. This trait would be advantageous in fluctuating environments, as it would allow females to delay oviposition until suitable conditions arise.

Aphid density is a key driver of oviposition behaviour in aphid-eating hoverflies. In general, females lay more eggs when aphid colonies are abundant (Fig. 16) (Wnuk and Starmach 1977). Reproductive output is also affected by temperature. While no direct studies are available for *S. scripta*, a study by Orengo-Green et al. (2022) showed that the total number of eggs laid by *S. rueppellii* females was higher when they were reared at a constant temperature of 25 °C than at 20 °C, particularly under a longer photoperiod (14L:10D vs. 12L:12D).

Conversely, females reared at a lower temperature lived longer, particularly under a longer photoperiod, and experienced a peak in oviposition earlier than those reared at a higher temperature. Bellefeville et al. (2019) investigated the impact of temperature on the number of eggs laid by the Silverfly *Leucopis glyphinivora* (Tanasijtshuk, 1958) and the American Hoverfly *Eupeodes americanus* (Wiedemann, 1830) when reared under constant laboratory conditions of 12, 15, and 18 °C. For the American Hoverfly, the mean number of eggs laid increased from around 30 at 12 °C to over 100 at 18 °C, suggesting a peak in oviposition at or above this temperature. For the Silverfly, the number of eggs increased between 12 and 15 °C and then decreased between 15 and 18 °C.

Oviposition behaviour and daily oviposition rate changes with female age. Almohamad et al. (2009) and Sadeghi et al. (2000) note that younger females are more selective and lay eggs closer to aphid colonies, while older females become less discriminating and may lay eggs even on uninfested plants. Females tend to lay more eggs early in life, likely to maximize reproductive success before senescence reduces fecundity. The peak of oviposition in *S. rueppellii* occurred around 10–12 days post adult-emergence, i.e. around one third of the total adult lifetime. In a laboratory experiment by Branquart and Hemptinne (2000), daily fecundity of *E. balteatus* also peaked around one third of the total adult lifetime.

Female fecundity may also be connected to the diet during their larval stage. In *S. rueppellii*, individuals that feed on *M. persicae* and *A. nerii* had significantly less eggs (25–32) compared to those on a diet on *R. padi* (50) (Amorós-Jiménez and Marcos-Garcia 2020). Not only is egg production connected to diet, but in the same publication, the authors also showed that *Sphaerophoria* fertility depends on the type of prey consumed by larvae. In this case, a diet of *M. persicae* and *A. nerii* was associated with much lower fertility (50% and 35% respectively), compared to a diet of *R. padi* (fertility of around 70%). Additionally, Honěk (1993), in his review about intraspecific variation in body size and fecundity, studied several species from different orders (Coleoptera, Diptera, Ephemeroptera, Heteroptera, and Homoptera) and showed that the number of ovarioles increased with insect body weight. The general relationship shows a 0.81% increase in ovariole number for each 1% increase in dry body weight.

Planned implementation in the model

Following Honěk (1993), we assume that the *S. scripta* potential fecundity (potential total number of eggs to be laid) depends linearly on female mass and thus is set at the female's emergence. As data on individual mass and fecundity were not available for *S. scripta*, we based the linear relationship on the minimum and maximum values reported/estimated in the literature, assuming that the minimum reported mass corresponds to the minimum reported fecundity, and the maximum reported mass corresponds to the maximum reported fecundity (Equation 30). Regarding fecundity, we take the data from Nangel and Drescher (1991). Regarding body mass, we assume a range between 6.6 and 33.3 mg (see explanation provided in section 'Foraging').

$$F_T = 12.097 \times M_f + 148.16 \qquad \text{Equation 30}$$

where F_T is the potential fecundity of a female, and M_f is the mass of a female.

The actual lifetime egg number laid will depend on environmental conditions (weather experienced), amount of food (pollen) consumed, as pollen is necessary for the maturation of eggs, and availability of oviposition sites (i.e., plants infested with aphids). We will further assume that *S. scripta* females experience enough mating events during their lifetime to fertilise all the possible eggs to be laid, i.e., the potential fecundity is not decreased because of missed mating. We assume a constant pre-oviposition time of 5 days based on Nengel and Drescher (1991).

S. scripta will employ a highly adaptive oviposition strategy; females will prefer to lay eggs in immediate proximity to high-density, young aphid colonies on infested leaves, using both prey-derived semiochemicals and plant volatiles to locate optimal sites. During local movements, females will prioritise oviposition sites with higher aphid densities, as these provide better resources for larval development. Females will only lay eggs when the aphid density at a specific location (in a 10 × 10 m grid cell at which aphid densities are provided) exceeds a predetermined threshold. This behaviour may be influenced by the habitat type, but due to the lack of species-specific data and the generalist feeding behaviour of *S. scripta* larvae, we assume a constant threshold, expressed as a minimum aphid biomass A_{th} required for oviposition. Based on Polak (1980), five *A. pisum* aphids (≈1.3 mg each) ensure larval survival, giving a baseline threshold of 6.5 mg of aphids. This value will be scaled by a mobility factor m_l to account for the limited foraging range of first-instar larvae. To replicate natural field variability, stochastic variation around this threshold will be included.

The probability of oviposition site selection will be modelled using a logistic function, which is appropriate for this coarse spatial resolution as it captures a biologically plausible threshold-like response: low-density patches are rarely selected, probability increases steeply after exceeding the minimum biomass, and saturates at high densities. This reflects the adaptive oviposition strategy of syrphids while avoiding unrealistic fine-scale selectivity. The function is expressed as (Equation 31):

$$P(A,C) = \begin{cases} \frac{1}{1+\exp[-k\times(A-A_{50})]}, A \geq A_{th} \\ 0, A < A_{th} \end{cases} \quad \text{Equation 31}$$

where A is aphid biomass (mg per 10 × 10 m cell), A_{th} is the daily biomass threshold (6.5 mg × m_l / f per cell with stochastic variation), A_{50} is the biomass giving 50% oviposition probability, and k is the steepness parameter.

S. scripta lay eggs individually; however more than one egg can be laid per plant if aphid densities are high (Fig. 16B). Furthermore, there may be more than one suitable plant for oviposition present in a 10 × 10 m grid cell, for which the aphid density/biomass is assessed. Thus, in the model, we assume a maximum number of eggs laid per 10 × 10 m grid cell, which will be scaled by aphid density/biomass. In addition, a female will avoid laying eggs in cells already occupied by eggs or larvae.

The expected daily egg production of a female hoverfly will be modelled as a product of baseline oviposition rate and environmental scaling factors reflecting temperature and photoperiod. Formally, the daily oviposition rate $E_d(t, A, T, P)$, where t denotes the female's reproductive age in days, A is the aphid biomass available at the oviposition site, T is the ambient temperature, and P is the photoperiod length in hours, is given by Equation 32:

$$E_d(t,A,T,P) = [f_A(A) \times f_{age}(t)] \times f_T(T) \times f_P(P) \quad \text{Equation 32}$$

where the first bracketed term represents the baseline daily oviposition under optimal temperature and photoperiod conditions, and $f_T(T)$ and $f_P(P)$ are scaling factors for temperature and photoperiod, respectively.

The baseline oviposition rate will be composed of a prey-dependent term, $f_A(A)$, and an age-dependent shape function, $f_{age}(t)$ (Fig. 17). The prey-dependent term is a logarithmic function of the aphid biomass A, limited to a maximum value A_{max} to avoid unrealistic values, and is expressed as (Equation 33):

$$f(A) = a \times \ln\left(\min\left(A, A_{max}\right)\right) + b \qquad \text{Equation 33}$$

where the parameters a = 10.270 and b = 20.841 represent averaged coefficients derived from Wnuk and Starmach (1977) for three hoverfly species: *E. corollae*, *S. vitripennis*, and *E. balteatus* (Table 8). As hoverflies in the experiment of Wnuk and Starmach (1977) were provided with plants infested with *A. fabae*, aphid biomass was calculated assuming an average individual aphid weight of 0.82 mg (see Table 5). An additional scaling factor may be required, as *A. fabae* appears to be a suboptimal prey species for *S. scripta* larvae. Larvae reared on *A. fabae* exhibit significantly higher aphid biomass requirements to complete development compared to those fed on alternative aphid species (see Fig. 11).

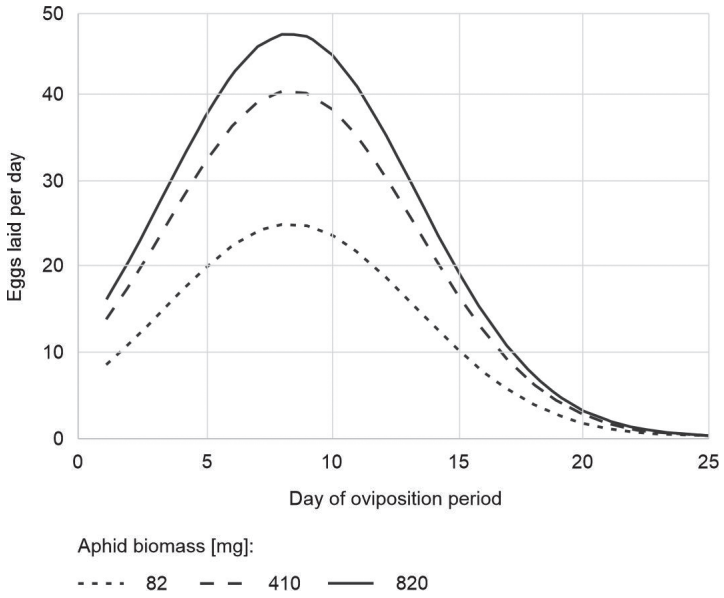

Figure 17. Dependence of daily oviposition rate of *Sphaerophoria scripta* female on its reproductive age and aphid biomass at the oviposition site. Modelled by combining Equation 33 and Equation 34.

The age-dependent oviposition function, $f_{age}(t)$, describing the temporal pattern of egg-laying over the oviposition period will be modelled using a Gaussian (normal) distribution normalized over the oviposition period, T_{ovip}, to ensure that total eggs sum to the maximum potential egg number (set to 550 eggs after Nangel and Drescher 1991). This is expressed as (Equation 34):

$$f_{age}(t) = \frac{1}{Z} \times exp\left(-\frac{(t-\mu)^2}{2 \times \sigma^2}\right) \qquad \text{Equation 34}$$

with Z is defined as (Equation 35):

$$Z = \sum_{1}^{T_{ovi}} exp\left(-\frac{(t-\mu)^2}{2\times\sigma^2}\right) \quad \text{Equation 35}$$

where the parameters μ = 8.33 and σ = 5 define the peak and spread of the oviposition curve. The peak was set at one-third of the oviposition period, consistent with the pattern observed for *S. rueppellii* at 25 °C under longer photoperiod (Orengo-Green et al. 2022). The oviposition period was set to 25 days, accounting for the mean female lifespan of 31 days with pre- and post-oviposition periods of 5 and 1 day, respectively (Nangel and Dreschel 1991).

The baseline oviposition rate is valid for the optimal temperature and photoperiod conditions, and thus will be further multiplied by a scaling factor depending on these variables (Fig. 18). Temperature will influence oviposition through the scaling factor $f_T(T)$, modelled by a normalised Weibull probability density function (PDF). This function was fitted to limited experimental data from Orengo-Green et al. (2022), scaled between 20 °C and 25 °C, where the mean total egg numbers showed a scaling factor of 0.34 to 1. In addition, the Weibull PDF was parameterised with a minimum temperature threshold T_{min} = 11 °C and assumed an optimum between 25 and 30 °C. The minimum temperature threshold was established based on the *Coccinella septempunctata* (Linnaeus, 1758) study by Xia et al. (1999), and that of Bellefeville et al. (2019) in which at a temperature of 12 °C, some oviposition of *L. glyphinivora* and *E. americanus* was observed. The temperature scaling function is given by Equation 36:

$$f_T(T) = \frac{WeibullPDF(T)}{WeibullPDF\left(T'\right)} \quad \text{Equation 36}$$

where

$$WeibullPDF(T) = \frac{k}{\lambda}\times\left(\frac{T-T_{min}}{\lambda}\right)^{k-1}\times exp\left(-\left(\frac{T-T_{min}}{\lambda}\right)^{k}\right) \quad \text{Equation 37}$$

with shape and scale parameters k = 4.321 and λ = 16.991 estimated from the fitting procedure and T' is the temperature that results in the maximum Weibull-PDF, i.e., the optimum temperature.

Photoperiod effects on oviposition will be incorporated through the scaling factor $f_P(P)$, which linearly scales oviposition between a minimum photoperiod threshold P_{min} = 11 hours and a maximum threshold P_{max} = 14 hours as (Equation 38):

$$f_P(P) = \min\left(1, \max\left[f_{min}, \frac{P-P_{min}}{P_{max}-P_{min}}\right]\right) \quad \text{Equation 38}$$

and is clipped between f_{min} and 1 to represent biological constraints on egg laying, where f_{min} is nonnegative and the minimum scaling factor based on photoperiod.

Dispersal

S. scripta is a migratory species (Raymond et al. 2013; Hlaváček et al. 2022) and exhibits two distinct scales of dispersal; routine daily movements associated with foraging and oviposition site selection, and seasonal long-distance

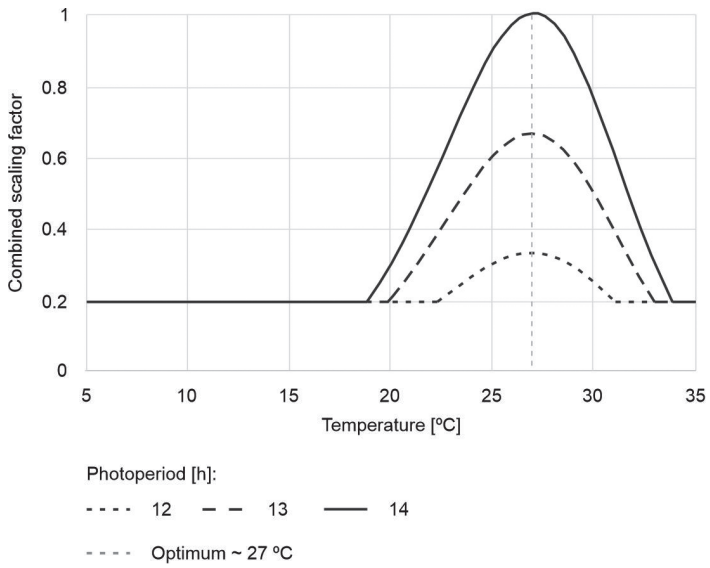

Figure 18. Distribution of the scaling factor for *Sphaerophoria scripta* female daily oviposition rate due to temperature and photoperiod. Modelled with Equation 36 and Equation 38. Here f_{min} is set to 0.2.

migrations that connect breeding and overwintering areas. *Sphaerophoria* spp. are expected in wild flower patches, as this taxon is typical of dry, open grassland habitats (Stubbs and Falk 2002).

Daily movement of adults

Several studies suggest that syrphid flies respond most strongly to landscape composition at spatial scales between 500 and 1,500 m (Kleijn and Van Langevelde 2006; Meyer et al. 2009; Madureira et al. 2023), although species-specific differences exist. For example, *Sphaerophoria* spp. appear unaffected by the proportion of arable land at any scale (Haenke et al. 2009). Dispersal patterns in syrphids vary, with capture-recapture studies indicating that non-migrant syrphids typically move up to 100 m, occasionally reaching 400 m (Conn 1976; Wratten et al. 2003); however, gut content analyses over seven-day periods provide only net displacement, limiting understanding of their daily movement. Foraging behaviour can be context-dependent: *Sphaerophoria* spp. demonstrate cautious, darting flight in response to camouflaged predators like *Thomisus labefactus* (Karsch, 1881) (Araneae, Thomisidae), but not when predators are overtly visible (Yokoi and Fujisaki 2009).

Perception range in *E. balteatus* estimated from field observations is 200 m (Arrignon et al. 2007).

Long-distance migrations

The timing of migration is a complex phenomenon influenced by a range of factors, including endogenous mechanisms such as the circadian clock (Denlinger et al. 2017) and abiotic factors such as weather conditions (Hlaváček et al. 2022). Recent work by Hlaváček et al. (2022) demonstrated that the peak migration of *S. scripta* typically occurs in September and October, with notable interannual variability in both timing and sex-specific patterns. In one observed

year, females initiated migration earlier than males, although males remained consistently abundant throughout the period. In the following year, both sexes exhibited synchronous migration. Despite these variations, a female-biased sex ratio was consistently observed, with females comprising 64% and 77% of migrants across the two years. This pattern may be partially explained by the greater fat reserves in females, which can sustain longer flights and enhance survival in the harsher climates of higher latitudes (Guo et al. 2019). These energy reserves, which would otherwise be allocated to ovarian development, may also contribute to enhanced flight capabilities in females.

Planned implementation in the model

We will treat *S. scripta* as a partially migratory species. Specifically, we assume that the proportion of females from the last autumn generation will exhibit migratory behavior, departing from the local landscape before oviposition. Those which stay will lay eggs which hatch into larvae which, in the last stage, will start the overwintering. A given female from the autumn generation will initiate migration movement with a defined probability p_m.

There are two movement types planned for implementation: short-range movement and long-range movement. Short-range movement simulates intensive search behavior when the adult hoverfly scans the local surroundings in search of food (nectar and pollen) and oviposition sites (aphid prey for larvae). Based on foraging speeds reported for honey bees and bumble bees (Osborne et al. 2013; Wright 2013, cited in Becher et al. 2016), and the assumed 1 m/s foraging speed estimated for *E. balteatus* by App et al. (2025), we assume that *S. scripta* forages at approximately 0.8–1.2 m/s, depending on individual body mass. This range reflects both its smaller size relative to bees and its likely non-linear, cruising search behavior during resource exploration. Long-range movement simulates the extensive search for a different type of landscape element or vegetation. This movement could be part of dispersal behavior as a response to insufficient resources at the current location. To estimate the maximum flight speed and potential flight range of *S. scripta* across its body mass range, we applied allometric scaling principles derived from Ellington's (1984) analysis of insect hovering flight. Ellington (1984) found that wing loading (q) scales with body mass ($q \propto M^{0.23}$), while flight speed (V) varies with the square root of wing loading ($V \propto q^{0.5}$). Collett and Land (1978) measured *E. tenax* flight behavior and velocities in the field as being at least 10 m/s but for short periods of time only. Using *E. tenax*'s mean body mass of 148 mg and allometric scaling principles from Ellington (1984), we can estimate *S. scripta*'s maximum speed when flying to range from approximately 6.6 m/s at 6.6 mg to 8.1 m/s at 33.3 mg (with 7.8 m/s for an mean body mass of 16.5 mg).

To determine whether remaining in a current location for foraging is energetically profitable for *S. scripta*, the balance (Equation 39) between potential energy gain per bout (gut-limited) (Equation 40) and the energy loss per bout (Equation 41) associated with local foraging movements (assuming foraging flight speed of 1 m) and flower handling will be evaluated:

$$E_{gain}^{bout} > E_{loss}^{bout} \quad \text{Equation 39}$$

where:

$$E_{gain}^{bout} = min\left[E_{max(G_v)}, \epsilon_f \times N_{patch} \times \pi r_p^2 \times \frac{t_s^{bout}}{h_f}\right] \quad \text{Equation 40}$$

where $E_{max(Gv)}$ is maximum energy that can be stored in the crop per bout (Equation 24), ϵ_f is hoverfly foraging efficiency (fraction of available resources acquired based on visitation and handling, calibrated parameter), r_p is perception range, N_{patch} is patch-level nectar production (in mg/m^2/day) by plants accessible by *S. scripta*, t_s^{bout} is time spent in a patch (where t_s = time spent in local foraging flights within the patch t_{local_fligh} + total flower handling time in the bout t_{handle}) and h_f is time within a day spend on foraging (calculated based on weather conditions and photoperiod, see section 'Diurnal activity').

$$E_{loss}^{bout} = C_f \times t_{local_flight} + C_{rest} \times t_{handle} \quad \text{Equation 41}$$

where C_f is flight energy consumption rate and C_{rest} is energy consumption when resting/handling on flowers (see 'Foraging' section).

A patch will be deemed profitable if the daily energy that can be obtained from accessible nectar sources exceeds the energy required for local search flights within the perceptual range (assuming, for simplicity, that energy gain comes only from nectar). This approach ensures that *S. scripta* preferentially remains in patches where resource availability is sufficient to offset the energetic cost of local search, and otherwise engages in long-range movements to locate more rewarding habitat. The long-range foraging movement will be restricted by a maximum daily dispersal ability and can be carried out in N_f movement bouts. This movement is driven by the availability and distance to foraging resources. The maximum daily dispersal ability D_{tmax} (for movements between floral patches) will be calculated from the available daily flight time (h_m) and the flight speed v. The maximum distance achieved during one bout will be restricted by available usable energy calculated based on percentage of stomach filling (Table 9).

When dispersing for oviposition sites, a hoverfly will be driven by aphid density / aphid biomass updated in a landscape daily with a resolution of 10 × 10 m. Within the perception range a hoverfly (the same as for foraging) will be capable of performing local search movements for cells providing a minimum aphid density / aphid biomass needed for larvae to survive (see section 'Reproduction and oviposition'). During this local search, energy will be spent in a similar way as described above for foraging. If not enough aphids are available locally, then hoverfy switches to long-range movement, occurring with similar rules as long-range movement for foraging patches.

Table 9. Flight energy budget and flying capacity of *Sphaerophoria scripta* provided for an individual of a mean body mass of 16.5 mg. For local search movement a speed of 1 m/s is assumed, while for long distance movement the maximum speed of 7.8 m/s. The maximum flying speed can only be achieved for short time periods.

Nectar glucose [%]	Usable energy [J/µL]	Full stomach usable energy [J]	Max flight time [min]	Local search distance [m]	Long movement distance [m]
20	0.6	1.3	9.3	558	4352
50	1.56	3.34	24.1	1446	11279

Dispersal activity will be tracked individually for each hoverfly, both in terms of time and energy spent and distance travelled, and once daily limits are reached a hoverfly will suspend its activity for that day. Importantly, daily time available for flying (h_m) includes long-range movements for both foraging and oviposition sites.

In the model, a hoverfly will switch between four behavioral states – foraging, flying/dispersing, reproduction, and resting – according to a state-dependent energy budget. Energy reserves will be represented at the individual level and divided into:

1. short-term energy state ($E_{current}$, sugars available in the hemolymph, replenished via nectar feeding), and
2. long-term reserves ($Fat_{reserve}$, stored fat mobilized only when energy balance is negative, assumed to be 5% of the hoverfly's mass).

The model will simulate daytime activities under time and energetic constraints, with behavioral decisions depending on internal energy state, resource distribution, and movement costs.

The daily activity budget will be divided based on observations of Gilbert (1985a); 67.4% of daylight will be allocated to foraging and within-patch flower visits, 8.7% to inter-patch flights, and 21.7% to resting, used only when other activities are complete. Time budgets will set upper limits for each activity type; actual durations will vary daily based on resource availability and behavioral decisions.

Each activity (flying, foraging, reproduction, and resting) will consume energy at a rate dependent on body mass. Cost of flying activities will be calculated as (Equation 42):

$$E_{fly} = C_f \times h_m \qquad \text{Equation 42}$$

where h_m is time spend on flying.

During a foraging bout, the hoverfly will attempt to fill its gut to maximum capacity with the potential energy gain per bout depending on nectar sugar concentration (Equation 40). The total daily nectar intake will be constrained by gut-emptying time (t_{empty}), determining the maximum number of bouts per day (N_{max}).

Egg maturation requires pollen ingestion, modelled as a daily pollen intake threshold ($P_{threshold}$) before oviposition can begin. Once mature eggs are available and $E_{current}$ exceeds an oviposition energy threshold (E_{ovip}), the hoverfly switches to searching for oviposition sites.

The energy cost of oviposition will be calculated as (Equation 43):

$$E_{ovip} = N_{eggs,laid} \times E_{egg} \qquad \text{Equation 43}$$

where $N_{eggs,laid}$ is number of eggs laid per day, an E_{egg} is energy needed for laying an egg (~0.05–0.2 J/egg, based on lipid- protein content of syrphid eggs; estimation from aphidophagous species). Maximum daily egg-laying rate is imposed as an additional stopping rule.

Resting will occur when all other activities are completed or constrained by time budgets. The resting metabolic cost will be calculated as (Equation 44):

$$E_{rest} = C_r \times h_r \quad \text{Equation 44}$$

where h_r is time spend on resting.

At the end of each day, remaining energy will be computed as (Equation 45):

$$E_{end} = E_{current} + E_{gut} + E_{unused_eggs} - E_{rest_night} \quad \text{Equation 45}$$

where E_{gut} is energy remaining in the gut (if feeding ended late), E_{unused_eggs} = ($Eggs_{mature}$ – $Eggs_{laid}$) × E_{egg}, assuming non-laid eggs are reabsorbed and converted to fat (similar assumption as in App et al. 2025). E_{rest_night} is overnight resting metabolic cost.

Then, the daily fat balance will be updated as (Equation 46):

$$Fat_{reserve(t+1)} = Fat_{reserve(t)} + (E_{end} - E_{threshold}) \quad \text{Equation 46}$$

where $Fat_{reserve(t)}$ is the reserve level at the start of day t, and $Fat_{reserve(t+1)}$ is the updated level for the following day. When the daily energy balance E_{end} exceeds the threshold $E_{threshold}$, the surplus is stored as fat, increasing $Fat_{reserve}$. Conversly, when E_{end} is below the threshold, fat reserves are mobilized to cover the deficit, decreasing $Fat_{reserve}$. This formulation ensures that fat reserves function as a dynamic energy buffer, capable of both recovery and depletion depending on the daily energy balance.

The energy available at the start of the next day will be calculated as (Equation 47):

$$E_{current}^{next} = \min\left(E_{max}, E_{baseline} + \alpha_{mobil} \times Fat_{reserve(t+1)}\right) \quad \text{Equation 47}$$

where α_{mobil} is the fraction of fat that can be mobilized overnight, and $E_{baseline}$ is the minimum short-term energy level (sugar pool) that a hoverfly naturally maintains overnight or at rest, even without recent feeding (it will be a calibrated parameter).

This structure allows day-to-day feedback, with reproductive output and survival probability depending on the previous day's energetic balance.

In the model, a hoverfly will switch between the foraging and oviposition behavior once enough energy is gained from nectar consumption and enough pollen is consumed for egg maturation. Thus, two thresholds will be introduced, one for percentage of filling of the stomach needed for oviposition expressed in energetic terms ($E_{ovip_threshold}$, calibrated parameter), and a second related to pollen consumption ($P_{threshold}$). Here we assume that there is a certain amount of pollen needed for maturation of a single egg (P_{egg}, calibrated parameter). Thus if, for a given day, we know a daily egg production rate, we know how much pollen needs to be consumed to allow the eggs to mature. Only if this is achieved, and if enough energy has been obtained, can a female switch to reproductive behavior. We assume that pollen can be consumed at the same time as nectar. As pollen intake rate is unknown, this will be a calibrated parameter

in the model, allowing to scale the amount of pollen consumed with the time a hoverfly spends in a given location, assuming a certain amount of pollen is available within the perception range of a hoverfly.

Four types of dispersal actions will be considered:

1. Random movement/displacement after adult emergence.
2. Local (within perception range) movements to search for resources.
3. Long-range daily movements (summed up to a maximum daily dispersal ability) carried out in N_f bouts. This movement is driven by the availability and distance to foraging resources (when a hoverfly is in foraging behavior) or by prey availability (when a hoverfly is in reproduction behavior, i.e. is looking for oviposition sites).
4. Movement to a hibernation site.

We plan to represent the movement using the following rules:

1. At the beginning of each day, the available sugar energy $E_{current}$ is determined as the sum of baseline carbohydrate levels and a mobilized fraction of fat reserves (Equation 46), whereas pollen reserves ($P_{current}$) are assumed to be minimal due to daily utilisation for egg maturation.
2. Determine if $E_{current} > E_{forage_threshold}$. If not, foraging for nectar is triggered. Foraging will continue until gut volume is filled or patch profitability decreases below a minimum threshold. Pollen foraging is triggered when $P_{current} < P_{threshold}$. The two foraging modes alternate depending on current needs.
3. Evaluate if reproduction goals are achieved (enough nectar/energy and pollen). If yes, then egg laying will be triggered if there are eggs to lay.
4. If egg-laying, evaluate the location for egg-laying potential by evaluating the oviposition site selection probability function.
5. If the oviposition site selection probability function is passed, then lay an egg, otherwise determine the current energy level.
6. If current energy level drops below a minimum threshold, or no eggs to lay, search for forage; otherwise, move to a new host area (or stay if egg-laying is successful).
7. If there are enough eggs and movement steps left, search for a host plant or nectar source and repeat the behaviors.
8. Activate resting when time budget is reached or no further foraging/oviposition is profitable.
9. Calculate the energy level at the end of day.

This behavior requires the specification of two functions, one for oviposition site acceptance and one for foraging site acceptance. The first is given by Equation 31, and the latter is related to assessment of patch profitability (Equation 39). At each step, the current level of energy $E_{current}$ is evaluated, i.e., flying energy cost is subtracted after each flight (inter-patch or to oviposition sites), and reproduction cost is subtracted after each egg laying. Thus, if $E_{current}$ falls below forage threshold during oviposition or dispersal, a hoverfly will switch back to foraging.

The above logic does not include hibernation and migration behaviors. Individuals from the last autumn generation will be assigned to one of two seasonal strategies, depending on a migration probability (p_m): (i) migration mode or

(ii) overwintering/hibernation mode, producing a larval overwintering generation. In migration mode, reproduction is halted; unlaid eggs are reabsorbed, and their energy is converted into fat. Foraging is directed exclusively toward sugar intake to build long-term energy reserves until a fat threshold is reached. Once this threshold and appropriate environmental conditions (e.g., a photoperiod threshold) are met, the hoverfly migrates (and is removed from the landscape). In overwintering/hibernation mode, individuals continue to follow the standard logic, ovipositing until the daily maximum egg-laying potential is reached or until energy constraints prevent further reproduction.

Overwintering/hibernation

S. scripta does not typically overwinter as an adult but instead survives winter conditions predominantly during an immature stage. In temperate regions, individuals have been reported to overwinter mainly as late third-instar larvae buried in soil or leaf litter, resuming development after spring warming (Dusek and Laksa 1974). However, this overwintering is likely based on temperature-induced quiescence rather than a true larval diapause, as evidence for larval diapause is lacking (Bańkowska 1964). Although facultative diapause at the imaginal stage has been reported, adult hibernation is considered ecologically unlikely due to the species' sensitivity to humidity (Bańkowska 1964). Contrarily, other studies have reported overwintering in the pupal stage, primarily within the soil, though occasionally on the soil surface or on trees (Kantyerina 1979).

Overwintering larvae of aphidophagous hoverflies, including *S. scripta*, typically occupy sheltered terrestrial microhabitats that offer thermal stability and protection from environmental stressors. The common overwintering sites are within the leaf litter, among grass tussocks, or at the soil-litter interface in habitats such as field margins, hedgerows, and woodland edges. However, in the study of Raymond et al. (2014) on immature hoverflies overwintering in agricultural fields, *S. scripta* larvae were the most common, next to *M. mellinum* and *E. balteatus*. This suggests that agricultural fields are important overwintering sites for aphidophagous hoverflies overwintering in their immature stages. Raymond et al. (2014) suggested that such a choice of overwintering site is probably mostly driven by the presence of aphid colonies in the crops in autumn.

Larvae are usually found at shallow depths, ranging from the surface to approximately 3–5 cm into the soil, where decaying plant material or moist detritus provides insulation and high humidity. These microhabitats buffer larvae against freezing conditions and may facilitate supercooling or freeze tolerance. Bale and Hart (1997) found that overwintering larvae of *S. ribesii* are strongly freeze tolerant; they were able to survive exposures to sub-zero temperatures as low as -30 °C, although they were not able to pupate. The lowest temperature at which, after exposure for short time, larvae were still able to pupate and emerge as adults was -20 °C, but survival rate was very low.

Unfortunately, studies on overwintering regulation in *Sphaerophoria* species are rare. Dusek and Laksa (1974) reported offset of *S. scripta* larvae overwintering near Olomouc in mid-May 1972. They also classified *S. scripta* and *S. rueppellii* as typical inhabitants of field biotopes where aphids are more abundant later in the spring. In related Palearctic syrphids, diapause is typically induced by environmental cues such as decreasing photoperiod (below ~10–11 h) and

declining temperatures, which trigger larval developmental arrest and fat body hypertrophy. For instance, in *E. balteatus*, reproductive diapause is initiated during the second and third instars when daylength drops below approximately 11 h, with overwintering success strongly influenced by temperature and humidity extremes (Hondelmann 2007). Although specific studies on diapause regulation in *S. scripta* are limited, it is likely that this species employs a similar photoperiod-mediated diapause strategy.

Planned implementation in the model

In autumn, adult hoverflies preferentially exploit landscape elements with dense and structurally complex vegetation—such as field margins, hedgerows, woodland edges, meadows, extensively managed grasslands, and agricultural fields infested with aphids late in the season—which provide late-season floral resources and aphid-infested host plants, while also incidentally offering suitable microhabitats for overwintering of late-instar larvae or pupae.

Start and end of overwintering will be primarily driven by photoperiod, with temperature factor acting as an additional trigger which may fasten the onset and offset of hibernation. Thus, a threshold date H_{Sdate} after which the start of hibernation is mandatory will be applied. This threshold will be set as day in the year at which the photoperiod falls below a certain number of hours (Ph_{start}). However, if *S. scripta* larva experience cold temperatures earlier, the start of overwintering will come earlier. Thus a certain number of days (H_{days}) with minimum night temperatures below a threshold (Th_{start}) will be required to initiate hibernation of *S. scripta*. H_{days}, Th_{start} will be initially set to 5 days and 12° C, respectively, and H_{date} will be set as date corresponding to photoperiod of 11 h (assumed after *E. balteatus*).

Offset of hibernation will also be related to photoperiod and temperature. A certain number of days (E_{days}) with maximum day temperatures above a threshold (Th_{end}) will be required; however, emergence will also be restricted by date, not being earlier than a given day (E_{date}) corresponding with photoperiod of Ph_{end}. E_{days} and Th_{end}. It will be initially set to 5 days and 10° C, respectively, and E_{date} will be set as date corresponding to photoperiod of 11 h.

As no data on distribution of individual larvae entering and leaving the hibernation sites is available, we will assume this process to follow a non-linear saturation function, with fast initial increase and gradual slowdown (Equation 48):

$$C_A(t) = 100 \times \left(1 - e^{-kt}\right) \qquad \text{Equation 48}$$

where $C_A(t)$ is cumulative percentage of individuals entering and leaving habitat site, and k (rate constant) and t (time in days) are parameters which will be fitted in the calibration process.

Mortality

Mortality of egg-to-pupa stages

The mortality of aphidophagous hoverflies during its immature stages is generally high, although exact rates depend on species, and vary depending on habitat conditions, prey availability, and natural enemies. Like other aphidophagous

syrphids (e.g. *E. balteatus*, *E. corollae*), *S. scripta* experiences its greatest losses during the egg and early larval stages. Survival rates documented by Nengel and Drescher (1991) were 33.1 ± 8.1% from oviposition to third instar, 53.5 ± 9.7% from third instar to pupation, and 80.6 ± 9.7% from pupation to adult emergence. These losses are primarily due to predation by ants, lacewings, ladybirds, spiders, and other generalist predators, as well as intraguild predation by other aphid predators, including syrphid larvae (Rojo et al. 2003). Additional mortality arises from egg desiccation, failure to hatch, and parasitism.

Although no specific studies on *S. scripta* are available, the study of Amorós-Jiménez et al. (2012) on *S. rueppellii* shows that mortality in *Sphaerophoria* species is primarily driven by temperature and humidity. Relative humidity is a particularly critical determinant of mortality of egg and larval stages; at 50% relative humidity, larval mortality reached 100% across all tested temperatures (20 °C, 25 °C, 30 °C), and egg mortality was significantly higher than at 90% RH, exceeding 80% at some temperature-humidity combinations. In contrast, pupal mortality was largely unaffected by humidity, suggesting that the pupal stage is more tolerant of desiccation. Temperature also had an impact; higher temperatures (30 °C) led to a notable increase in pupal mortality, regardless of humidity conditions. Impact of mortality in egg and larva stages was less pronounced, especially at high relative humidity of 90%.

Aphid type and density seems to be important factor determining mortality at larval stages of aphidophagous hoverflies. Increasing mortality of larvae with decreasing aphid density was reported for *E. balteatus* (Putra and Yasuda 2006). Interestingly, when comparing high and low prey availability, Amorós-Jiménez et al. (2012) reported no significant effect on larval or pupal mortality; larvae experienced 25% mortality under both regimes, and pupal mortality ranged from 5–15%. In addition, Amorós-Jiménez and Marcos-García (2020) found that larvae reared on *R. padi* and *M. persicae* attained higher survival rates (70% and 74%, respectively), whereas those fed on *A. nerii* survived at only ~40%.

Another important source of mortality in aphidophagous hoverflies is parasitism. Under certain conditions, field data suggest that the impact of parasitoids on hoverfly populations can be substantial and, in some cases, potentially severe, particularly in intensively managed agricultural landscapes (Sommaggio et al. 2014). Despite this, a comprehensive understanding of the dynamics between aphidophagous hoverflies and their parasitoids remains limited, especially with respect to species-specific effects and population-level consequences.

Parasitoids of aphidophagous hoverflies such as *S. scripta* primarily attack the preimaginal stages, including larvae and pupae. Many parasitoid taxa exploit Syrphinae hosts as koinobiont endoparasitoids, laying eggs in or on early larval instars and allowing the host to continue developing for some time before the parasitoid larva consumes it from within (Schneider 1969; Rotheray 1981, 1984). Consistent with this mode of parasitism, studies by Wnuk (1974) and Wnuk and Wojciechowicz (1993) indicate that parasitization does not measurably reduce the feeding capacity of syrphid larvae during their development. Instead, parasitoids primarily affect hoverfly populations by preventing successful adult emergence, thereby exerting a delayed but negative effect on future syrphid population sizes. The host ultimately dies prior to adult emergence,

and the adult parasitoid emerges from the host puparium. This mode of action is characteristic of several Ichneumonidae, such as *Diplazon laetatorius* (Fabricius, 1781), widely regarded as one of the most frequent and ecologically important syrphid parasitoids (e.g., Schneider 1969; Rotheray 1984; Jankowska 2004; Sommagio et al. 2014). Other parasitoid families associated with aphidophagous syrphids include Pteromalidae (e.g., *Pachyneuron* Walker, 1833 species), which often attack later instar larvae or pupae as pupal parasitoids, and Encyrtidae (e.g., *Syrphophagus aeruginosus* Dalman, 1820), which also emerge from the puparium (e.g., Schneider 1969; Rotheray 1984; Jankowska 2004; Sommagio et al. 2014). In contrast to koinobionts, some parasitoids manipulate host development differently, but in all cases the outcome for the host is mortality before adulthood.

Parasitoids locate syrphid hosts using chemical cues associated with aphid colonies and the host itself. Volatile aphid-derived odours guide parasitoids to infested plants, while contact cues on the larval cuticle trigger ovipositor insertion. Final host acceptance and oviposition appear to depend on internal cues, likely from larval haemolymph (Rotheray 1981, 1984). Field surveys of parasitoid impact on syrphid larvae and pupae report highly variable parasitism rates, reflecting both temporal variation and ecological context (e.g. country, crop type, and landscape complexity). In a three-year study of parasitoids of aphidophagous hoverflies on cabbage vegetables in Poland, Jankowska (2004) documented substantial interannual variation, with overall parasitism rates ranging from 14.4% to 46.4%. *D. laetatorius* was the most frequent parasitoid, reaching parasitism levels of up to 21.7%. Similarly, Wnuk and Wojciechowicz (1993), also working in Polish cabbage systems infested by *B. brassicae*, reported that 27–40% of syrphid larvae were parasitised. Very high parasitism pressure has been recorded in cereal systems; in maize crops in Poland, Krawczyk et al. (2011) found that total parasitism ranged from 32.8% to 84.4%, with *Pachyneuron grande* (Thomson, 1878) as the dominant parasitoid. Comparable patterns were observed in a three-year study in northeastern Italy by Sommaggio et al. (2014), where *Pachyneuron* species dominated intensively managed maize fields, while *Diplazon* species were more prevalent in wheat and extensive habitats. In that study, parasitism rates varied from 32% in extensive habitats to 48% in wheat and up to 78% in maize, highlighting the strong influence of crop type and landscape simplification on parasitism pressure. High parasitism levels have also been documented outside Europe. On lettuce farms in Iran, Mohammadi-Khorambadi et al. (2016) found that *Enizemum ornatum* (Gravenhorst, 1829), *D. laetatorius*, and *Pachyneuron formosum* (Walker, 1833) parasitized 45.0%, 14.0%, and 1.83% of syrphid larvae, respectively. In a two-year survey of lettuce and broccoli crops in Argentina, Díaz Lucas et al. (2020) reported parasitism rates ranging from 8% to 100%. *D. laetatorius* was recorded in both crops, whereas *Pachyneuron* species were found exclusively in broccoli, further supporting crop-specific differences in parasitoid assemblages and host exploitation.

Unfortunately, none of the published studies focus exclusively on *Sphaerophoria* species. Typically, field surveys collect all aphidophagous hoverflies present in a study system, rear them under laboratory conditions, and record the parasitoids that emerge. In many cases, parasitism rates are reported per parasitoid species rather than per host species. When host-specific data are

available, the number of *Sphaerophoria* individuals examined is often very small compared to other hoverfly species, particularly *E. balteatus*. Consequently, parasitism rates reported for aphidophagous hoverflies are difficult to extrapolate directly to *S. scripta*. Nevertheless, parasitoid species repeatedly recorded from *Sphaerophoria* hosts across different studies provide valuable qualitative information on host-parasitoid associations. An overview of parasitoids reported for *Sphaerophoria* species, together with their mode of action and the developmental stages attacked, is therefore presented in Table 10.

Planned implementation in the model

Background mortality will be defined separately for the egg-to-pupa stages. This mortality is a daily probability applied at the start of each daily time step. For all the immature stages of *S. scripta*, this background mortality probability will depend on both temperature and humidity and will be calculated based on the polynomial regression models fitted to the mortality data on immature stages of *S. rueppellii* (Amorós-Jiménez et al. 2012) (Fig. 19, Equation 49).

$$M(T, RH) = a_1 \times T^2 + a_2 \times T + a_3 \times RH^2 + a_4 \times RH + a_5 \times T \times RH + a_6 \quad \text{Equation 49}$$

The effects of aphid species and prey density on larval mortality will not be included in the model directly. The influence of aphid species has only been investigated for a limited number of taxa (*R. padi*, *M. persicae*, and *A. nerii*), and

Table 10. Parasitoids of *Sphaerophoria* spp., mode of action, and stages attacked.

Parasitoid species	Family	Mode of action	Stage attacked	Reference
Diplazon laetatorius (Fabricius, 1781)	Ichneumonidae (Diplazontinae)	Larval endoparasitoid	Late larva → adult emerges from puparium	Sommaggio et al. (2014); Rotheray (1984); Schneider (1969)
Diplazon pectoratorius (Gravenhorst, 1829)	Ichneumonidae (Diplazontinae)	Larval endoparasitoid	Larva → puparium	Rotheray (1984)
Diplazon tetragonus (Thunberg, 1822)	Ichneumonidae (Diplazontinae)	Larval endoparasitoid	Larva → puparium	Rotheray (1984)
Diplazon signatus (Fabricius, 1781)	Ichneumonidae (Diplazontinae)	Larval endoparasitoid	Larva → puparium	Schneider (1969)
Enizemum ornatum (Gravenhorst, 1829)	Ichneumonidae	Larval endoparasitoid	Larval instars	Sommaggio et al. (2014); Rotheray (1984)
Promethes monticola (Förster, 1869)	Ichneumonidae	Larval endoparasitoid	Larva → puparium	Schneider (1969)
Syrphophilus bizonarius (Gravenhorst, 1829)	Ichneumonidae	Larval endoparasitoid	Larva → puparium	Sommaggio et al. (2014)
Pachyneuron formosum (Walker, 1833)	Pteromalidae	Pupal endoparasitoid / ectoparasitoid	Pupa (occasionally late larva)	Sommaggio et al. (2014); Schneider (1969)
Pachyneuron grande (Thomson, 1878)	Pteromalidae	Pupal endoparasitoid	Pupa	Sommaggio et al. (2014); Krawczyk et al. (2011)
Syrphophagus aeruginosus (Dalman, 1820)	Encyrtidae	Larval–pupal endoparasitoid	Larva → puparium	Sommaggio et al. (2014); Krawczyk et al. (2011)
Cheiloneurus boldyrevi (Trjapitzin, 1963)	Encyrtidae	Pupal endoparasitoid / hyperparasitoid	Pupa	Sommaggio et al. (2014)
Trichosteresis foersteri (Kieffer, 1907)	Ceraphronidae	Larval endoparasitoid	Larva → puparium	Sommaggio et al. (2014); Schneider (1969)
Lygocerus sp. (Förster, 1869)	Ichneumonidae	Larval endoparasitoid	Larva → puparium	Schneider (1969)

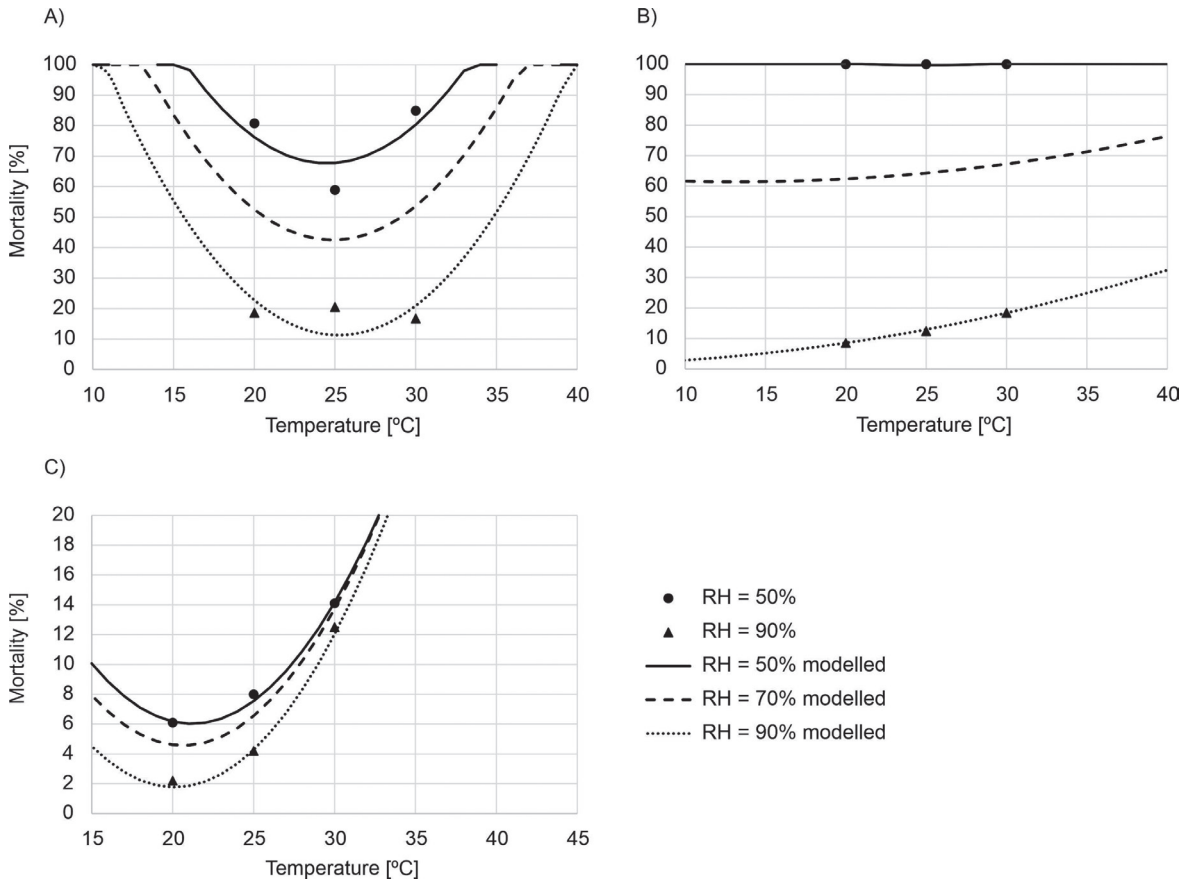

Figure 19. Impact of temperature and relative humidity (RH) on mortality of immature stages of *Sphaerophoria rueppellii*: (**A**) egg, (**B**) larva, (**C**) pupa. Points represent measurement data from experiments of Amorós-Jiménez et al. (2012). Lines represent the fitted polynomial regression models (Equation 49) with parameters presented in Table 11.

Table 11. Parameters of the polynomial regression models for *Sphaerophoria rueppellii* mortality at different life stages. Models were fitted based on data from Amorós-Jiménez et al. (2012).

Developmental stage	a_1	a_2	a_3	a_4	a_5	a_6	R^2
Egg	0.422	-19.94	-0.0074	-0.0001	-0.015	339.7576	0.95
Larva	0.021	-2.2875	-0.0199	-0.0001	0.0247	162.6233	0.99
Pupa	0.105	-4.7375	-0.0016	0	0.0057	57.2263	0.99

remains uncharacterised for other aphid species. Furthermore, unlike findings reported for other aphidophagous syrphids such as *E. balteatus*, the effect of aphid prey density on larval mortality in *Sphaerophoria* species has not been confirmed. In the only study conducted on *S. rueppellii*, no significant relationship was observed. We will, however, include a density-dependent mortality factor refelecting the competition among larvae and possible cannibalism. Density dependence will be introduced by limiting the number of *S. scripta* that could be present in a surrounding of any larva, to a fixed number of larvae. Additional larvae will be removed from the simulation (died because of food limitation, or eaten). The size of the surrounding will be defined separately for each larval instar, reflecting their increasing mobility with age.

Parasitism-induced mortality and landscape dependence

In addition to the background and density-dependent mortality, parasitism-induced mortality will be incorporated as a distinct process acting on immature stages of *S. scripta*. Aphidophagous hoverfly parasitoids typically oviposit into late larval instars, but host mortality is delayed, with parasitised larvae continuing to feed, grow, and pupate normally before dying at or shortly before adult emergence. To reflect this biology, parasitism will not be implemented as an immediate stage-specific mortality factor.

Parasitism will be modelled as a two-step process. Individuals reaching susceptible larval stages (late second and third instars) are assigned a baseline daily parasitism probability (p_{para0}), derived from cumulative parasitism rates (P_{para}) observed over n days of larval susceptibility (Equation 50):

$$p_{para0} = 1 - (1 - P_{para})^{1/n} \quad \text{Equation 50}$$

Because species-specific parasitism rates for *S. scripta* are largely unavailable, the cumulative parasitism rate used in the model will be based on values reported for *D. laetatorius*, one of the most common and consistently reported parasitoids of *Sphaerophoria* species (Table 10). In the three-year field study by Jankowska (2004), a substantial fraction of the aphidophagous hoverfly larvae collected belonged to the *Sphaerophoria* species (11% in 1993, 48% in 1994, and 35% in 1995), making this dataset one of the strongest empirical datasets for this genus. Across the study period, *D. laetatorius* exhibited a mean parasitism rate of 21.7%, which will therefore be used as the reference cumulative parasitism rate (P_{para}) for parameterising parasitism pressure in the model. This parameter will subsequently be refined during the model calibration phase to ensure consistency with observed population dynamics under field conditions.

The effective daily parasitism probability (p_{paraL}) will be then adjusted for landscape-dependent variation (Equation 51):

$$p_{paraL} = p_{para0} \times L \quad \text{Equation 51}$$

where (L) is a dimensionless modifier reflecting habitat complexity ($L > 1$) in simplified landscapes, ($L < 1$) in complex landscapes. Parasitised larvae develop normally, with no reduction in aphid consumption, and all parasitised individuals experience mortality at the pupal-adult transition, representing successful parasitoid development and emergence from the host puparium.

This formulation allows parasitism-induced mortality to be incorporated as a delayed-lethal process, mechanistically distinct from background mortality defined in Equation 49, while enabling modulation of parasitism risk by landscape structure.

Pesticide responses

To simulate pesticide responses in *S. scripta*, we adopt a modelling framework analogous to that used in the development of the ApisRAM honey bee colony model (Duan et al. 2022). Pesticide exposure can occur through the consumption of contaminated nectar, contact, and overspray. By considering these three exposure pathways, we provide an accurate representation of how model

hoverflies may encounter pesticides in contaminated environments. $P_B(t)$ is used to represent the accumulated pesticide burden for the individual until day t. $P_B(t)$ is updated by all three exposure paths and is used to calculate the stress caused by pesticide exposure. The new pesticide exposure on day t is represented by $P_N(t)$ which is calculated by Equation 52.

$$P_N(t) = P_I(t) + P_C(t) + P_O(t) \quad \text{Equation 52}$$

where $P_I(t)$ is the new contamination from intake, $P_C(t)$ is from the contact exposure and $P_o(t)$ is from the overspray exposure.

Intake exposure pathway

Foraging hoverflies may be exposed by collecting pollen and nectar from contaminated flowers. The pesticide amount in the consumed resource is represented by $P_I(t)$ and is assumed to move directly to the hoverfly's body ($P_N(t)$).

Overspray and contact exposure pathways

The overspray exposure pathways are only relevant to any hoverfly stage present at the moment of pesticide spraying. Contact exposure can occur when a mobile stage moves in a contaminated area. In both cases, a simple one-time absorption model is used; i.e., we assume that the pesticide is absorbed into the hoverfly's body once, with separate parameters for contact and overspray.

Contact exposure specifically pertains to foraging adults and occurs when a hoverfly touches a contaminated plant surface during foraging. The amount of pesticide transferred to the body through contact is controlled by two user-defined parameters as shown in Equation 53.

$$P_c = s_c \times S \times P_s \quad \text{Equation 53}$$

where P_S is the pesticide amount per square meter on the plant surface, S is a constant representing the area of the hoverfly that is in contact with the surface. Here, we might imagine that foot, abdomen, and wing contact could occur. S_C is the absorption rate that determines the amount of pesticide P_S that will be transferred to the body. This implementation does not consider foraging time, but both parameters can be adjusted to make this approach more or less conservative.

Overspray exclusively occurs when hoverflies (adults or larvae) are active in a field where simultaneous pesticide spraying occurs and/or where drift occurs in the adjacent area. Two parameters, starting time and ending time, for a pesticide spray event are used to control whether overspray can happen. Overspray can only occur if a hoverfly is in the exact location when the pesticide is being sprayed. When the overspray happens, the contaminated pesticide amount (P_O) going to the hoverfly's body is calculated using Equation 54.

$$P_o = s_o \times Sa \quad \text{Equation 54}$$

where S represent a proportion of the body surface, as for Equation 28, a is the pesticide spraying application rate, S_o is the absorption rate for overspray.

Toxicology

To determine the effect of the pesticide body burden, the initial model only considers acute mortality. To do this requires three parameters. The first is a threshold for effect, P_t, above which there is a daily probability of mortality P_m. The third threshold D is the daily decay rate of the pesticide in the hoverfly's body. This approach will implement a first model for implementing pesticide effects and assumes that an ALMaSS or equivalent landscape model is available to generate the pesticide concentration in the nectar and vegetation, as well as overspray.

Other mortalities

There will be a number of other mortalities considered in the model, an important one being the daily background mortality of adult hoverflies. However, empirical data on adult background mortality under natural conditions remain scarce. The only available estimates for *Sphaerophoria* species derive from laboratory-based studies, where survival was assessed under controlled conditions, often as part of unrelated experimental treatments. For instance, Violi et al. (2025) evaluated various marking techniques for *S. rueppellii* to support mark-release-recapture studies aimed at enhancing biological control strategies. In this study, Kaplan-Meier survival analysis of the untreated control group revealed a steady decline in survival probability over time. The mean lifespan of control females was 5.4 days, with the longest-lived individual surviving 12 days.

Despite these findings, extrapolating laboratory-derived survival data from *S. rueppellii* to estimate background mortality in *S. scripta* would not be reliable due to interspecific differences, limited sample size (n = 10), and the absence of natural mortality factors such as predation and environmental stressors. Consequently, the model will employ a generalized daily background mortality rate for adult females, treated as a calibration parameter.

Overwintering mortality will be assessed once, at the conclusion of the overwintering period, prior to adult emergence. Given the limited knowledge regarding mortality dynamics during overwintering, this parameter will also be incorporated as a model input.

Additionally, mortality associated with agricultural management practices will be considered. Immature stages of *S. scripta* occur either on aphid-infested plants (eggs and larvae) or in the soil/near the plant base (pupae). Mortality risk depends on both the spatial location of the stage and its temporal overlap with specific crop operations. Eggs and larvae are only susceptible during the main aphid season, when they feed within colonies on crop plants, whereas pupae may be affected by soil-disturbing operations irrespective of aphid presence. Based on these considerations, Table 12 summarises the mortality probabilities assigned to each agricultural activity for the different immature stages. These values are expert-derived estimates in the absence of species-specific data and will be further refined during model calibration. Note that in ALMaSS, pesticide applications are often treated in detail, and their implementation will be considered on a case-by-case basis when applying the model.

Table 12. Agricultural activities that have non-zero probability of mortality in immature stages of *Sphaerophoria scripta*.

Activity	Egg mortality	Larva mortality	Pupa mortality	Notes
Harrowing	0	0	0.5	Soil disturbance can affect pupae; eggs/larvae absent before sowing
Ploughing	0	0	0.5	Soil disturbance pre-sowing; eggs/larvae absent
Stubble cultivator	0	0	0.5	Post-harvest soil disturbance; affects pupae
Autumn roll	0	0	0.5	Soil compaction/rolling can crush pupae
Autumn sowing	0	0	0.3	Minor impact on pupae near surface
Bed forming	0	0	0.3	Soil preparation may disturb pupae
Bulb harvesting	0	0	0.3	Soil disturbance; pupae may be affected
Harvest	0	0	0.2	Minor impact on soil/lower plant pupae
Mechanical weeding	0.3	0.3	0.2	Direct disturbance of leaves/aphid colonies; minor pupae disturbance

Discussion

We propose a mechanistic, stage-structured model of *S. scripta* population dynamics that synthesizes temperature-dependent development, prey-specific larval survival, adult nutritional ecology, foraging behaviour and movement into a unified, modular framework. The model presented here is grounded in a relatively substantial body of literature. However, many of the processes incorporated remain characterised by uncertain parameter values or mechanisms. Much of the information informing the model derives from laboratory studies and, in several cases, from studies of other hoverfly species, rather than *S. scripta* itself. Thus, some crucial information about the species is still missing or uncertain, and here we outline some of the thinking behind our choices.

The available data were insufficient to estimate detailed thermal performance curves for the developmental stages of *S. scripta*. As a result, temperature-dependent development of eggs and pupae were modelled using linear degree-day relationships fitted to development rates, reflecting the approximately linear response observed within the experimentally tested temperature range. For both stages, data at higher temperatures are lacking, precluding reliable estimation of upper thermal limits. In the pupal stage, the degree-day model suggests a lower developmental threshold of 3.6 °C; however, the associated confidence interval is wide (-7.5 to 8.0 °C), indicating limited information on low-temperature constraints and substantial parameter uncertainty. In contrast, larval development showed a unimodal response to temperature and was therefore modelled using a Gaussian function fitted to development rates under ad libitum feeding conditions. Although this approach better reflects the biological expectation of an optimal temperature, the larval stage remains the most uncertain due to sparse, heterogeneous data. Notably, the primary focus of most existing studies was not the exploration of temperature effects on development, but rather the influence of diet or other ecological factors. These studies often employed single temperatures or narrow thermal ranges, limiting their utility for modelling thermal responses. In addition, although for modelling the temperature-dependent development of larvae, we included only results from studies in which aphids were provided ad libitum, the studies differed in terms of other laboratory settings, resulting in quite a variability of obtained results for

the same temperatures. Given that the larval stage appears particularly sensitive to environmental variability, uncertainties in thermal parameters may disproportionately influence predictions of larval development duration.

Larval development in aphidophagous hoverflies is strongly dependent on aphid prey availability. In our model, we assume that prey limitation impacts larval development additively across temperatures. However, the only available empirical data linking prey density and *S. scripta* larval development were obtained at 20 °C (Polak 1980). We extrapolated these findings to other temperatures, recognising that this may not hold true universally. Larvae may exhibit greater sensitivity to prey limitation near thermal extremes, with reduced sensitivity at temperatures closer to their thermal optimum.

Aphid consumption patterns during larval development were drawn from studies on various *Sphaerophoria* species reared on different aphid species. To facilitate comparisons, we developed a recalculation method converting aphid densities to biomass consumed. Further, we rescaled daily aphid biomass consumption by other *Sphaerophoria* species to match *S. scripta*, based on interspecific comparisons of larval mass. These results support the statement by Adams et al. (1987) that aphidophagous hoverflies require a specific biomass intake for pupation under ad libitum conditions. However, an exception was noted when *S. scripta* larvae were fed on *A. fabae*, suggesting that certain aphid species may be nutritionally suboptimal, necessitating higher consumption to achieve pupation thresholds. This aligns with the concept of essential and alternative prey types, as documented in other aphidophagous predators such as ladybirds (Evans et al. 1999; Berkvens et al. 2010).

Empirical data on juvenile survival for *S. scripta* are sparse. For this reason, we adopted temperature and humidity-related mortality functions fitted to data from *S. rueppellii* (Amorós-Jiménez et al. 2012). However, these data are limited to three temperatures (20, 25, 30 °C) and two humidity levels (50%, 90%), restricting confidence in predictions beyond these conditions. Additionally, no significant effect of prey availability on larval mortality was reported for *S. rueppellii*, in contrast with findings for other hoverflies (e.g. *E. balteatus*, Putra and Yasuda 2006). The limited design of the *S. rueppellii* study, which considered only two prey regimes, may partly explain this discrepancy. No other studies have explored *Sphaerophoria* larval mortality under varying prey densities. While Polak (1980) examined larval development at a range of aphid densities, mortality data were not reported. Therefore, the first model version excludes prey density effects on mortality, pending the availability of suitable data.

Other mortality factors, including overwintering losses, are poorly documented. *S. ribesii* larvae are known to be strongly freeze tolerant (Bale and Hart 1997), but no temperature-dependent survival functions could be defined for *S. scripta*. Similarly, background mortality in adults remains insufficiently quantified, and thus, for model implementation, both will be defined as parameters requiring fitting.

The floral preferences of *Sphaerophoria* species are not well characterised. While our model includes flowering plants documented as pollen and nectar sources for *S. scripta* in plant-pollinator interaction databases, quantitative information on the relative importance of specific floral traits (e.g. colour or shape) and pollen nutritional requirements remains limited.

Experimental evidence from *S. rueppellii* indicates that hoverfly foraging is influenced by visual floral traits such as colour, shape, and flower abundance (Gasol et al. 2019), but these effects could not yet be parameterised for *S. scripta*. Consequently, we assumed that all documented flowering species were equally important, with patch attractiveness driven primarily by resource quantity. In the case of nectar, a preference for sucrose concentrations near 50% was included (modelled with Gaussian function), based on *S. ribesii* (Gilbert 1981), in the absence of data for *S. scripta*.

Several foraging and energy budget parameters were estimated through allometric scaling from other hoverflies. Stomach volume (Gilbert 1983) and flight and resting energy costs (Sotavalta and Laulajainen 1961) were estimated and rescaled based on results for *E. tenax*, while flight speeds were inferred using allometric relationships from Ellington (1984). Although this introduces uncertainty, the scarcity of species-specific studies necessitated such an approach. Notably, a similar rescaling strategy was applied by App et al. (2025) in modelling of *E. balteatus*.

Reproductive parameters of *S. scripta* are likely shaped by energy reserves, nutrient intake, environmental conditions, and prey availability for larvae. Yet, these mechanisms remain largely unquantified. Patterns of daily egg production were derived from *S. rueppellii* and rescaled to the maximum egg production of *S. scripta* inferred from Nengel and Drescher (1991). No direct data are available on how larval prey availability affects adult reproduction in *S. scripta*, so we assumed patterns similar to those of other aphidophagous hoverflies (i.e., *E. balteatus*, *S. vitripennis*, *E. corollae*; Wnuk and Starmach 1977). Pollen availability is known to constrain egg production, as Nengel and Drescher (1991) reported no oviposition without pollen access. Our model implements a simplified approach by requiring daily pollen intake above a threshold to start reproductive behaviour, as the relationship between pollen quantity and daily egg output is unknown.

Dispersal functions were designed to integrate with foraging and oviposition behaviours, with daily activities driven by reproductive and foraging objectives. These depend on resource distributions and are limited by *S. scripta* movement abilities. Model calibration will therefore focus on evaluating behavioural parameters in relation to the spatial and temporal resource patterns generated by the landscape model. Such alignment is essential to ensure that emergent population dynamics realistically reflect field conditions.

Given the ecological significance of migration for *S. scripta*, we assume that females of the autumn generation may exhibit migratory behaviour with a certain probability. However, as the primary objective of the current model is to inform risk assessment, the probability of migration will be set to zero in the first version of the model. This simplification is intended to prevent the confounding and dilution of potential pesticide effects, thereby enabling clearer interpretation of local risk dynamics.

While the model lacks some of the detailed parameterisation characteristic of other ALMaSS models, it provides a dynamic framework capable of responding to variations in weather, habitat configuration, and resource availability. This first formal implementation serves as a structured synthesis of current ecological knowledge, intended for refinement through post-deployment calibration using a pattern-oriented modelling (POM) approach. Our prior work has

demonstrated POM's utility in improving realism and predictive accuracy in individual-based models of beneficial insects. This model represents a robust starting point for iterative development, designed to facilitate scenario analyses of pesticide effects within managed landscapes.

Framing the model

This section outlines the key assumptions and limitations associated with the design of this model and its integration within social-ecological systems simulations. Following Topping et al. (2015), the model aims to describe population changes in time and space without including all possible known behaviours, seeking to balance false inclusions and exclusions by focusing on processes that significantly influence population dynamics.

The *S. scripta* model synthesises extensive literature, though many processes involve uncertain parameters and mechanisms, primarily derived from laboratory studies and other hoverfly species. The model embodies several critical assumptions and simplifications that constrain its applicability and interpretation.

Domain of applicability

This model is designed to simulate the population dynamics of aphidophagous hoverflies in temperate European agricultural landscapes, with specific focus on responses to environmental variability, resource availability, and pesticide applications. The parameterisation using *S. scripta* data makes it most directly applicable to multivoltine syrphid species with similar ecological traits; generalist aphid predators during larval stages, polylectic adult pollinators, and facultative migrants capable of multiple generations per year.

The phenology in the present model is parameterised primarily for northern and central European conditions, where part of the *S. scripta* population is expected to overwinter at immature stages. However, evidence from emergence-trap studies in agricultural landscapes in south-western and central-western France demonstrate that *S. scripta* commonly overwinters as pre-imaginal stages and emerges locally in spring (Raymond et al. 2014). These regions are characterised by a continental Mediterranean climate, suggesting that similar overwintering strategies are likely in other southern European regions, such as northern Italy. Consequently, while the general life-cycle structure implemented in the model remains applicable, direct application to Mediterranean regions requires reparameterisation of overwintering intensity and phenology to reflect local climatic conditions.

The ALMaSS framework constrains the model to landscapes typically spanning 100 km^2, operating at 1 m^2 spatial resolution with daily time steps over multi-year to decadal periods. This scale captures local population dynamics, seasonal migration patterns, and landscape-level resource heterogeneity, but may not fully represent large-scale metapopulation processes or continental migration networks that characterise some hoverfly species. The daily time resolution is appropriate for capturing development, mortality, and movement decisions but cannot resolve within-day behavioural sequences or circadian rhythms in foraging activity.

Key biological processes and data limitations

Thermal performance and development

The sparse data available for the thermal performance relationships in this model mean that care must be taken in overinterpreting temperature-related scenarios, especially if they include extreme temperatures not likely to be well supported by the stage-specific functions used here (linear degree-day models for egg and pupal stages, and a Gaussian thermal performance function for larval development).

Survival and mortality data

Sparse data exists on juvenile survival, with information only available for the related species *S. rueppellii*. Other mortality drivers are known but not well quantified. Critically, the impact of prey availability on larval mortality is not included in this version of the model due to insufficient data supporting the relationship between prey density and mortality for *Sphaerophoria* species, unlike findings for other aphidophagous hoverflies such as *Episyrphus balteatus*.

Cross-species parameter estimation

Many behavioural and physiological patterns are inferred based on data from other species within the genus (such as *S. rueppellii*) or at the broader level of aphidophagous hoverflies. While such cross-species extrapolation introduces uncertainty where species-specific adaptations may differ significantly from generic patterns, many key traits relevant to population dynamics (e.g. larval aphid predation, pollen dependence for egg maturation, and general phenology) are broadly conserved within aphidophagous Syrphinae. Consequently, this approach also enhances the generality of the model, allowing *S. scripta* to serve as a representative of the aphidophagous hoverfly guild. Species-specific refinements can be readily implemented through reparameterisation as additional empirical data become available.

Energetic budget and allometric scaling

The model simulates daytime activities under time and energetic constraints, with behavioral decisions depending on internal energy state, resource distribution, and movement costs. However, several physiological and behavioural parameters, including flight and resting energy expenditure, gut volume, and flight speed, were estimated using allometric scaling approaches. These estimates were derived by comparing body mass or body length of *S. scripta* with those of closely related syrphid species, introducing compound uncertainties from both the scaling relationships and the source data.

Migration and dispersal

Limited knowledge exists regarding the proportion of populations exhibiting migratory behaviour. The probability of exhibiting migratory behaviour is set as a fitted parameter which, for the sake of simplicity, is assumed to be zero in the first version of the model. This eliminates important population processes that could influence both local dynamics and pesticide exposure patterns.

Density dependence mechanisms

The model assumes that density dependence operates through two primary mechanisms, the availability of larval habitats and aphid prey availability. This simplified representation may miss other important density-dependent processes such as interference competition, disease transmission, or habitat modification effects.

Population genetics and local adaptation

The model assumes genetically uniform populations with fixed physiological and behavioural parameters. However, *S. scripta* populations across Europe likely exhibit local adaptations to climate, host plants, and agricultural practices. Genetic variability in thermal tolerance, development rates, or pesticide resistance could influence population responses to environmental stressors. Additionally, the model excludes gene flow between populations, which in highly mobile species like *S. scripta* could rescue local populations from pesticide impacts or introduce maladapted genotypes.

Complex foraging decisions and flower constancy

While the model incorporates nectar concentration preferences and pollen requirements, it simplifies the complex cognitive processes underlying pollinator foraging. Real hoverflies may exhibit flower constancy, learning, or risk-sensitive foraging that optimises energy gain while minimising predation risk. The model treats each foraging decision independently, potentially missing emergent patterns where experience influences subsequent choices or where local depletion of resources creates spatial foraging patterns not captured by simple attractiveness functions.

Detailed trophic interactions

The model focuses on aphid-hoverfly dynamics but simplifies the broader food web context. *Sphaerophoria scripta* larvae coexist with other aphid predators (ladybirds, lacewings, parasitoids), and these interactions may involve both competition and niche complementarity. In structurally complex habitats, spatial and temporal partitioning of aphid resources, differences in prey stage use, and behavioural specialisation can promote complementary predator effects, potentially enhancing aphid suppression rather than reducing prey availability. Similarly, adult hoverflies interact with other pollinators in ways that may involve resource competition or facilitation, depending on floral diversity and landscape context, and they themselves serve as prey for spiders, birds, and other predators. Although such multi-trophic and complementary interactions are not explicitly represented in the current model, they may generate indirect effects whereby pesticide impacts on co-occurring predator or pollinator communities secondarily influence hoverfly populations.

Microclimate and fine-scale habitat heterogeneity

The ALMaSS landscape simulation uses a combination of raster and patch representations to map the homogeneous landscape polygons (patches) onto a raster map. This means that, despite 1 m^2 resolution, the model treats cells

forming landscape polygons as spatially uniform. However, hoverflies respond to microclimatic variation within fields, seeking thermal refugia, exploiting boundary effects, or concentrating in resource-rich patches. Larvae may preferentially occupy specific positions on plants (leaf undersides, stem bases) that offer protection from adverse weather or natural enemies. This fine-scale heterogeneity could create population refugia during adverse conditions not represented in the current framework.

Detailed metamorphosis and physiological constraints

The model represents development as smooth, temperature-dependent transitions between life stages. In reality, metamorphosis involves complex physiological reorganisation that may be disrupted by environmental stressors. Nutritional stress during larval development can affect adult body size, longevity, and fecundity in ways more complex than simple linear relationships. Similarly, the model assumes successful development given adequate thermal conditions, missing potential failures during critical developmental windows.

Pathogen dynamics and immune responses

While basic background mortality is included, the model excludes explicit representation of pathogen dynamics. Viral pathogens associated with other pollinators, such as black queen cell virus, sacbrood virus, and deformed wing virus, have been detected in *Eristalis* hoverflies (Bailes et al. 2018), suggesting that some syrphids can carry pathogens shared with bees; however, these viruses have not been documented in aphidophagous species. Fungal epizootics affecting syrphids have not been reported (De Wint et al. 2024). Microbial associations have been observed in other syrphid species (e.g., saproxylic *Mallota dusmeti*; Sánchez-Galván et al. 2017), but their relevance to aphidophagous taxa is unclear. Overall, evidence of pathogen-driven epizootics affecting natural aphidophagous hoverfly populations or demographic rates is extremely limited and understudied. Consequently, the population-level consequences of such pathogen interactions, and their potential modulation by environmental stressors, remain poorly quantified and are not captured by the model's simple mortality functions.

Philosophical boundaries

Individual variation and population heterogeneity

The model represents individuals as identical except for stochastic variation in development timing. Real populations exhibit substantial variation in body size, metabolic rates, behavioural tendencies, and stress tolerance that could influence population resilience. By standardising individuals, the model may miss emergent properties arising from population heterogeneity, such as differential survival of stress-tolerant phenotypes during adverse conditions.

Deterministic development and stochastic reality

Thermal performance curves imply predictable development given environmental conditions. However, development rates exhibit substantial individual variation even under identical conditions, and environmental fluctuations may have non-linear effects on developmental outcomes. The model's deterministic approach may underestimate population variability and resilience mechanisms that arise from developmental asynchrony.

Spatial discreteness and movement behaviour

The grid-based landscape representation treats space as discrete cells with defined boundaries. Hoverfly movement likely occurs along continuous gradients of resource quality and environmental conditions. This discretisation may create artificial barriers to movement or miss important edge effects where landscape elements meet. Additionally, the model assumes individuals can accurately perceive resource quality within their detection radius, potentially overestimating the efficiency of resource location.

Additive stress and synergistic effects

The model assumes that multiple stressors (temperature, humidity, pesticides, resource limitation) combine in predictable, largely additive ways. However, synergistic interactions are common in biological systems, where the combined effect of multiple stressors exceeds the sum of individual effects. For example, temperature stress might increase pesticide susceptibility, or resource limitation might reduce detoxification capacity, creating non-linear responses to environmental challenges.

Implications of model framing

These simplifications reflect deliberate choices, balancing biological realism against parameter availability and computational feasibility. The extensive use of allometric scaling and cross-species parameter estimation highlights data limitations for this ecologically important but understudied species. Many key processes rely on assumptions derived from related species or theoretical considerations rather than empirical data specific to *S. scripta*.

For risk assessment applications, the model provides a framework for comparing relative risks across management scenarios rather than predicting absolute population outcomes. It is most valuable for identifying critical life stages vulnerable to pesticide exposure, evaluating how landscape composition influences population persistence, assessing the effectiveness of refuge areas in maintaining viable populations, and comparing the population-level consequences of different agricultural practices.

The model is less appropriate for predicting precise population abundances, assessing extinction probabilities in specific landscapes, evaluating long-term evolutionary responses to agricultural intensification, or extrapolating to hoverfly species with substantially different life histories (e.g., univoltine species, specialist predators, or non-migratory forms).

By acknowledging these boundaries explicitly, we position the model as a structured hypothesis about hoverfly population dynamics that can guide both risk assessment and future research priorities. The framework's value lies not in perfect biological representation, but in providing a quantitative tool for exploring how environmental variability and management practices interact to influence pollinator and biocontrol services in agricultural landscapes.

Acknowledgements

We thank Francis Gilbert for sharing unpublished data and publications on *S. scripta*, Aleksandra Walczyńska for assistance with temperature-dependent development analyses of preimaginal stages, and two anonymous reviewers for their valuable comments and suggestions.

Additional information

Conflict of interest

The authors have declared that no competing interests exist.

Ethical statement

No ethical statement was reported.

Use of AI

No use of AI was reported.

Funding

This study was supported by the PollinERA project. PollinERA receives funding from the European Union's Horizon Europe research and innovation Programme under grant agreement No.101135005. Views and opinions expressed are those of the author(s) only and do not necessarily reflect those of the European Union (EU) or the European Research Executive Agency (REA). Neither the EU nor REA can be held responsible for them.

Author contributions

Conceptualization: EZ, GS, XD, CJT. Formal analysis: EZ, XD. Funding acquisition: CJT. Investigation: EZ, GS. Supervision: CJT. Visualization: EZ. Writing - original draft: EZ, GS. Writing - review and editing: XD, CJT.

Author ORCIDs

Elżbieta Ziółkowska https://orcid.org/0000-0002-7213-2200
Grzegorz Sowa https://orcid.org/0000-0001-7855-0545
Xiaodong Duan https://orcid.org/0000-0003-2345-4155
Christopher John Topping https://orcid.org/0000-0003-0874-7603

Data availability

All of the data that support the findings of this study are available in the main text.

References

Adams THL, Chambers RJ, Dixon AFG (1987) Quantification of the impact of the hoverfly *Metasyrphus corollae* on the cereal aphid *Sitobion avenae* in winter wheat: laboratory rates of kill. Entomologia Experimentalis et Applicata 43: 153–157. https://doi.org/10.1111/j.1570-7458.1987.tb03599.x

Agarwala BK, Bhaumik AK, Gilbert FS (1989) Relative development and voracity of six species of aphidophagous syrphids in cruciferous crops. Proceedings: Animal Sciences 98: 267–274. https://doi.org/10.1007/BF03179408

Almohamad R, Verheggen F, Haubruge É (2009) Searching and oviposition behavior of aphidophagous hoverflies (Diptera: Syrphidae): a review. Biotechnologie, Agronomie, Société et Environnement 13: 467–481.

Amorós-Jiménez R, Marcos-García MÁ (2020) Fitness-related parameters of the aphid predator *Sphaerophoria rueppellii* (Diptera: Syrphidae) feeding on three different aphid pests. Boletín de la Asociación Española de Entomología 44: 299–315. https://doi.org/10.3390/insects11030166

Amorós-Jiménez R, Pineda A, Fereres A, Marcos-García MÁ (2012) Prey availability and abiotic requirements of immature stages of the aphid predator *Sphaerophoria rueppellii*. Biological Control 63: 17–24. https://doi.org/10.1016/j.biocontrol.2012.06.001

Amorós-Jiménez R, Pineda A, Fereres A, Marcos-García MÁ (2014) Feeding preferences of the aphidophagous hoverfly *Sphaerophoria rueppellii* affect the performance of its offspring. Biological Control 59: 427–435. https://doi.org/10.1007/s10526-014-9577-8

Amorós-Jiménez R, Robert CA, Marcos-García MÁ, Fereres A, Turlings TCJ (2015) A differential role of volatiles from conspecific and heterospecific competitors in the selection of oviposition sites by the aphidophagous hoverfly *Sphaerophoria rueppellii*. Journal of Chemical Ecology 41: 493–500. https://doi.org/10.1007/s10886-015-0583-9

App M, Hellwig N, Schneider-Hohenbrink A-K, Burmeister J, Schröder B, Thiele J (2025) SyrFitSources: An agent-based model to investigate the effects of land use on the population dynamics of aphidophagous hoverflies. Ecological Modelling 507: 111098. https://doi.org/10.1016/j.ecolmodel.2025.111098

Arrignon F, Deconchat M, Sarthou JP, Balent G, Monteil C (2007) Modelling the overwintering strategy of a beneficial insect in a heterogeneous landscape using a multi-agent system. Ecological Modelling 205: 423–436. https://doi.org/10.1016/j.ecolmodel.2007.03.006

Awadallah KT, Mahmoud TT, Khalil FM (1980) Egg-laying activities of the syrphid females *Metasyrphus corollae* and *Sphaerophoria scripta* (Diptera: Syrphidae). Mesopotamia Journal of Agriculture 15: 263–272.

Bailes EJ, Deutsch KR, Bagi J, Rondissone L, Brown MJF, Lewis OT (2018) First detection of bee viruses in hoverfly (syrphid) pollinators. Biology Letters 14: 20180001. https://doi.org/10.1098/rsbl.2018.0001

Bale JS, Hart AJ (1997) Factors affecting the freeze tolerance of the hoverfly *Syrphus ribesii* (Diptera: Syrphidae). Journal of Insect Physiology 44: 21–29. https://doi.org/10.1016/S0022-1910(97)00106-6

Bańkowska R (1961) Studies on the family Syrphidae in the Nida Valley. Fragmenta Faunistica 9: 153–201. [In Polish] https://doi.org/10.3161/00159301FF1961.9.13.153

Bańkowska R (1964) Studien über die paläarktischen Arten der Gattung *Sphaerophoria* St. Farg. Rt. Serv. (Diptera: Syrphidae). Annales Zoologici 22: 285–353. [In German]

Bańkowska R (1978) Aphid–aphidophage community in alfalfa cultures (*Medicago sativa* L.) in Poland. Part 3. Abundance regulation of *Acyrthosiphon pisum* (Harris) in a chain of oligophagous predators. Annales Zoologici 34: 39–77.

Becher MA, Grimm V, Knapp J, Horn J, Twiston-Davies G, Osborne JL (2016) Beescout: A model of bee scouting behaviour and a software tool for characterizing nectar and pollen landscapes for BEEHAVE. Ecological Modelling 340: 126–133. https://doi.org/10.1016/j.ecolmodel.2016.09.013

Bellefeuille Y, Fournier M, Lucas E (2019) Evaluation of two potential biological control agents against the foxglove aphid at low temperatures. Journal of Insect Science 19: 2. https://doi.org/10.1093/jisesa/iey130

Belyaev OA, Farisenkov SE (2019) A study on allometry of wing shape and venation in insects. Part 2. Diptera. Moscow University Biological Sciences Bulletin 74: 7–14. https://doi.org/10.3103/S0096392519010024

Berkvens N, Landuyt C, Deforce K, Berkvens D, De Clercq P (2010) Alternative foods for the multicoloured Asian lady beetle *Harmonia axyridis* (Coleoptera: Coccinellidae). European Journal of Entomology 107: 189–195. https://doi.org/10.14411/eje.2010.025

Bokina IG (2012) Hoverflies (Diptera: Syrphidae) in agrocenoses of the forest-steppe of Western Siberia and the influence of agrotechnological practice on their abundance. Entomological Review 92: 1053–1060. https://doi.org/10.1134/S001387381209014X

Branquart E, Hemptinne J-L (2000) Selectivity in the exploitation of floral resources by hoverflies (Diptera: Syrphinae). Ecography 23: 732–742. https://doi.org/10.1111/j.1600-0587.2000.tb00316.x

Campan M (1968) Preliminary observations on the activity rhythm of female *Eristalis tenax* at the oviposition site: influence of meteorological factors [Observations preliminaires sur le rythme d'activité des femelles d'Eristalis tenax (Dipteres, Syrphides) aux lieux de ponte influence des facteurs meteorologiques]. Revue du Comportement Animal 3: 69–76. [In French]

Campan M (1973) Study of seasonal variations in the frequency of visits to laying sites by females of *Eristalis tenax* (Diptera, Syrphidae) [Étude des variations saisonnières du rythme de fréquentation des lieux de ponte chez les femelles d'Eristalis tenax (Diptères, Syrphides).]. Bulletin de la Société d'Histoire Naturelle de Toulouse 109 : 119–130. [In French]

Capela N (2025) Resource quality and forage selection. Deliverable D1.3, Better-B project. https://www.better-b.eu

Chandler AEF (1968) The relationship between aphid infestations and oviposition by aphidophagous Syrphidae (Diptera). Annals of Applied Biology 61: 425–434. https://doi.org/10.1111/j.1744-7348.1968.tb04544.x

Collett TS, Land MF (1978) How hoverflies compute interception courses. Journal of Comparative Physiology 125: 191–204. https://doi.org/10.1007/BF00656597

Conn DLT (1976) Estimates of population size and longevity of adult narcissus bulb fly *Merodon equestris* (Fabricius) (Diptera: Syrphidae). Journal of Applied Ecology 13: 429–434. https://doi.org/10.2307/2401792

Cornelius M, Barlow CA (1980) Effect of aphid consumption by larvae on development and reproductive efficiency of a flower fly *Syrphus corollae* (Diptera: Syrphidae). The Canadian Entomologist 112: 989–992. https://doi.org/10.4039/Ent112989-10

Curran CH (1920) Observations on the more common aphidophagous syrphid flies (Diptera). The Canadian Entomologist 53: 53–55. https://doi.org/10.4039/Ent5253-3

D'Amen M, Birtele D, Zapponi L, Hardersen S (2013) Patterns in diurnal co-occurrence in an assemblage of hoverflies (Diptera: Syrphidae). European Journal of Entomology 110: 649–656. https://doi.org/10.14411/eje.2013.088

De Buck N (1990) Bloemboek en bestuivingsecologie van Zweevfliegen (Diptera, Syrphidae) in het bijzonder voor België (No. 60). Institut royal des Sciences naturelles de Belgique.

Denlinger DL, Hahn DA, Merlin C, Holzapfel CM, Bradshaw WE (2017) Keeping time without a spine: what can the insect clock teach us about seasonal adaptation? Philosophical Transactions of the Royal Society B 372: 20160257. https://doi.org/10.1098/rstb.2016.0257

De Wint FC, Nicholson S, Koid QQ, Zahra S, Chestney-Claassen G, Seelan J, Seelan S, Xie J, Xing S, Fayle TM, Haelewaters D (2024) Introducing a global database of entomopathogenic fungi and their host associations. Scientific Data 11: 1418. https://doi.org/10.1038/s41597-024-04103-4

Díaz Lucas MF, Passarelli LM, Maza N, Aquino DA, Greco NM, Rocca M (2020) Spatio-temporal variation of predatory hoverflies (Diptera: Syrphidae) and their relationship with aphids in organic horticultural crops in La Plata, Buenos Aires. Revista de la Sociedad Entomológica Argentina 79: 15–22. https://doi.org/10.25085/rsea.790403

Doyle T, Hawkes WL, Massy R, Powney GD, Menz MHM, Wotton KR (2020) Pollination by hoverflies in the Anthropocene. Proceedings of the Royal Society B 287: 20200508. https://doi.org/10.1098/rspb.2020.0508

Duan X, Topping CJ (2024) A general subpopulation model for the Animal Landscape and Man Simulation System (ALMaSS). Food and Ecological Systems Modelling Journal 5: e122467. https://doi.org/10.3897/fmj.5.122467

Duan X, Wallis D, Hatjina F, Simon-Delso N, Bruun Jensen A, Topping CJ (2022) ApisRAM formal model description. EFSA Supporting Publications 19: 7184E. https://doi.org/10.2903/sp.efsa.2022.EN-7184

Dunn L, Lequerica M, Reid CR, Latty T (2020) Dual ecosystem services of syrphid flies (Diptera: Syrphidae): pollinators and biological control agents. Pest Management Science 76: 1973–1979. https://doi.org/10.1002/ps.5807

Dušek J, Láska P (1974) Overwintering and spring emergence of some common species of aphidophagous syrphids (Diptera: Syrphidae). Folia Facultatis Scientiarum Naturalium Universitatis Purkynianae Brunensis 15: 71–75.

Ellington CP (1984) The aerodynamics of hovering insect flight. II. Morphological parameters. Philosophical Transactions of the Royal Society B 305: 17–40. https://doi.org/10.1098/RSTB.1984.0050

Evans EW, Stevenson AT, Richards DR (1999) Essential versus alternative foods of insect predators: benefits of a mixed diet. Oecologia 121: 107–112. https://doi.org/10.1007/s004420050911

Gafarov S (1979) Syrphid flies as a component of cotton agrobiocenoses in Tajikistan. Izvestiya Akademii Nauk Tadzhikskoy SSR, Otdeleniye Biologicheskikh Nauk 76: 41–45. [In Russian]

Garibaldi LA, Carvalheiro LG, Leonhardt SD et al. (2014) From research to action: enhancing crop yield through wild pollinators. Frontiers in Ecology and the Environment 12: 439–447. https://doi.org/10.1890/130330

Gasol NR, Avilla J, Alegre S, Alins G (2019) *Sphaerophoria rueppellii* adults change their foraging behavior after mating but maintain the same preferences to flower traits. Biological Control 64: 149–158. https://doi.org/10.1007/s10526-019-09928-2

Gilbert FS (1983) The foraging ecology of hoverflies (Diptera: Syrphidae): circular movements on composite flowers. Behavioral Ecology and Sociobiology 13: 253–257. https://doi.org/10.1007/BF00299672

Gilbert FS (1985a) Diurnal activity patterns in hoverflies (Diptera: Syrphidae). Ecological Entomology 10: 385–392. https://doi.org/10.1111/j.1365-2311.1985.tb00736.x

Gilbert FS (1985b) Ecomorphological relationships in hoverflies (Diptera: Syrphidae). Proceedings of the Royal Society B 224: 91–105. https://doi.org/10.1098/rspb.1985.0023

Gilbert FS (2015) Hoverflies. Naturalist' Handbook 5. Cambridge University Press, Cambridge, 96 pp.

Grimm V, Railsback SF (2005) Individual-based modeling and ecology. Princeton University Press, Princeton, 448 pp. https://doi.org/10.1515/9781400850624

Guo JW, Yang F, Li P et al. (2019) Female bias in an immigratory population of *Cnaphalocrocis medinalis* moths based on field surveys and laboratory tests. Scientific Reports 9: 18388. https://doi.org/10.1038/s41598-019-54721-x

Hlaváček A, Lučan RK, Hadrava J (2022) Autumnal migration patterns of hoverflies (Diptera: Syrphidae): interannual variability in timing and sex ratio. PeerJ 10: e14393. https://doi.org/10.7717/peerj.14393

Hondelmann P (2007) Overwintering of the hoverfly *Episyrphus balteatus*: Long-distance migration or local overwintering? PhD Thesis, University of Hannover. https://doi.org/10.1111/j.1570-7458.2007.00568.x

Hondelmann P, Poehling H-M (2007) Diapause and overwintering of the hoverfly Episyrphus balteatus. Entomologia Experimentalis et Applicata 124: 189–200. https://doi.org/10.1111/j.1570-7458.2007.00568.x

Honěk A (1993) Intraspecific variation in body size and fecundity in insects: a general relationship. Oikos 66: 483–492. https://doi.org/10.2307/3544943

Honěk A (1996) Geographical variation in thermal requirements for insect development. European Journal of Entomology 93: 303–312.

Honěk A, Kocourek F (1988) Thermal requirements for development of aphidophagous Coccinellidae (Coleoptera), Chrysopidae, Hemerobiidae (Neuroptera), and Syrphidae (Diptera): some general trends. Oecologia 76: 455–460. https://doi.org/10.1007/BF00377042

Hopper JV, Nelson EH, Daane KM, Mills NJ (2011) Growth, development and consumption by four syrphid species associated with the lettuce aphid, *Nasonovia ribisnigri*, in California. Biological Control 58: 271–276. https://doi.org/10.1016/j.biocontrol.2011.03.017

Ingels B, Van Hassel P, Van Leeuwen T, De Clercq P (2015) Feeding history affects intraguild interactions between *Harmonia axyridis* (Coleoptera: Coccinellidae) and *Episyrphus balteatus* (Diptera: Syrphidae). PLoS ONE 10: e0128518. https://doi.org/10.1371/journal.pone.0128518

Jankowska B (2004) Parasitoids of aphidophagous Syrphidae occurring in cabbage aphid (*Brevicoryne brassicae* L.) colonies on cabbage vegetable. Journal of Plant Protection Research 44: 299–305.

Kantyerina NF (1979) Biological characteristics of syrphid flies (Diptera: Syrphidae) in the Orlovski Region. Byulleten Nauchno-Tekhnicheskoi Informatsii Vsesoyuznogo Nauchno-Issledovatelskogo Instituta Zernobobovykh i Krupianykh Kultur 24: 37–40. [In Russian]

Khan AA, Shah MA, Majid S (2016) Functional response of four syrphid predators associated with green apple aphid (Hemiptera: Aphididae) in laboratory. Journal of Economic Entomology 109: 78–83. https://doi.org/10.1093/jee/tov264

Klecka J, Hadrava J, Biella P, Akter A (2018) Flower visitation by hoverflies (Diptera: Syrphidae) in a temperate plant-pollinator network. PeerJ 6: e6025. https://doi.org/10.7717/peerj.6025

Kleijn D, Van Langevelde F (2006) Interacting effects of landscape context and habitat quality on flower visiting insects in agricultural landscapes. Basic and Applied Ecology 7: 201–214. https://doi.org/10.1016/j.baae.2005.07.011

Krawczyk A, Hurej M, Jackowski J (2011) Syrphids and their parasitoids from maize crop. Journal of Plant Protection Research 51: 93–97. https://doi.org/10.2478/v10045-011-0017-9

Krsteska V (2008) Population dynamics of aphidophagous hoverflies on tobacco plants. Acta Entomologica Serbica 13: 27–41.

Li H, Wu K (2023) An efficient breeding method for *Eupeodes corollae* (Diptera: Syrphidae), a pollinator and insect natural enemy in facility-horticulture crops. Horticulturae 9: 664. https://doi.org/10.3390/horticulturae9060664

Madureira M, Rodrigues I, Pereira JA (2024) Ground-cover vegetation composition shapes the abundance of *Sphaerophoria scripta* (Diptera: Syrphidae) in Mediterranean olive groves. Journal of Insect Science 24: 7. https://doi.org/10.1093/jisesa/ieae110

Madureira M, Rodrigues I, Villa M, Pereira JA (2023) The surrounding landscape shapes the abundance of *Sphaerophoria scripta* and *Melanostoma mellinum* (Diptera: Syrphidae) in Portuguese vineyards. Agricultural and Forest Entomology 25: 206–216. https://doi.org/10.1111/afe.12544

Meyer B, Jauker F, Steffan-Dewenter I (2009) Contrasting resource-dependent responses of hoverfly richness and density to landscape structure. Basic and Applied Ecology 10: 178–186. https://doi.org/10.1016/j.baae.2008.01.001

Mohammadi-Khoramabadi A, Lotfalizadeh H, Gharali B (2016) A study on parasitoids of the hoverflies (Dipt.: Syrphidae) and their natural effects on them in organic aphid-infested lettuce farms of Yazd Province, Iran. Entomologia Generalis 36: 107–115. https://doi.org/10.1127/entomologia/2016/0131

Mushtaq S, Rana SA, Rana N, Maalik S, Ehsan N (2014) Developmental duration and predatory efficiency of *Episyrphus balteatus* on four aphid species in Pakistan. International Journal of Agriculture & Biology 16: 614–618.

Nengel S, Drescher W (1990) Studies on the biology of *Sphaerophoria scripta* L. (Diptera: Syrphidae). In VI International Symposium on Pollination 288: 98–102. https://doi.org/10.17660/ActaHortic.1991.288.10

Nicholas S, Thyselius M, Holden M, Nordström K (2018) Rearing and long-term maintenance of *Eristalis tenax* hoverflies for research studies. Journal of Visualized Experiments 135: e57711. https://doi.org/10.3791/57711

Orengo-Green JJ, Casas JL, Marcos-García MÁ (2022) Effect of abiotic climatic factors on the gonadal maturation of the biocontrol agent *Sphaerophoria rueppellii* (Wiedemann, 1830) (Diptera: Syrphidae). Insects 13: 573. https://doi.org/10.3390/insects13070573

Osborne JL, Smith A, Clark SJ, Reynolds DR, Barron MC, Lim KS, Reynolds AM (2013) The ontogeny of bumblebee flight trajectories: From naïve explorers to experienced foragers. PLoS ONE 8: e78681. https://doi.org/10.1371/journal.pone.0078681

Parry HR, Bithell M (2011) Large scale agent-based modelling: a review and guidelines for model scaling. In: Heppenstall A, Crooks A, See L, Batty M (Eds) Agent-Based Models of Geographical Systems. Springer, Dordrecht, 269–286. https://doi.org/10.1007/978-90-481-8927-4_14

Parry HR, Evans AJ (2008) A comparative analysis of parallel processing and super-individual methods for improving the computational performance of a large individual-based model. Ecological Modelling 214: 141–152. https://doi.org/10.1016/j.ecolmodel.2008.02.002

Parry HR, Evans AJ, Morgan D (2006) Aphid population response to agricultural landscape change: A spatially explicit, individual-based model. Ecological Modelling 199: 451–463. https://doi.org/10.1016/j.ecolmodel.2006.01.006

Patro B, Behera MK (2002) Biology and feeding potential of *Sphaerophoria javana* Weid. (Diptera: Syrphidae) on the bean aphid, Aphis craccivora Koch. Journal of Biological Control 16: 165–167.

Pekas A, De Craecker I, Boonen S, Wäckers FL, Moerkens R (2020) One stone; two birds: concurrent pest control and pollination services provided by aphidophagous hoverflies. Biological Control 149: 104328. https://doi.org/10.1016/j.biocontrol.2020.104328

Pineda A, Marcos-García MA (2008) Use of selected flowering plants in greenhouses to enhance aphidophagous hoverfly populations (Diptera: Syrphidae). International Journal of Entomology 44: 487–492. https://doi.org/10.1080/00379271.2008.10697584

Pleasants JM, Chaplin SJ (1983) Nectar production rates of *Asclepias quadrifolia*: causes and consequences of individual variation. Oecologia 59: 232–238. https://doi.org/10.1007/BF00378842

Polak B (1980) The influence of food density and the size of food rations on the consumption and development of aphidophagous Syrphidae (Diptera). Annals of Zoology 35: 105–115.

Putra NS, Yasuda H (2006) Effects of prey species and its density on larval performance of two species of hoverfly larvae, *Episyrphus balteatus* de Geer and *Eupeodes corollae* Fabricius (Diptera: Syrphidae). Applied Entomology and Zoology 41: 389–397. https://doi.org/10.1303/aez.2006.389

Rader R, Bartomeus I, Garibaldi L, Garratt M, Howlett B, Winfree R, Cunningham S, Mayfield M, Arthur A, Andersson G, Bommarco R, Brittain C, Carvalheiro L, Chacoff N, Entling M, Foully B, Freitas B, Gemmill-Herren B, Ghazoul J, Griffin S, Gross C, Herbertsson L, Herzog F, Hipolito J, Jaggar S, Jauker F, Klein A, Kleijn D, Krishnan S, Lemos C, Lindstrom S, Mandelik Y, Monteiro V, Nelson W, Nilsson L, Pattemore D, Pereira N, Pisanty G, Potts S, Reemer M, Rundlof M, Sheffield C, Scheper J, Schuepp C, Smith H, Stanley D, Stout J, Szentgyorgyi H, Taki H, Vergara C, Viana B, Woyciechowski M (2016) Non-bee insects are important contributors to global crop pollination. Proceedings of the National Academy of Sciences of the United States of America 113: 146–151. https://doi.org/10.1073/pnas.1517092112

Rader R, Cunningham SA, Howlett BG, Inouye DW (2020) Non-bee insects as visitors and pollinators of crops: biology, ecology, and management. Annual Review of Entomology 65: 391–407. https://doi.org/10.1146/annurev-ento-011019-025055

Raymond L, Plantegenest M, Vialatte A (2013) Migration and dispersal may drive high genetic variation and significant genetic mixing: the case of two agriculturally important, continental hoverflies (*Episyrphus balteatus* and *Sphaerophoria scripta*). Molecular Ecology 22: 5329–5339. https://doi.org/10.1111/mec.12483

Raymond L, Sarthou JP, Plantegenest M, Gauffre B, Ladet S, Vialatte A (2014) Immature hoverflies overwinter in cultivated fields and may significantly control aphid populations in autumn. Agriculture, Ecosystems & Environment 185: 99–105. https://doi.org/10.1016/j.agee.2013.12.019

Reilly J, Bartomeus I, Simpson D, Allen-Perkins A, Garibaldi L, Winfree R (2024) Wild insects and honey bees are equally important to crop yields in a global analysis. Global Ecology and Biogeography 33: e13843. https://doi.org/10.1111/geb.13843

Reynolds SK, Clem CS, Fitz-Gerald B, Young AD (2024) A comprehensive review of long-distance hover fly migration (Diptera: Syrphidae). Ecological Entomology 49: 749–767. https://doi.org/10.1111/een.13373

Rojo S, Hopper KR, Marcos-Garcia MA (1996) Fitness of the hoverflies Episyrphus balteatus and Eupeodes corollae faced with limited larval prey. Entomologia Experimentalis et Applicata 81: 53–59. https://doi.org/10.1111/j.1570-7458.1996.tb02014.x

Rojo S, Gilbert FS, Marcos-Garcia MA, Nieto JM, Durante MP (2003) A world review of predatory hoverflies (Diptera, Syrphidae: Syrphinae) and their prey. CIBIO Ediciones, Alicante, 319 pp.

Rotheray GE (1981) Host searching and oviposition behavior of some parasitoids of aphidophagous Syrphidae. Ecological Entomology 6: 79–87. https://doi.org/10.1111/j.1365-2311.1981.tb00974.x

Rotheray GE (1984) Host relations, life cycles and multiparasitism in some parasitoids of aphidophagous Syrphidae (Diptera). Ecological Entomology 9: 303–310. https://doi.org/10.1111/j.1365-2311.1984.tb00853.x

Ružička Z, Gonzales Cairo V (1976) The effect of larval starvation on the development of *Metasyrphus corollae* (Diptera). Vestnik Ceskoslovenské Společnosti Zoologické 40: 206–213.

Sadegui H, Gilbert FS (2000) Aphid suitability and its relationship to oviposition preference in predatory hoverflies. Journal of Animal Ecology 69: 771–784. https://doi.org/10.1046/j.1365-2656.2000.00433.x

Sánchez-Galván IR, Ferrer J, Galante E, Marcos-García MA (2017) Bacteria and hoverflies (Diptera: Syrphidae) in tree hollows from the Iberian Mediterranean forest. Environmental Entomology 46: 137–142. https://doi.org/10.1093/ee/nvw158

Schneider F (1969) Bionomics and physiology of aphidophagous Syrphidae. Annual Review of Entomology 14: 103–124. https://doi.org/10.1146/annurev.en.14.010169.000535

Sommaggio D, Burgio G, Guerrieri E (2014) The impact of agricultural management on the parasitization of aphidophagous hoverflies (Diptera: Syrphidae). Journal of Natural History 48: 301–315. http://dx.doi.org/10.1080/00222933.2013.791953

Sotavalta O, Laulajainen E (1961) On the sugar consumption of the drone fly (*Eristalis tenax* L.) in flight experiments. Annales Academiae Scientiarum Fennicae Series A IV. Biologica 53.

Speight MCD (2010) Species accounts of European Syrphidae (Diptera) 2010. Syrph the Net, the database of European Syrphidae, vol. 59. Dublin: Syrph the Net publications.

Speight MCD (2024) Species accounts of European Syrphidae, 2024. Syrph the Net, the database of European Syrphidae (Diptera), Vol. 115. Dublin: Syrph the Net publication, 381 pp.

Stubbs AE, Falk SJ (2002) British Hoverflies: An Illustrated Identification Guide. Second edition. British Entomological & Natural History Society, Reading, 469 pp.

Stürken K (1964) Die Bedeutung der Imaginalernährung für das Reproduktionsvermögen der Syrphiden. Angew Zool 25: 385–417. [In German]

Tenhumberg B (2004) Predicting predation efficiency of biocontrol agents: Linking behavior of individuals and population dynamic. In: Pahl-Wostl C, Schmidt S, Jakeman T (Eds) Complexity and Integrated Resources Management, Transactions of the 2nd Biennial Meeting of the International Environmental Modelling and Software Society (Vol 2), Manno, Switzerland, 864–869.

Thomsen P, Xiaodong D, Topping CJ (2024) Formal model for *Acyrthosiphon pisum*, *Aphis fabae*, *Myzus persicae* and *Sitobion avenae* using the ALMaSS subpopulation approach. Food and Ecological Systems Modelling Journal 5: e123747. https://doi.org/10.3897/fmj.5.123747

Thyselius M (2022) A behavioural investigation into Eristalis tenax. Pursuit, approach estimation, locomotor activity and rearing. PhD Thesis, University of Uppsala, ACTA UNIVERSITATIS UPSALIENSIS.

Thyselius M, Nordström K (2016) Hoverfly locomotor activity is resilient to external influence and intrinsic factors. Journal of Comparative Physiology A 202: 45–54. https://doi.org/10.1007/s00359-015-1051-2

Topping CJ (2022) The Animal Landscape and Man Simulation System (ALMaSS): a history, design, and philosophy. Research Ideas and Outcomes 8: e89919. https://doi.org/10.3897/rio.8.e89919

Topping CJ, Duan X (2024) Managing large and complex population operations with agent-based models: The ALMaSS Population_Manager. Food and Ecological Systems Modelling Journal 5: e117593. https://doi.org/10.3897/fmj.5.117593

Topping CJ, Duan X (2025) The formal model for the butterfly *Pieris napi* (Lepidoptera, Pieridae) agent-based model in the Animal Landscape and Man Simulation System (ALMaSS). Food and Ecological Systems Modelling Journal 6: e142802. https://doi.org/10.3897/fmj.6.142802

Topping CJ, Hansen TS, Jensen TS, Jepsen JU, Nikolajsen F, Odderskær P (2003) ALMaSS, an agent-based model for animals in temperate European landscapes. Ecological Modelling 167: 65–82. https://doi.org/10.1016/S0304-3800(03)00173-X

Topping CJ, Alrøe HF, Farrell KN, Grimm V (2015) Per Aspera ad Astra: Through complex population modeling to predictive theory. The American Naturalist 186: 669–674. https://doi.org/10.1086/683181

Topping CJ, Marcussen LK, Thomsen P, Chetcuti J (2022) The formal model article format: justifying modelling intent and a critical review of data foundations through publication. Food and Ecological Systems Modelling Journal 3: e91024. https://doi.org/10.3897/fmj.3.91024

Villa M, Santos SA, López-Sáez JA, Pinheiro L, Marrão R, Aguiar C, Pereira JA (2021) Pollen feeding by syrphids varies across seasons in a Mediterranean landscape dominated by the olive orchard. Biological Control 156: 104556. https://doi.org/10.1016/j.biocontrol.2021.104556

Violi M, Costi E, Monari E, Sommaggio D, Maistrello L (2025) Exploring marking methods for the predatory hoverfly *Sphaerophoria rueppellii* (Diptera: Syrphidae). Insect Science. https://doi.org/10.1111/1744-7917.70020

Wnuk A (1974) Pasożyty mszycożernych bzygowatych (Diptera, Syrphidae). Polish Journal of Entomology 44: 865–875. [in Polish]

Wnuk A, Fusch R (1977) Obserwacje nad efektywnością ograniczania liczebności mszycy kapuścianej *Brevicoryne brassicae* (L.) przez bzygowate (Diptera, Syrphidae). Polish Journal of Entomology 47: 147–155. [in Polish]

Wnuk A, Wojociechowicz E (1993) Drapieżne bzygowate (Diptera: Syrphidae) występujące w koloniach mszycy kapuścianej *Brevicoryne brassicae* (L.) na kapuście i kalafirze. Polish Journal of Entomology 62: 215–229. [in Polish]

Wojciechowicz-Żytko E (2000) The effectiveness of aphidophagous syrphid larvae [Diptera, Syrphidae] in the control of *Aphis fabae* Scop. [Homoptera, Aphidodea] on broad bean. Journal of Plant Protection Research 40: 152–157.

Wojciechowicz-Żytko E, Dobińska-Graczyk M (2025) Urban green space as a reservoir of predatory syrphids (Diptera, Syrphidae) for aphid control in cities. Agronomy 15: 953. https://doi.org/10.3390/agronomy15040953

Wojciechowicz-Żytko E, Wilk E (2023) Surrounding semi-natural vegetation as a source of aphidophagous syrphids (Diptera, Syrphidae) for aphid control in apple orchards. Agriculture 13: 1040. https://doi.org/10.3390/agriculture13051040

Wotton KR, Gao B, Menz MH, Morris RK, Ball SG, Lim KS, Reynolds DR, Hu G, Chapman JW (2019) Mass seasonal migrations of hoverflies provide extensive pollination and crop protection services. Current Biology 29: 2167–2173. https://doi.org/10.1016/j.cub.2019.05.036

Wratten SD, Bowie MH, Hickman JM, Evans AM, Sedcole JR, Tylianakis JM (2003) Field boundaries as barriers to movement of hover flies (Diptera: Syrphidae) in cultivated land. Oecologia 134: 605–611. https://doi.org/10.1007/s00442-002-1128-9

Wright E (2013) The effect of pathogens on honeybee learning and foraging behaviour. PhD Thesis, University of Warwick.

Xia JY, Van der Werf W, Rabbinge R (1999) Temperature and prey density on bionomics of *Coccinella septempunctata* (Coleoptera: Coccinellidae) feeding on *Aphis gossypii* (Homoptera: Aphididae) on cotton. Environmental Entomology 28: 307–314. https://doi.org/10.1093/ee/28.2.307

Yokoi T, Fujisaki K (2009) Hesitation behaviour of hoverflies *Sphaerophoria* spp. to avoid ambush by crab spiders. Naturwissenschaften 96: 195–200. https://doi.org/10.1007/s00114-008-0459-8

Ziółkowska E, Bednarska AJ, Laskowski R, Topping CJ (2023) The formal model for the solitary bee *Osmia bicornis* L. agent-based model. Food and Ecological Systems Modelling Journal 4: e102102. https://doi.org/10.3897/fmj.4.102102

Ziółkowska E, Walczyńska A, Topping CJ (2025) The formal model for the hoverfly *Eristalis tenax* (Diptera, Syrphidae) agent-based model in the Animal Landscape and Man Simulation System (ALMaSS). Food and Ecological Systems Modelling Journal 6: e152847. https://doi.org/10.3897/fmj.6.152847